NASA CR–72388
BRL NO. 4220

Final Report

Design, Fabrication and Test of a Flueric Servovalve

By
C.E. Vos

15 February 1968

Prepared Under Contract No. NAS 3–7980

NATIONAL AERONAUTICS AND SPACE ADMINISTRATION

Bendix
Research Laboratories

NOTICE

This report was prepared as an account of Government sponsored work. Neither the United States, nor the National Aeronautics and Space Administration (NASA), nor any person acting on behalf of NASA:

A.) Makes any warranty or representation, expressed or implied, with respect to the accuracy, completeness, or usefulness of the information contained in this report, or that the use of any information, apparatus, method, or process disclosed in this report may not infringe privately owned rights; or

B.) Assumes any liabilities with respect to the use of, or for damages resulting from the use of, any information, apparatus, method or process disclosed in this report.

As used above, "person acting on behalf of NASA" includes any employee or contractor of NASA, or employee of such contractor, to the extent that such employee or contractor of NASA, or employee of such contractor, prepares, disseminates, or provides access to any information pursuant to his employment or contract with NASA, or his employment with such contractor.

Requests for copies of this report should be referred to:

National Aeronautics and Space Administration
Office of Scientific and Technical Information
Attention: AFSS – A
Washington, D.C. 20546

NASA CR–72388
BRL NO. 4220

Final Report

Design, Fabrication and Test of a Flueric Servovalve

By
C.E. Vos

February 1968

Prepared Under Contract No. NAS 3–7980

NATIONAL AERONAUTICS AND SPACE ADMINISTRATION

Submitted to:

Technical Management
NASA Lewis Research Center
Cleveland, Ohio 44135
Advanced Systems Division
Vernon D. Gebben

Research
Laboratories

ABSTRACT

Two different models of a pneumatic-input servovalve that operates without the use of moving mechanical parts were designed and fabricated. The servovalve has the output characteristics of a four-way open-centered valve and is designed to operate with either N_2 at room temperature or H_2 at temperatures from 56°K (100°R) to 333°K (600°R), supply pressure of 148 N/cm^2 (215 psia), exhaust pressure of 34.5 N/cm^2 (50 psia), and maximum control pressure of 48.5 N/cm^2 (70.4 psia). This final report presents descriptions of the flueric circuits, component and circuit development, and evaluation test results.

TABLE OF CONTENTS

LIST OF ILLUSTRATIONS

LIST OF TABLES

SECTION 1

INTRODUCTION

The objective of this effort was to develop a flueric servovalve for a nuclear rocket control drum actuator. The flueric servovalve was developed for this application because of its potential for high reliability and good performance. Having no moving mechanical parts, it should be particularly advantageous for operation in cryogenic, high-temperature, and radiation environments. The servovalve has a pneumatic input signal, its output characteristics are similar to those of a four-way open-centered servovalve, and it incorporates frequency-variant load-pressure feedback.

The initial concept of a pneumatic servovalve using vortex pressure amplifiers was demonstrated under NASA Contract NAS 3-5212, "Design, Fabrication and Test of a Fluid Interaction Servovalve." This servovalve operated with a supply pressure of 62 N/cm^2 (90 psia) and was approximately three times larger than the servovalve developed under the subject contract. Vortex elements in the power stage of the laboratory-model servovalve were designed with a chamber diameter of 3.3 cm (1.3 inches) compared with 1.1 cm (0.437 inch) for the vortex chambers of the present servovalve. The initially developed servovalve had a maximum pressure recovery of 31.0 N/cm^2 (45 psi), which represented 60% of supply pressure, and a maximum flow recovery of 44% of supply flow. This laboratory-model servovalve demonstrated the valve functional relationships; however, it did not produce the desired linearity, flow recovery, and output pressure stability. The ultimate objective of the effort under the subject contract (NAS 3-7980) was to refine the servovalve performance to meet the requirements of the AG-20 actuator used for NASA Contract NAS 3-6201, "Replacement of Electronics with Fluid Interaction Devices."

The following requirements were apparent and formed the initial technical approach:

(1) Incorporation of dual-exit vortex amplifiers in the power stage to increase flow recovery and reduce input-signal power.

(2) Addition of regenerative feedback in the pilot stage to further reduce input-signal power.

(3) Incorporation of frequency-variant load-pressure feedback to provide for improved actuator system response.

(4) Environmental compatibility through proper selection of materials to meet the temperature requirement of the control drum actuation system. During the breadboard effort, it was not necessary to meet this Item (4).

(5) Resizing the servovalve to meet pressure and flow requirements.

(6) Improve stability and linearity of servovalve developed under Contract NAS 3-5212.

The present contract, NAS 3-7980, for "Design, Fabrication and Test of a Flueric Servovalve," has been carried through Phase 1 breadboard demonstrations. A state of the art has been established, and areas for potential improvement have been identified.

During Phase 1, two servovalve concepts were evaluated. The first concept employed two vortex pressure amplifiers for the power stage. The second concept employed a four-element vortex valve bridge power stage, and an ejector and a jet-on-jet proportional amplifier were added to the pilot stage.

The major portion of the development effort was related to the refinement of flow interactions and geometrical modifications. A summary of this effort is found in Section 2. Section 3 describes the development of the vortex pressure amplifier servovalve. It contains a description of the servovalve circuit, results of developmental tests of the servovalve components, and results of an evaluation test of the complete servovalve. Subsequent developmental tests of the vortex pressure amplifier to improve stability are also described in Section 3. Section 4 covers the development of the vortex valve bridge servovalve. It includes a description of the complete circuit, developmental tests of the vortex bridge power stage, and development of the Venjet amplifiers, and it explains the benefits obtained by adding the ejector and jet-on-jet proportional amplifier to the pilot stage. Evaluation test results of the vortex bridge servovalve conclude Section 4. Conclusions and recommendations are presented in Section 5.

The material in the appendixes provides the background for this report. Appendix A details the design specifications. Appendix B describes the vortex valve, the vortex amplifier, the Venjet amplifier, the jet-on-jet amplifier, and the ejector. Appendix C provides a glossary of symbols and terms. Dimensions of components are given in Appendix D. Appendix E describes the test equipment and test procedures used in evaluating the servovalves.

SECTION 2

SUMMARY

The ultimate objective of this contract is to refine the servovalve performance to meet the requirements of the AG-20 actuator used for NASA Contract NAS 3-6201, "Fabrication and Test of a Flueric Position Servo." The servo is designed to control the position of a nuclear rocket control drum.

Two types of servovalves, one incorporating a vortex pressure amplifier-type power stage and one a vortex bridge-type power stage, have been designed and evaluated. Test results indicate that these flueric servovalves have most of the desired performance characteristics, but lack either the desired output stability or power recovery. Of the two servovalves, the vortex pressure amplifier unit demonstrated the highest pressure and flow recovery, having a pressure recovery of 59% and a flow recovery of 54%. The unit with the vortex bridge-type power stage demonstrated a pressure recovery of 54% and a flow recovery of 20%. Although the servovalve with the vortex pressure amplifier power stage has demonstrated the best power recovery, it appears to have the greater problem with stability.

Because of the good pressure and flow recovery performance demonstrated by the vortex pressure amplifier type servovalve and because of its good reliability potential, it is recommended that a basic technology study be carried out to determine causes of and solutions for instabilities in flueric components and circuits, and that the results of this study be combined with the technology established in this contract as a means of completing the development of a flueric servovalve.

2.1 SERVOVALVE: VORTEX PRESSURE AMPLIFIER POWER STAGE CONFIGURATION

The power stage of the first type of servovalve consists of two vortex pressure amplifiers, which are operated in push-pull and produce a pressure-flow characteristic similar to the conventional four-way-bridge spool-type servovalve. The pilot stage is made up basically of two Venjet amplifiers and two summing vortex valves. The function of the pilot stage is to amplify the input signal, and to convert it to a control pressure at a higher pressure level compatible with the power stage. The Venjet amplifier enables a high output pressure to be controlled by a low chamber pressure which, in turn, is controlled by a summing vortex valve. The output of each Venjet amplifier provides the control signal to one of the power stage vortex pressure amplifiers.

Flueric components for the servovalve were designed, fabricated and tested. The testing of the components revealed that with the smaller-size lower-flow vortex elements it was not possible to achieve the turn-down ratio (ratio of maximum output flow to minimum output flow) that

had been possible with the larger-size elements. As a result, it became apparent that it would not be possible to increase the flow recovery of the servovalve to the desired value of 55% of supply flow. In subsequent tests a flow recovery of 50% and a pressure recovery of 67.5 N/cm^2 (98 psi) with a supply pressure of 148 N/cm^2 (215 psia) was achieved. The output pressure noise level was 9.4 N/cm^2 (13.7 psi), and response tests indicated that the final configuration would have more than adequate response. It was low in pressure recovery, and the output pressure was unstable. The low pressure recovery could be tolerated because it was possible to meet the final goal of operating the AG-20 actuation system, but the output stability had to be improved.

In an investigation to establish the cause of the instability, it was found that there was a reversal of the slope of the output pressure-flow characteristic curves of the power stage vortex pressure amplifier. The slope-reversal region is an unstable or oscillatory region and results in low-frequency variations in the servovalve output pressure. The slope reversal was thought to be related to the dynamic and static characteristics of the vortex flow field in the area between the vortex chamber exit orifice and the probe receiver entrance. Changes made in the geometry of this area eliminated the slope reversal in the single-exit vortex pressure amplifier, but when the changes were incorporated in a dual-exit device the slope reversal reappeared. In general, changes in geometry which eliminated the slope reversal also resulted in lower pressure and flow recovery.

2.2 SERVOVALVE: VORTEX BRIDGE POWER STAGE CONFIGURATION

A vortex valve bridge power stage consisting of four vortex valves arranged in a bridge circuit was evaluated as an alternative to the vortex pressure amplifier power stage. A jet-on-jet proportional amplifier and ejector were added to the pilot stage to maintain overall flow recovery. The addition of the jet-on-jet proportional amplifier also provides additional power gain in the pilot stage so that the regenerative-feedback vortex pressure amplifiers used with the vortex pressure amplifier configuration were no longer needed.

During the initial development, only one-half of the bridge circuit was tested. Existing components were used and, because of pressure limitations, tests were operated with pressures below design. The supply pressure to the circuit was 79.2 N/cm^2 (115 psia) and the exhaust pressure was 10.3 N/cm^2 (15 psia), as compared with a required 121 N/cm^2 (175 psia) and 34.5 N/cm^2 (50 psia). There were no areas of reverse slope in the characteristic curves and the circuit had a maximum output pressure variation of 0.069 N/cm^2 (0.1 psi) peak-to-peak. The pressure recovery was 66%. It was concluded that with proper sizing and the optimization of the turndown ratios of the circuit elements, adequate pressure recovery could be achieved.

Components for a complete bridge circuit designed for higher power recovery were fabricated next. Also, a jet-on-jet pressure amplifier was

acquired and an ejector was built. Tests with one-half of the circuit indicated that the complete bridge circuit would have a pressure swing of 71 N/cm^2 (103 psi) and an output noise level of 2.8 N/cm^2 (4 psi). The complete bridge circuit along with the jet-on-jet amplifier and ejector developed a differential pressure of 70 N/cm^2 (101 psi) and had an output noise level of 6.9 N/cm^2 (10 psi). These tests also established that the jet-on-jet amplifier and ejector functioned as anticipated. It was concluded that a breadboard model of the complete servovalve using the vortex bridge circuit rather than the pressure amplifier should be built and acceptance-tested.

The vortex bridge was selected on the basis of superior output pressure stability characteristics found during the initial tests and the premise that acceptable pressure recovery, flow recovery, and stability could be achieved with additional optimization of component performance. The exhaust valves of the bridge circuit were changed to single-exit devices to improve stability,and the control flow to these elements was reduced. The pilot stage of the complete servovalve incorporates Venjet amplifiers in the control signal input circuits to the jet-on-jet proportional amplifier. In testing the complete servovalve, it was found that the addition of the Venjet amplifiers increased the output noise of the servovalve above that obtained when the power stage was controlled with a pilot stage consisting of only a jet-on-jet proportional amplifier. An investigation indicated that the Venjet, itself, had an output noise level of 2.8 N/cm^2 (4 psi) peak-to-peak at a frequency of approximately 100 hz. In subsequent development of the Venjet, geometry of the nozzle and receiver was varied and the noise level was reduced to 0.83 N/cm^2 (1.2 psi) peak-to-peak. The addition of the Venjets to the servovalve still resulted in an increase in output noise level of the servovalve. The output noise of concern was low-frequency noise that did not correlate with the high-frequency noise of the Venjet.

The Venjets and summing vortex valves of the final servovalve were oversized relative to the jet-on-jet amplifier. These components were originally sized to operate with the pressure amplifier power stage. Also, being a breadboard, components were not closely connected and dynamic performance could not be fully evaluated. In the final acceptance test, the servovalve had a pressure recovery of 61 N/cm^2 (89 psi), a flow recovery of 20%, and an output noise level of 7.9 N/cm^2 (11.4 psi) peak-to-peak. With properly sized Venjets and vortex summing valves, the flow recovery of this servovalve would be 31%. A complete summary of servovalve performance is presented in the following section.

2.3 BREADBOARD SERVOVALVE PERFORMANCE

Table 2-1 summarizes the performance characteristics of the two basic types of flueric servovalves that were built and evaluated.

The characteristic load pressure versus load flow curves for the servovalves are shown in Figures 2-1 and 2-2. Figure 2-3 shows the characteristic curves of a vortex bridge power stage with good flow and

Table 2-1 - Breadboard Flueric Servovalve Performance Using Nitrogen

Item	Specified*	Power Stage Vortex Pressure Amplifier	Power Stage Vortex Bridge
(1) Supply Pressure	148 N/cm^2 (215 psia)	148 N/cm^2 (215 psia)	148 N/cm^2 (215 psia)
(2) Exhaust Pressure	34.5 N/cm^2 (50 psia)	34.5 N/cm^2 (50 psia)	34.5 N/cm^2 (50 psia)
(3) Flow Recovery	55% min.	50%	20%
(4) Rated Input Signal	7 N/cm^2 (10 psi) max.	10 N/cm^2 (14.5 psi)	4.8 N/cm^2 (5.6 psi)
(5) Input Signal Pressure Bias	45 N/cm^2 (65.3 psia) max.	53.7 N/cm^2 (76.7 psia)	49.3 N/cm^2 (71.7 psia)
(6) Total Input Power	2.1 watts max.	10.5 watts	7.8 watts
(7) Rated No-Load Flow	2.76 gm/sec (0.0063 pps)	3.0 gm/sec (0.0067 pps)	1.0 gm/sec (0.0022 pps)
(8) Pressure Recovery	82 N/cm^2 (119 psi)	67 N/cm^2 (98 psi)	61.2 N/cm^2 (89 psi)
(9) Linearity-Deviation Gain Variation	10% max. 2 times average max.	19% 2 times	16% 1.7 times
(10) Stability	0.4 N/cm^2 (0.58 psi) p-p max.	9 N/cm^2 (13.1 psi)	7.9 N/cm^2 (11.4 psi)
(11) Transient Response	62.5% F.V. in 0.055 sec (on H_2) 90.0% F.V. in 0.210 sec (on H_2)	0.110 sec 0.190 sec	0.14 sec 0.29 sec
(12) Frequency Response Phase Shift and Amplitude Ratio	20° max. @ 6 hertz (on H_2) 90° max. @ 60 hertz (on H_2) ±2 db max. @ 0-60 hertz (on H_2)	20° @ 5 hertz 90° @ 45 hertz ±1.7 db	20° @ 1.9 hertz 90° @ 10 hertz ±2 db @ 0-8 hertz
(13) Threshold	0.5% max.	1%	not measured
(14) Hysteresis	3% max.	3%	5%

P-5349

*NASA Contract No. NAS 3-7980. Specified performance is with nitrogen except where hydrogen is indicated.

pressure recovery, but with the slope-reversal characteristic that causes instability. The superior power recovery of this design is apparent.

Previously mentioned tests were conducted with nitrogen gas. Both servovalve concepts also were tested by using hydrogen as the supply gas. The blocked port pressure gain characteristics of the vortex bridge servovalve tested with hydrogen and then with nitrogen are shown in Figure 2-4. The pressure gain characteristics are essentially the same, and linearity is very good except when approaching maximum output pressure. In tests of the servovalve with the pressure amplifier power stage, changing of gases resulted in a null shift. This shifting was due primarily to a mismatching of the components.

The results of frequency response tests of the vortex pressure amplifier servovalve show that the response of the servovalve will be adequate. The breadboard components were packaged to achieve flexibility rather than compactness. Repackaging to decrease connecting line volumes and using hydrogen rather than nitrogen would bring the performance within the specified values.

The dynamic response of the vortex bridge servovalve is not representative of its potential capability because the components were manifolded with long communicating lines. Since the vortex bridge servovalve would have dynamic response comparable to the vortex pressure amplifier servovalve, a compact vortex bridge servovalve should meet all dynamic performance requirements.

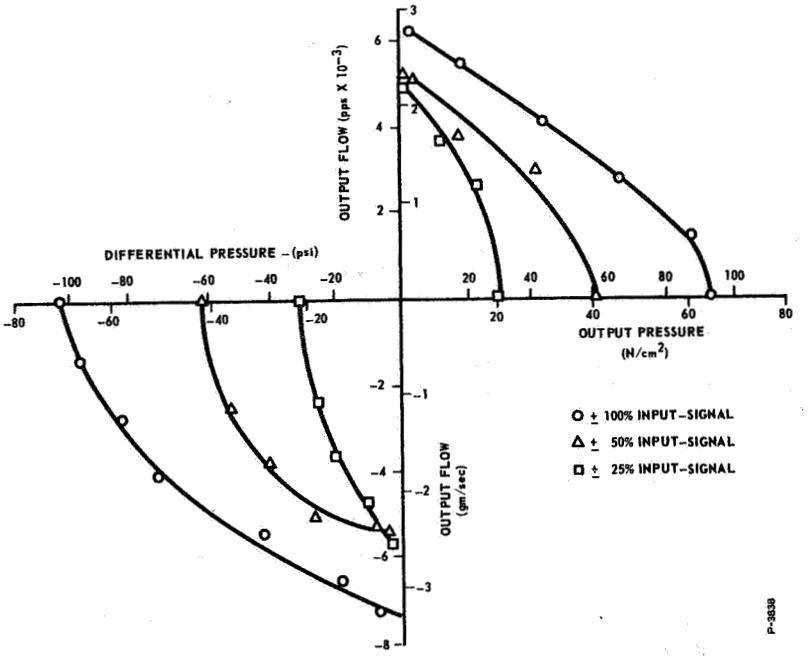

Figure 2-1 - Breadboard Flueric Servovalve Output Flow Versus Differential Pressure

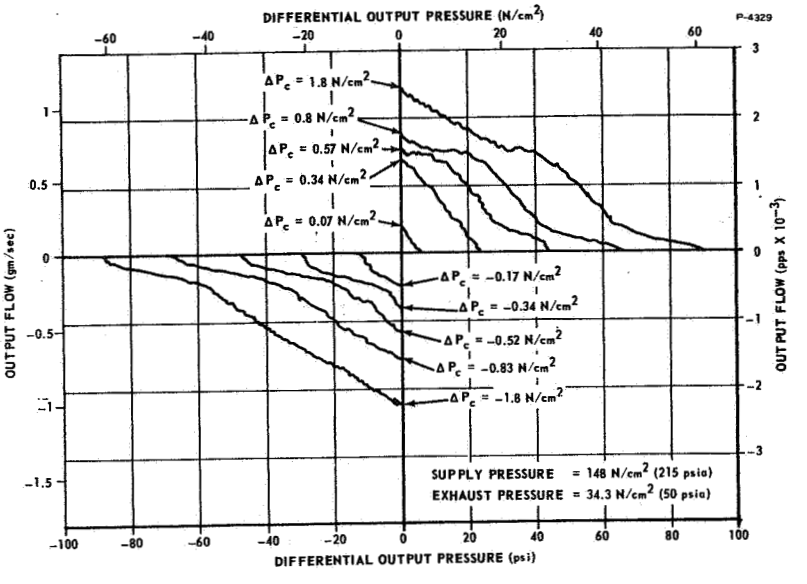

Figure 2-2 - Output Flow Versus Output Pressure - Vortex Valve Bridge Power Stage Stable Configuration

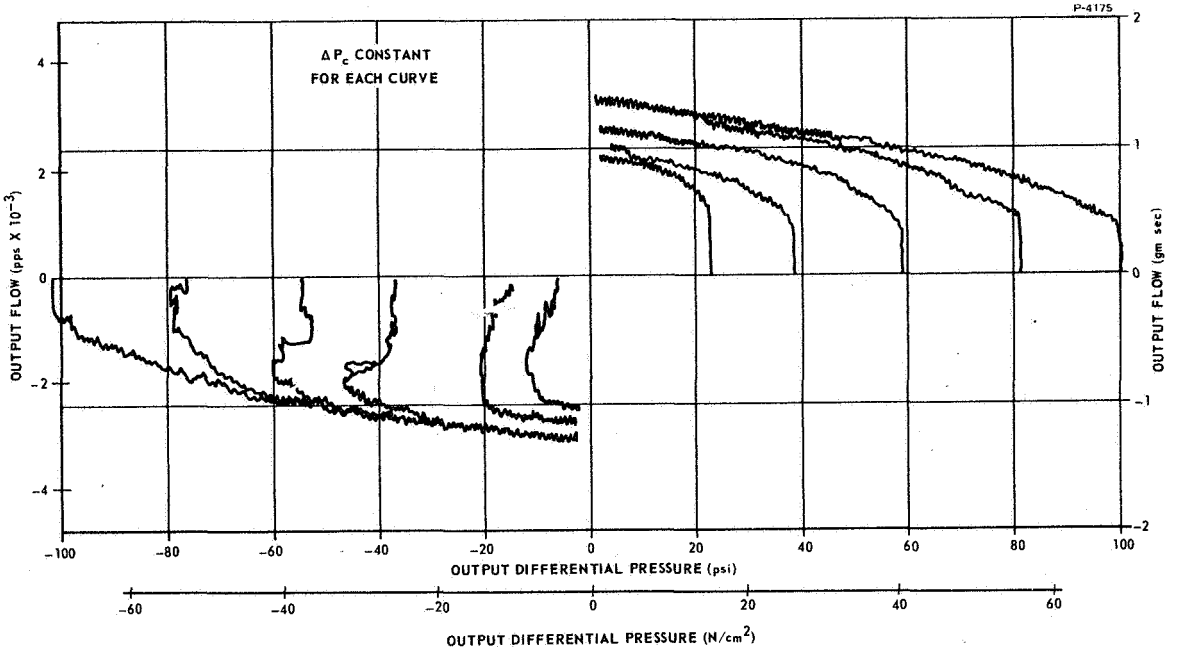

Figure 2-3 - Output Pressure Versus Output Flow Characteristics of Vortex Valve Bridge Power Stage

2.4 FLUERIC SERVOVALVE POTENTIAL PERFORMANCE

The potential performance is the predicted maximum performance that may be achieved from a flueric servovalve when using components and circuits with characteristics already established experimentally in the size and pressure ranges under consideration.

Figure 2-5 shows the potential load pressure versus load flow curves for a vortex pressure amplifier servovalve and a vortex bridge servovalve. Also shown is the specified characteristic curve. The load flow has been normalized by showing it as a fraction of supply flow, and the output pressure has been normalized with respect to the pressure difference between valve supply pressure and exhaust pressure.

The characteristics of the vortex pressure amplifier servovalve are derived from the characteristic curves shown in Figure 2-1. The flow recovery of this servovalve is improved by the addition of a jet-on-jet proportional amplifier to the pilot stage, which increases the maximum flow recovery from 50% to 76% of supply flow. A schematic of this servovalve concept is shown in Figure 2-6.

The characteristic curves of the vortex bridge servovalve are derived from the curves shown in Figure 2-3, and are based on using a properly sized pilot stage. Table 2-2 summarizes the potential performance for these two servovalve concepts.

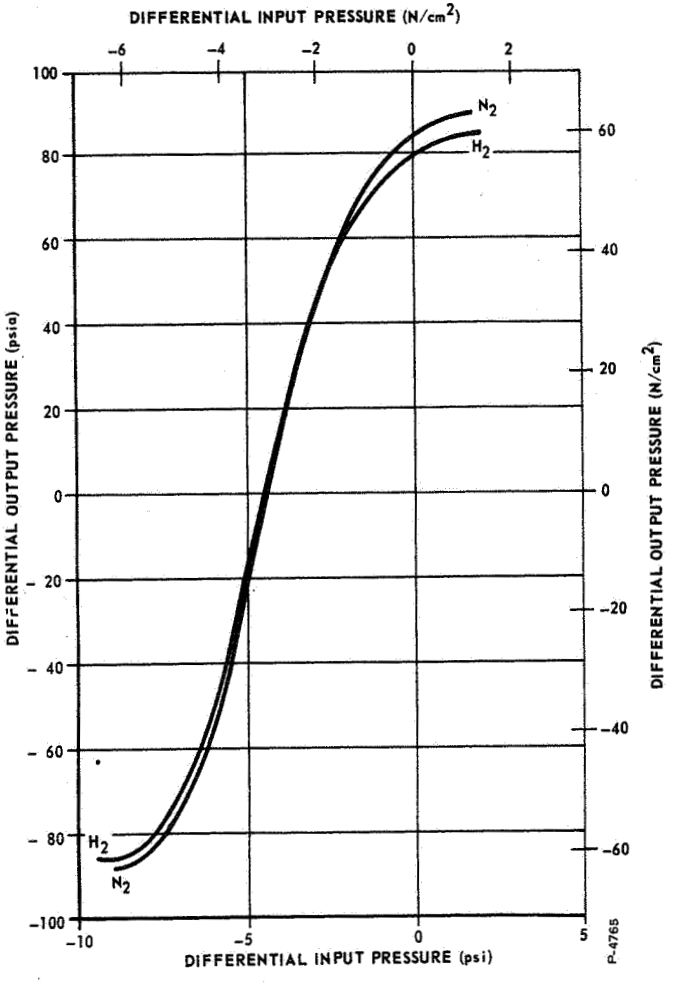

Figure 2-4 - Breadboard Servovalve Differential Output Pressure Versus Differential Input Pressure

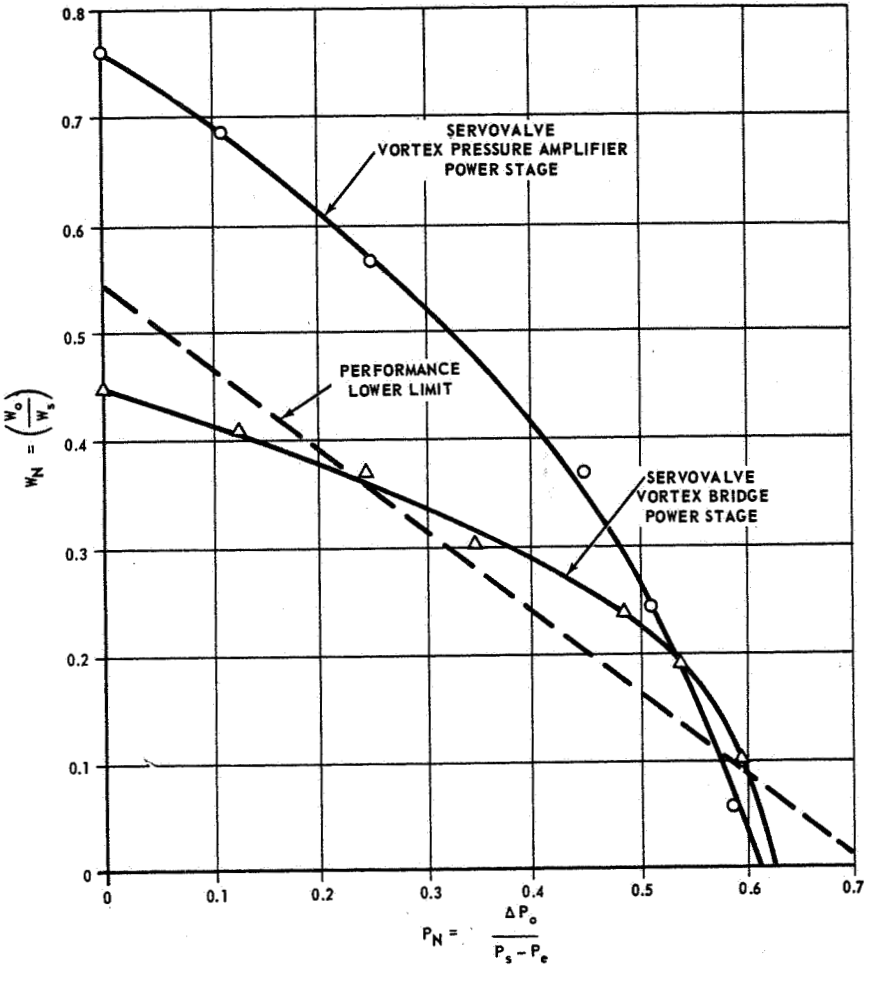

Figure 2-5 - Potential Load Pressure Versus Load Flow of Flueric Servovalves

Table 2-2 - Performance Potential of Flueric Servovalve

Item	Performance Goal	Potential of Vortex Bridge Servovalve	Potential of Vortex Pressure Amplifier Servovalve
Flow Recovery	55%	45%	76%
Pressure Recovery	72%	61%	63%
Rated Output Flow (nitrogen)	2.76 gm/sec (0.0063 pps)	2.76 gm/sec (0.0063 pps)	2.76 gm/sec (0.0063 pps)
Input Signal Power (nitrogen)	2.1 watts	4.2 watts	2.9 watts

P-4765

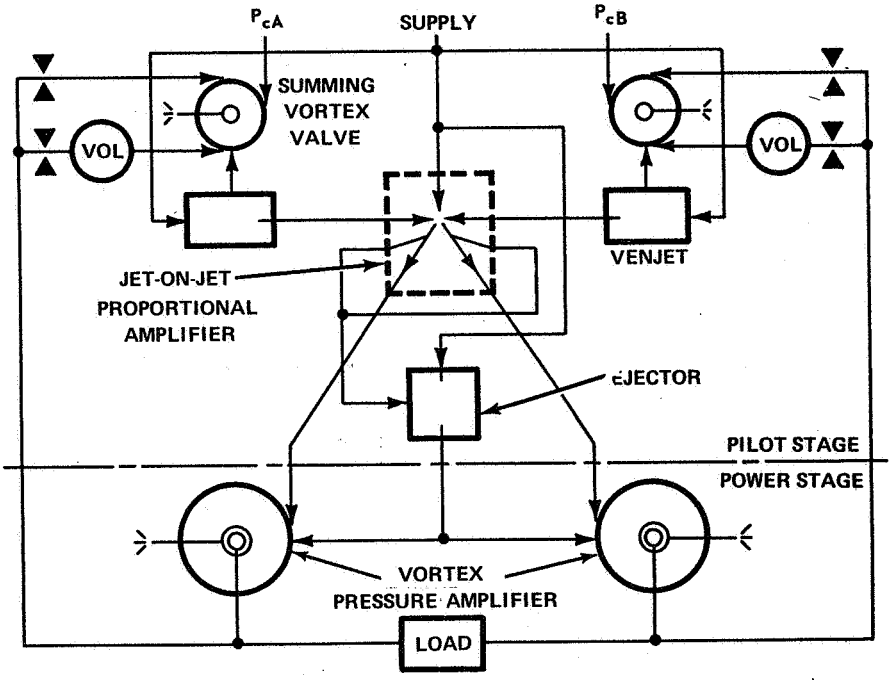

Figure 2-6 - Flueric Servovalve Schematic - Vortex Pressure Amplifier Power Stage and Jet-on-Jet Proportional Amplifier Pilot Stage

2.5 CONCLUSIONS

It has been established that a flueric servovalve with performance capabilities comparable to a flapper-nozzle type servovalve can be built. A problem with stability still exists. All techniques evaluated thus far to improve stability have resulted in reduction of pressure and flow recovery. In the case of the vortex bridge servovalve, a severe loss in power recovery resulted. If the full potential of this type of servovalve is to be realized, it will be necessary to develop techniques for stabilization that do not result in severe losses in performance.

2.6 RECOMMENDATIONS

Since the flueric servovalve has demonstrated good performance capabilities excluding stability, and offers important advantages in reliability and maintenance, it is recommended that further development effort be carried on to improve stability. This effort should include a basic technology study to determine causes of and solutions for instabilities in flueric components and circuits. Analytical techniques should be developed to describe flueric elements by mathematical models and to analyze and optimize circuits by computer. The effort should be concluded by applying the resulting technology along with the technology described in this report in further development of a flueric servovalve with a jet-on-jet proportional amplifier type pilot stage and a vortex pressure amplifier type power stage.

SECTION 3

DEVELOPMENT OF VORTEX PRESSURE AMPLIFIER SERVOVALVE

The breadboard vortex pressure amplifier servovalve uses a similar but more sophisticated flueric circuit than that used in the laboratory-model servovalve developed under NASA Contract NAS 3-5212.* The laboratory-model servovalve used two single-exit vortex pressure amplifiers for the power stage and two Venjet amplifiers controlled by dual-exit vortex valves for the pilot stage. In the initial design approach of the breadboard vortex pressure amplifier, the following changes were made from the laboratory-model servovalve.

(1) Incorporation of dual-exit vortex amplifiers in the power stage to increase flow recovery and reduce input-signal power.

(2) Addition of regenerative feedback in the pilot stage to reduce input-signal power further.

(3) Incorporation of frequency-variant load-pressure feedback to provide for improved actuator system response.

(4) Sizing the servovalve much smaller to meet flow requirements.

After the flueric components were designed and fabricated, developmental and evaluation tests were performed on each component separately. The components were then assembled together and the complete breadboard servovalve was experimentally evaluated. A stability problem was found and the main source of the instability was traced to a "negative resistance" (i.e., reverse slope) region in the pressure-flow characteristics of the power stage vortex pressure amplifiers, as shown in Figure 3-1. Developmental tests were performed on the power stage vortex pressure amplifier in which the stability was improved slightly but the oscillation due to negative resistance was not eliminated.

3.1 DESCRIPTION OF CIRCUIT

The servovalve circuit is made up of a power stage and pilot stage as shown schematically in Figure 3-2. Components making up the circuit are described in Appendix B.

The power stage consists of two vortex pressure amplifiers, shown schematically in Figure 3-3, which are operated in push-pull and produce a pressure-flow characteristic similar to the conventional four-way-bridge spool-type servovalve. An increase of control pressure P_{c1} diverts

*"Design Fabrication and Test of a Fluid Interaction Servovalve (Final Report)," Bendix Report BRL-2978, NASA Report NASA-CR-54463 (N65-31178), May 17, 1965.

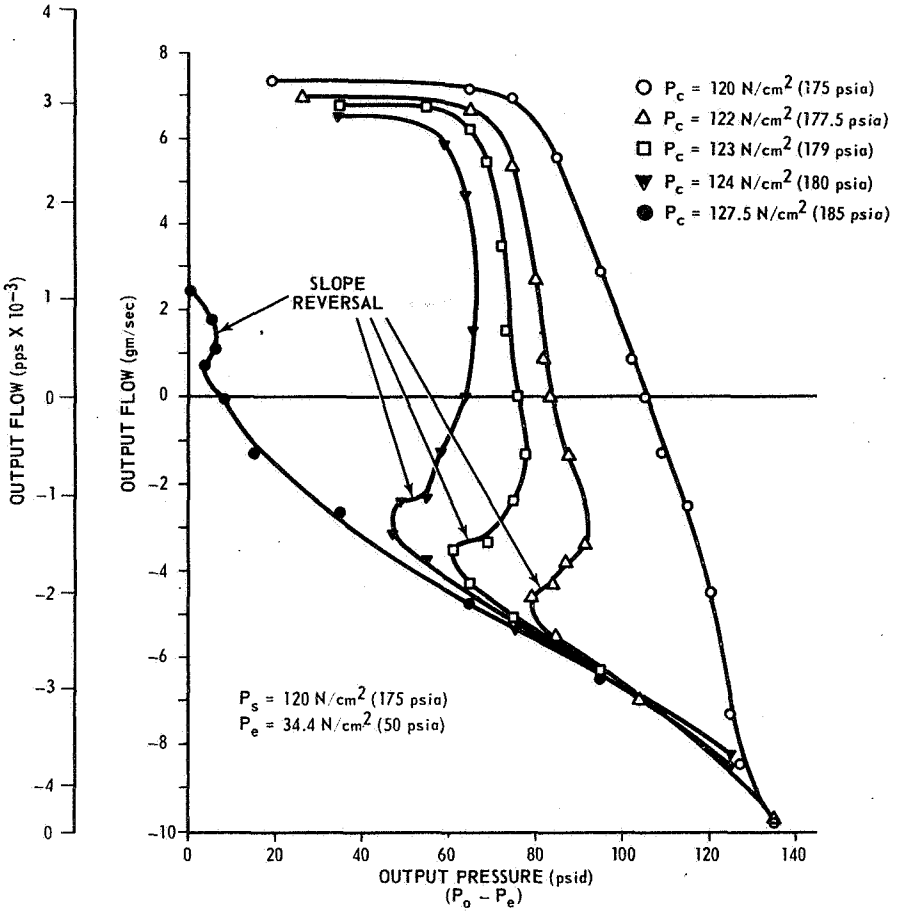

Figure 3-1 - Vortex Pressure Amplifier Receiver Output Flow Versus Output Pressure

the flow leaving the output orifice of valve V_1 and thereby reduces the recovered pressure P_1. A simultaneous reduction of P_{c2} converges the flow leaving V_2 to increase P_2. The result is a differential pressure $P_2 - P_1$ across the load.

When the two valves are operated to drive an actuator load, it is necessary for one valve to absorb reverse flow from the actuator when the load is moving. The vortex amplifier receiver is designed to provide this type of operation. With the outlet flow at a minimum value and fully diverted to exhaust, the backflow is exhausted with minimum back pressure by providing sufficient area between the valve and receiver.

An orifice in the supply line to the power stage drops the pressure from 148 N/cm^2 (215 psia) to about 120 N/cm^2 (175 psia). The quiescent control pressures to the power stage are set at a value that results in a quiescent supply flow to each vortex pressure amplifier equal to one-half

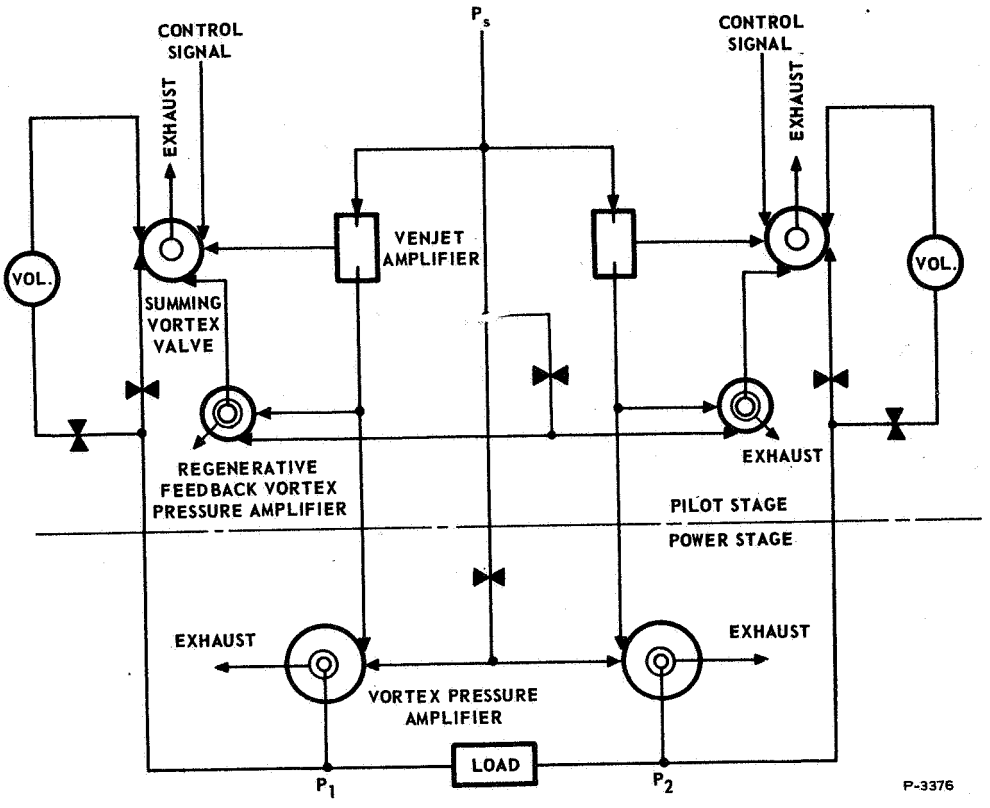

Figure 3-2 - Vortex Pressure Amplifier Servovalve - Schematic

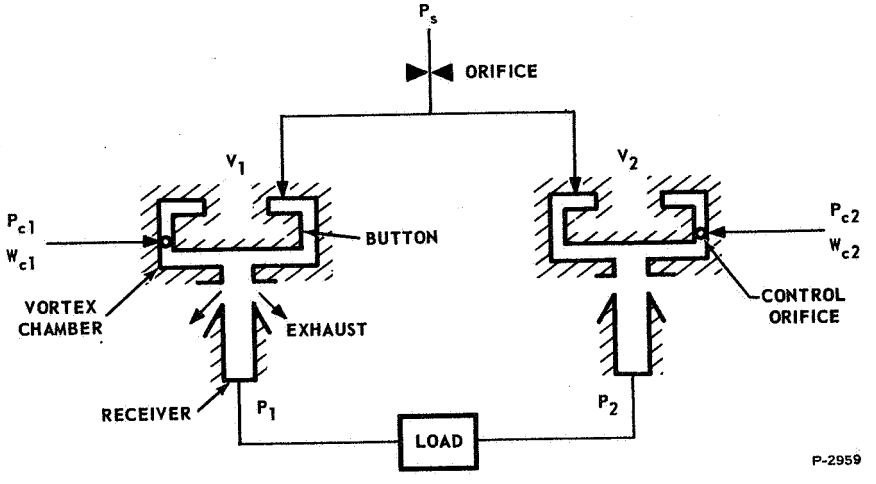

Figure 3-3 - Schematic of Power Stage

of the maximum supply flow to the power stage. When the control pressures are varied about the quiescent condition by an input signal to the valve, one control pressure to the power stage increases and the other decreases. This change in control pressures results in an increase in supply flow to one vortex pressure amplifier and a decrease in the supply flow to the other. Also, the supply flow to each vortex pressure amplifier is almost independent of the receiver load or output flow. Thus the supply flow to the power stage and consequently the supply pressure, remain relatively constant. Each vortex pressure amplifier is of the dual-exit type, which has a higher flow gain than a single-exit amplifier. A dual-exit pressure amplifier has an exit orifice and a probe-type receiver on each side of the vortex chamber at the center, as shown in Figure 3-4.

The function of the pilot stage is to amplify the input signal, and to convert it to a control pressure at a higher pressure level compatible with the power stage. The pilot stage is made up basically of two Venjet amplifiers and two summing vortex valves. The Venjet amplifier enables a high output pressure to be controlled by a low chamber pressure which, in turn, is controlled by a summing vortex valve. The primary control flow to the summing vortex valve is one of the servovalve input signals. The output of each Venjet is the control signal to one of the power stage vortex pressure amplifiers.

The effective restriction of the summing vortex valve is a function of the pressure differential between the Venjet chamber pressure and the sum of the control input signals to the summing vortex valve. The control signal to the summing vortex valve need only be slightly higher than the Venjet chamber pressure to restrict the chamber vent flow. The Venjet chamber pressure is the supply pressure of the summing vortex valve, and the valve supply flow is the vent flow of the Venjet. As the primary control input pressure to the summing vortex valve increases, the vent flow from the Venjet chamber decreases and the Venjet chamber pressure increases, causing the Venjet receiver pressure and flow to increase. A schematic of a Venjet amplifier controlled by a vortex valve is shown in Figure 3-5.

Regenerative feedback between each Venjet and its summing vortex valve is incorporated to improve the power gain of the pilot stage. The output pressure change of the Venjet is used to provide the feedback signal. However, simple feedback of this pressure to the summing vortex valve would not be adequate because the flow change would be proportional to the output pressure. To produce a large change in feedback flow, the Venjet output pressure is introduced into the supply port of another vortex valve that is biased through its control port at a pressure near the maximum output pressure of the Venjet. The flow no longer changes proportionally to the output pressure change; instead, the feedback flow is controlled by the difference between the bias pressure and the Venjet output pressure, and a much larger flow change is possible. When Venjet output pressure is maximum, the pressure difference is zero, and the valve

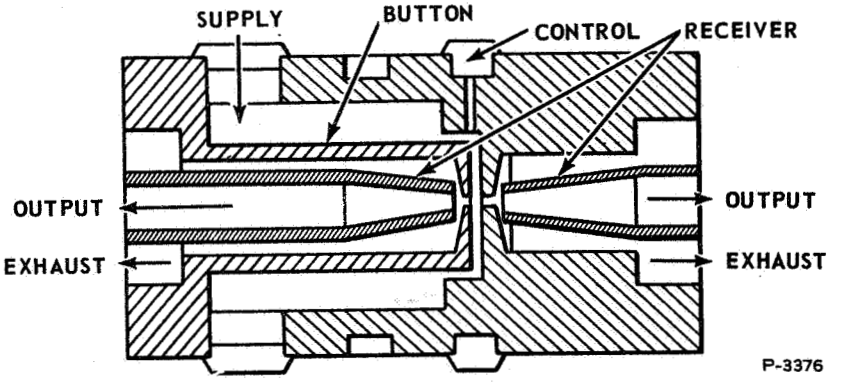

Figure 3-4 - Dual-Exit Vortex Pressure Amplifier

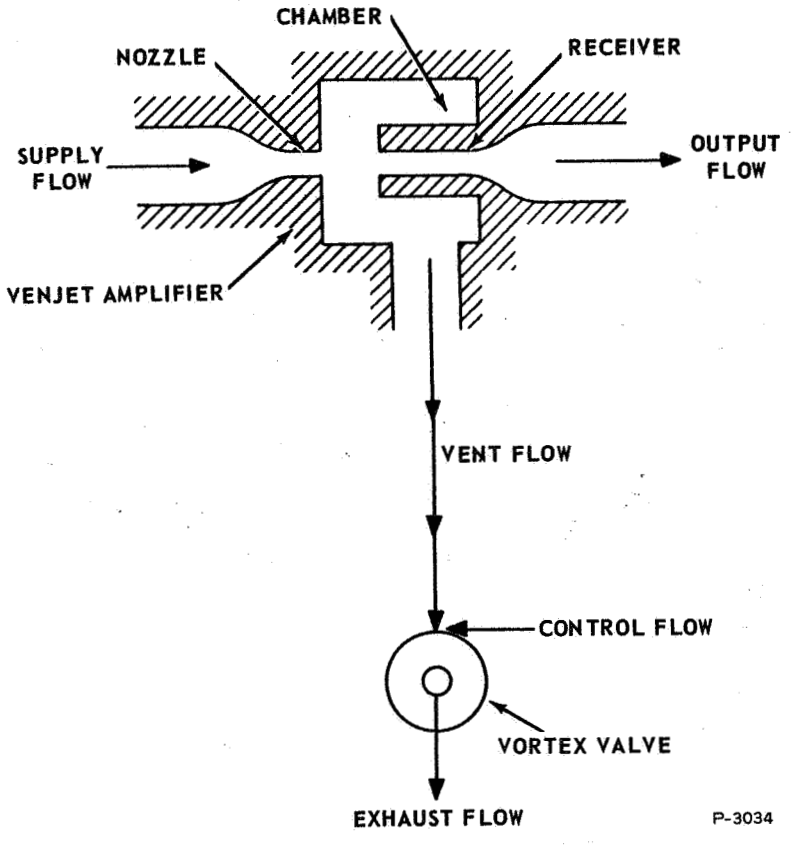

Figure 3-5 - Schematic of Venjet Amplifier - Vortex Valve Circuit

permits maximum flow to feed back to the summing vortex valve. When Venjet output pressure is smaller than the bias pressure, the bias flow turns down the valve, reducing feedback flow. The feedback enters a control port of the summing vortex valve in the same direction as the control input signal so that it increases the gain. Proper sizing of the feedback vortex valve produces the required feedback gain.

In addition to the input signal and regenerative-feedback signal, the summing vortex valve contains two additional opposing control ports. These ports receive the load-pressure feedback signal. The port in the same direction as the input signal receives the direct load pressure signal through a gain-adjusting orifice. The same pressure is passed through a similar orifice in series with a volume to the opposing control port. This volume and orifice form a lag circuit which at high frequencies reduces the opposing flow to zero. However, at low frequencies the same amount of flow passes through the volume as through the branch without the volume, and the two cancel each other out. The effect is to reduce gain when input frequencies are high. This frequency-variant pressure feedback is termed dynamic pressure feedback.

3.2 COMPONENT DEVELOPMENT AND TEST RESULTS

3.2.1 Power Stage Vortex Pressure Amplifier

(1) Chamber Diameter Development

In the initial tests of the vortex pressure amplifier, a negative resistance characteristic was found which resulted in a vertical portion of the supply flow versus control pressure curve as shown in Figure 3-6. Negative resistance in a vortex device ordinarily can be eliminated by increasing the viscous losses in one of several ways: (a) shortening chamber length to increase viscous drag, (b) enlarging chamber diameter to lengthen the flow path, or (c) roughening, or adding protrusions or grooves to the chamber walls. The first attempt was to eliminate the negative resistance by shortening the vortex chamber length, but this method was not effective. Returning to the original chamber length, the chamber and button diameters were increased, keeping the annular area around the button constant. The vortex chamber diameter, originally 0.660 cm (0.260 in.), was first increased to 0.940 cm (0.370 in.). This change eliminated some, but not all, of the negative resistance. The chamber diameter was next increased to 1.112 cm (0.438 in.), and this change eliminated all of the negative resistance. The flow versus control pressure curve is shown in Figure 3-7.

(2) Exit Orifice Length

When the second power stage vortex pressure amplifier was built, it incorporated a longer exit orifice as a means of improving both output pressure stability and pressure recovery. The vortex chamber exit orifice length of the first amplifier was 30% of the orifice diameter.

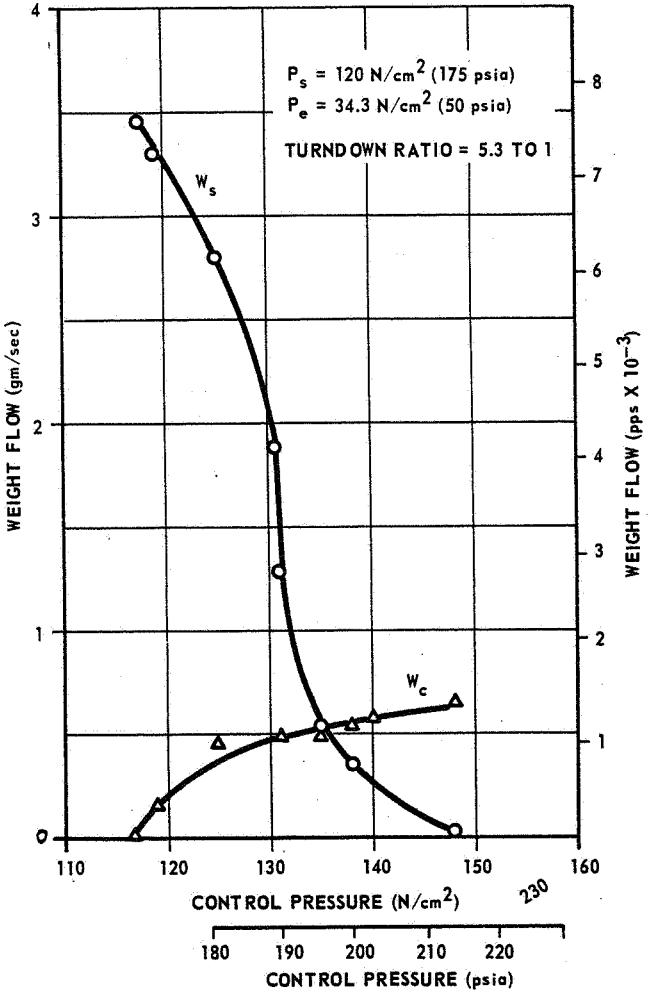

Figure 3-6 - Flow Versus Control Pressure Characteristics of Power Stage Vortex Pressure Amplifier With Small Chamber Diameter

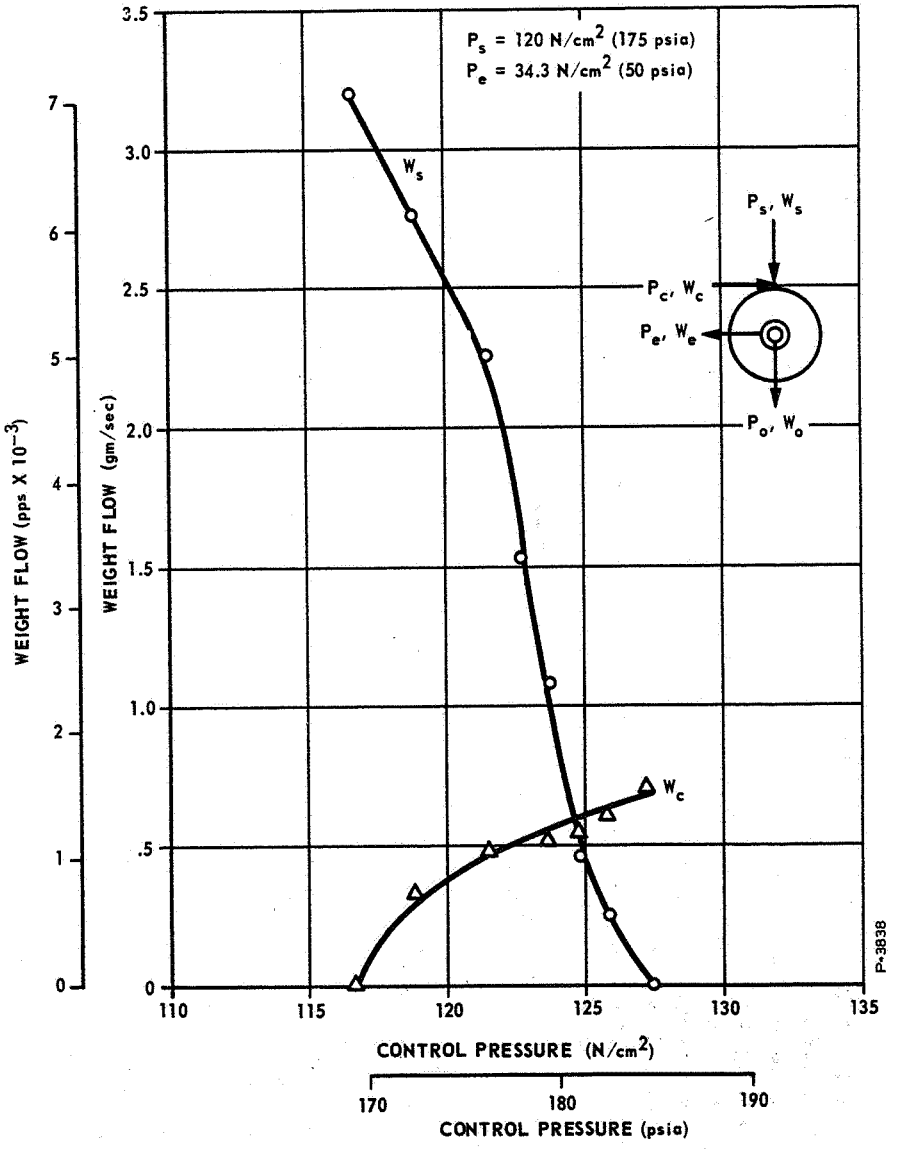

Figure 3-7 - Flow Versus Control Pressure Characteristics of Power Stage Vortex Pressure Amplifier With Large Chamber Diameter

The blocked output pressure under the zero control flow condition intermittently fluctuated between 91% and 75% of the vortex amplifier supply pressure. It was thought that a longer exit orifice would tend to straighten and focus the jet; so the orifice length of the second amplifier was increased to four times the orifice diameter. This change eliminated the intermittent output pressure fluctuation, and increased the maximum blocked output pressure to 96% of the supply pressure. However, the minimum blocked output pressure was higher also, so that the maximum pressure differential was only slightly higher.

3.2.2 Venjet Amplifier

The objectives of the Venjet amplifier test were to determine the pressure gain characteristics and the maximum pressure and flow recovery. A schematic of the Venjet amplifier is shown in Figure 3-8. This test was performed at room temperature using both nitrogen and hydrogen. Previous to the performance of this test, it was uncertain whether or not there would be a shift in the output pressure versus chamber pressure curve in changing from nitrogen to hydrogen. The following data indicate that there is virtually no difference in performance.

The output pressure and flow characteristics are shown as a function of the chamber pressure in Figure 3-9. The load orifice simulated the orifice area of one of the servovalve power stage vortex amplifiers. The pressure downstream of the load was 120 N/cm^2 (175 psia), and corresponded to the supply pressure of the power stage. The supply pressure to the Venjet was 148.1 N/cm^2 (215 psia). Under the test load condition, the maximum output pressure was 127 N/cm^2 (184 psia) with a flow recovery of 56%. The blocked output (zero load flow) versus chamber pressure is shown in Figure 3-10.

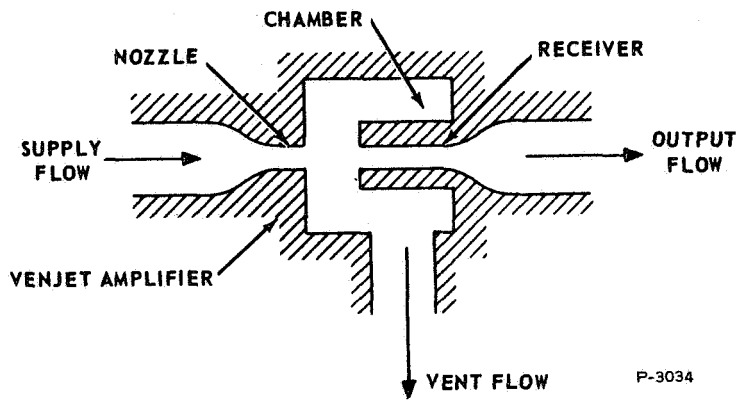

Figure 3-8 - Schematic of Venjet Amplifier

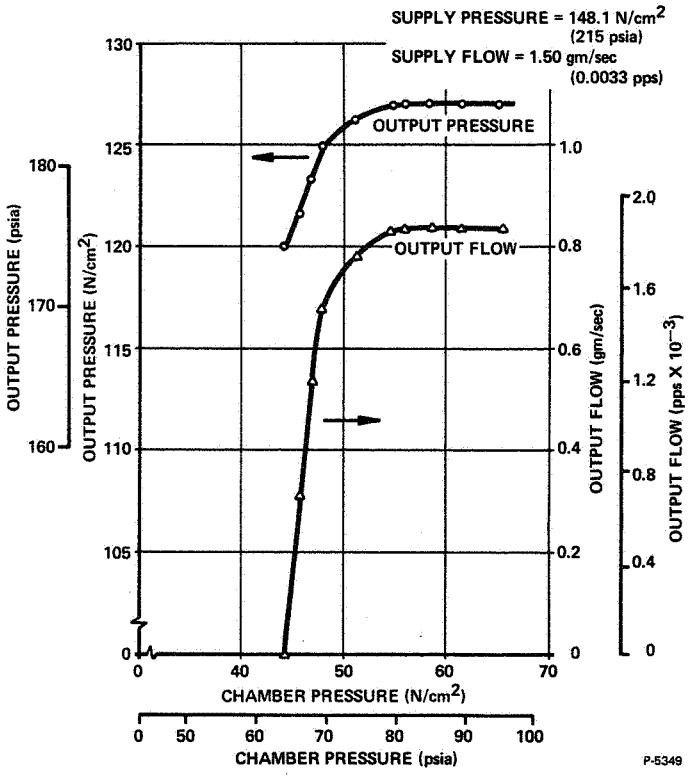

Figure 3-9 - Output Pressure and Flow Versus Chamber Pressure of Venjet Amplifier With Simulated Load

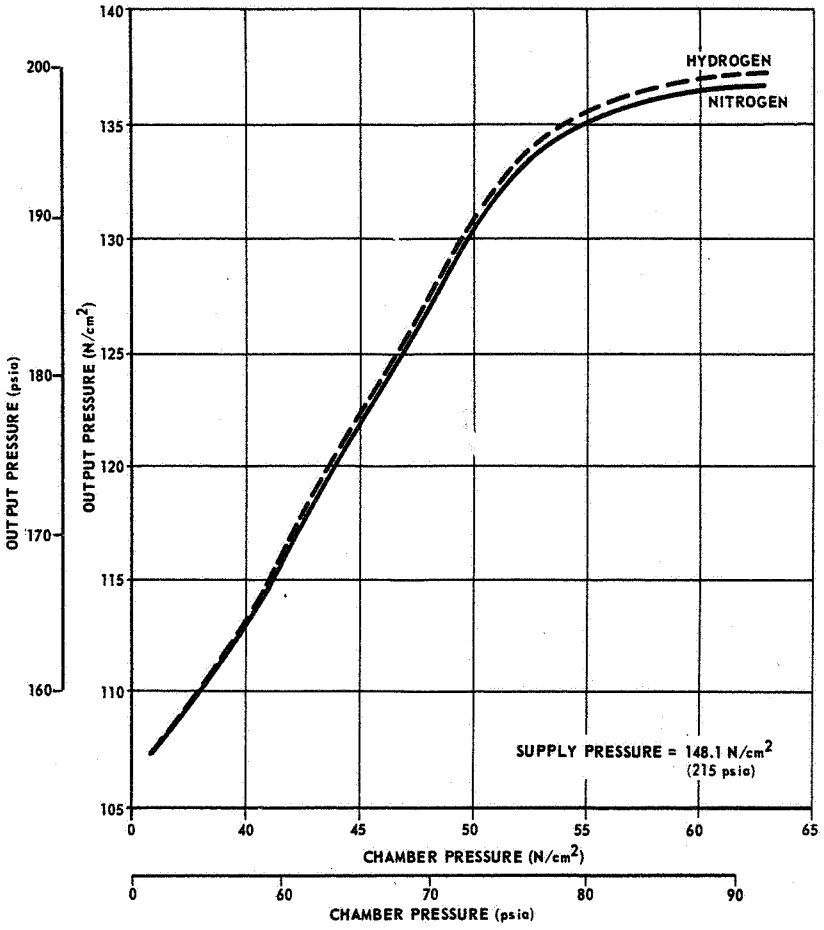

Figure 3-10 - Comparison of Gain Characteristics of Venjet Amplifier With Hydrogen and Nitrogen With Blocked Load

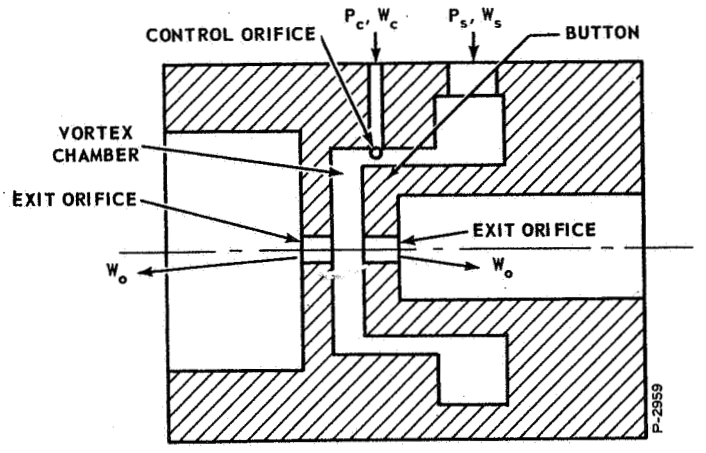

Figure 3-11 - Dual-Exit Vortex Valve

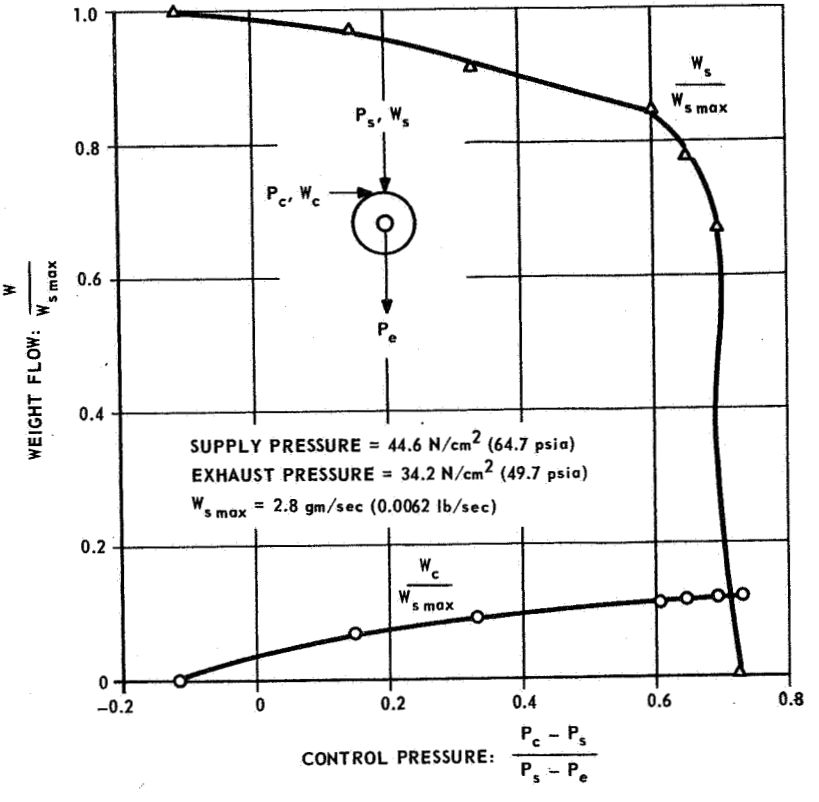

Figure 3-12 - Flow Versus Control Pressure Characteristics of Summing Vortex Valve

3.2.3 Summing Vortex Valve

The primary objective of the summing vortex valve test was to determine turndown ratio. The summing vortex valve, shown schematically in Figure 3-11, is of the dual-exit type with four control inputs: the input signal, the regenerative feedback signal, and the two inputs from the dynamic pressure feedback network.

Data in Figure 3-12 show supply flow and control flow measured at various control pressures. A turndown ratio of 8.3:1 was obtained. A negative resistance region was found which results in a hysteresis effect if the supply pressure is held constant. However, in the servovalve, the supply pressure to the summing vortex valve increases as the control pressure increases, so that no hysteresis effect occurs.

3.2.4 Regenerative-Feedback Vortex Pressure Amplifier

The objective of this test was to determine the turndown ratio and the pressure-flow recovery characteristics of the regenerative-feedback vortex pressure amplifier. A schematic of the pressure amplifier is shown in Figure 3-13. The amplifier is of the dual-exit type with dual receivers. The test was performed with room temperature nitrogen at a supply pressure of 127 N/cm^2 (185 psia). The supply flow, control flow, and output pressure were measured at various values of control pressure. The control flow, supply flow, and blocked output pressure are plotted as a function of supply flow in Figure 3-14. The turndown ratio of this device is small, only 1.65:1, but is still adequate for this application. The output flow versus output pressure characteristic with zero control flow is shown in Figure 3-15.

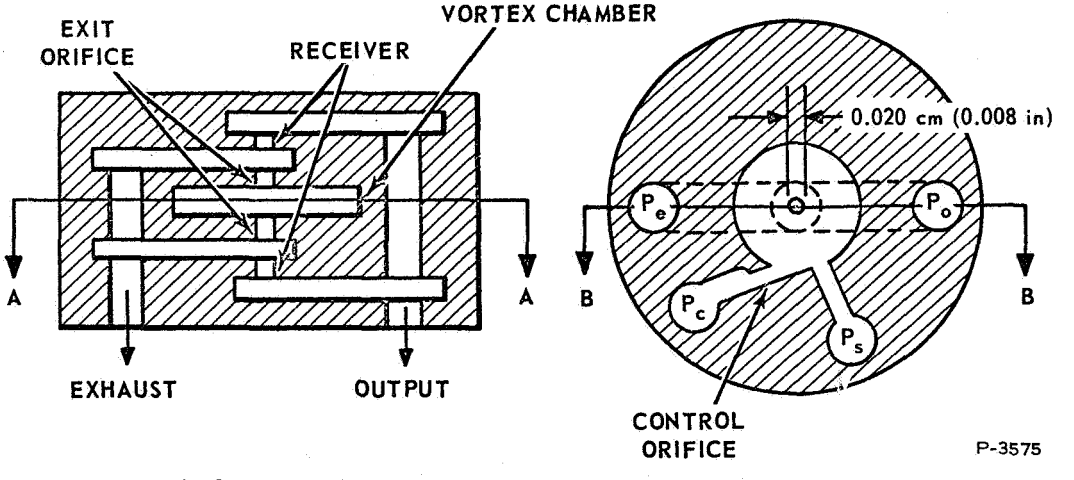

Figure 3-13 - Schematic of Regenerative-Feedback Vortex Pressure Amplifier

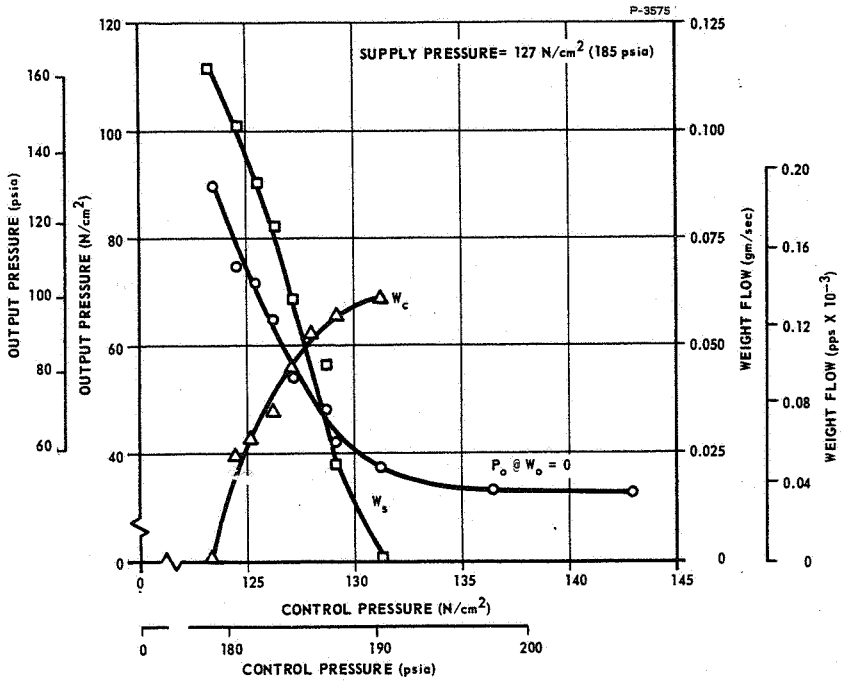

Figure 3-14 - Flow and Output Pressure Versus Control Pressure Characteristics of Regenerative-Feedback Vortex Pressure Amplifier

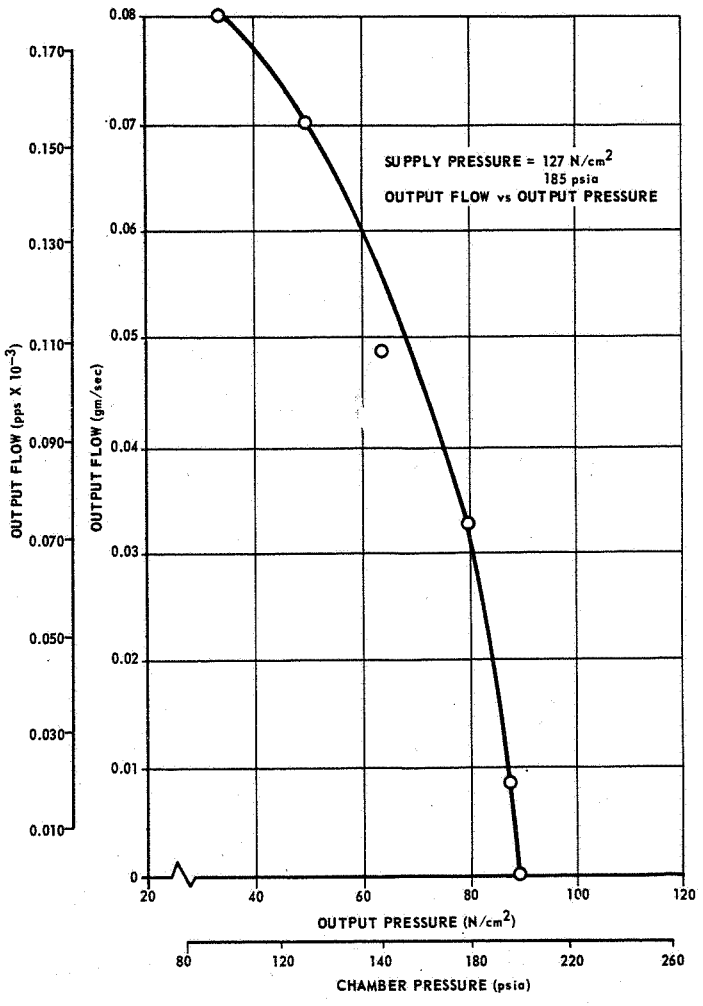

Figure 3-15 - Flow-Pressure Recovery Characteristics of Regenerative-Feedback Vortex Pressure Amplifier

3.3 BREADBOARD SERVOVALVE EVALUATION TEST

The objectives of the evaluation test were to determine how well the complete servovalve would perform and what interface problems might exist between the components of the servovalve. In the servovalve evaluation test, the linearity, flow recovery, pressure recovery and input-signal power were measured, first using nitrogen as the gaseous medium and then using hydrogen. The other performance items were measured using nitrogen only.

The breadboard servovalve test performance is compared with the specified requirements in Table 3-1. The measured performance met, or came close to meeting, the specified requirements in supply flow, rated no-load flow, transient response, frequency response, threshold, and hysteresis. The test results also pointed out several areas which required an improvement in performance. These are pressure recovery, linearity, and stability.

Preliminary checks of the servovalve performance prior to the evaluation test indicated that the servovalve would not operate properly with regenerative feedback in the pilot stage. There was a large area of hysteresis along with a bistable type of operation. One side of the servovalve had been previously tested satisfactorily with regenerative feedback in the pilot stage. But, when testing the complete servovalve, the difference in the gain characteristics of the two power stage vortex pressure amplifiers caused the regenerative-feedback vortex pressure amplifiers to operate improperly. Therefore, as a temporary expedient to permit the evaluation test to proceed without delay, the regenerative-feedback amplifiers were disconnected from the servovalve circuit and the test was performed without them. The effect of this was to increase the maximum input-signal pressure slightly and to increase the total maximum input-signal power by a factor of about two.

Table 3-1 - Breadboard Flueric Servovalve Performance

Item	Specified*	Measured (N_2)	Measured (H_2)
3.1.5 Supply Flow	1.82 rated no-load output flow max.	2.0	1.93
5.2 Rated Input Signal	7 N/cm^2 (10 psi) max.	10 N/cm^2 (14.5 psi)	9.3 N/cm^2 (13.5 psi)
5.3 Input Signal Pressure Bias	45 N/cm^2 (65.3 psia)	53.7 N/cm^2 (76.7 psia)	51.2 N/cm^2 (74.2 psia)
5.5 Total Input Power	2.1 watts max. N_2 @ 530°R 7.7 watts max. H_2 @ 530°R	10.5 watts	31.0 watts
6.2 Rated No-Load Flow	2.76 gm/sec (0.0063 pps) N_2 @ 530°R 0.782 gm/sec (0.00173 pps) H_2 @ 530°R	3.0 gm/sec (0.0067 pps)	0.816 gm/sec (0.0018 pps)
6.4 Pressure Recovery	82 N/cm^2 (119 psi)	67 N/cm^2 (98 psi)	57 N/cm^2 (83 psi)
6.5 Linearity-Deviation Gain Variation	10% max. 2 times avg. max.	19% 2 times	25% 3.6 times
6.7 Stability	0.4 N/cm^2 (0.58 psi) p-p	9 N/cm^2 (13.1 psi)	Not Measured
6.8 Transient Response	62.5% F.V. in 0.055 sec 90.0% F.V. in 0.210 sec	0.110 sec 0.190 sec	Not Measured
6.9 Frequency Response Phase Shift and Amplitude Ratio	20° max. @ 6 hertz 90° max. @ 60 hertz ±2 db max. @ 0-60 hertz	20°@5 hertz 90°@45 hertz ±1.7 db	Not Measured
6.11 Threshold	0.5% max.	1%	Not Measured
6.11 Hysteresis	3% max.	3%	Not Measured

P-3830

*See Appendix A

Because of the oscillation of the power stage differential output pressure, the load pressure dynamic feedback circuit could not be evaluated, and therefore it, too, was disconnected from the servovalve for this test.

The supply flow was 2.0 and 1.93 times the rated no-load flow on nitrogen and hydrogen, respectively, as compared with the specified value of 1.82 times rated no-load output flow.

The threshold was measured by applying a sine-wave input and gradually decreasing the amplitude while recording the output of the servovalve. The threshold is defined as the increment of input signal required to produce a change in the output signal. Thus, if the input sine wave is reduced until the output amplitude becomes zero, the input amplitude at that point is a measure of the threshold. Actually, the threshold of the servovalve should be zero, because of the nature of its flueric components, which have no inherent hysteresis. Thus, the output amplitude should go to zero only when the input amplitude is reduced to zero. However, the oscillation in the output obscured measurements at low input amplitude so that the test data only show that the threshold is not more than 1%.

Input-signal power is defined as the product of the input-signal volumetric flow and the pressure difference between the input-signal pressure and the servovalve exhaust pressure. The maximum total input-signal power was excessively high for two reasons. The regenerative feedback was not used and thus more control flow was required. Also, the input-signal pressure is high because of the pressure level characteristics of the Venjet amplifier. The Venjet amplifier output pressure versus chamber pressure curve is at a higher chamber pressure than was desired.

A typical trace of the transient response is shown in Figure 3-16. The response time values listed in Table 3-1 are the average of several traces. The differential output reached 62.9% of the step in 0.110 second and settled within 90% of the final value in 0.190 second.

The frequency response data is shown in Figure 3-17. The input signal was 6.2% of the rated input signal rather than 2% as called out in the specifications, so that the differential output pressure sine-wave data would not be obscured by the output pressure oscillation. The phase shift was 90 degrees at 45 hertz. The differential output pressure amplitude variation was less than ± 1.7 db from 0 to 80 hertz. This phase shift without amplitude variation indicates that a signal delay of approximately 8 milliseconds occurs in the breadboard servovalve.

The results of the frequency-response and transient-response tests show that the response of the servovalve will be more than adequate. The breadboard servovalve components were packaged separately in order to achieve flexibility rather than compactness. Repackaging to decrease connecting line volumes and using hydrogen rather than nitrogen would bring the performance well within the specified limits.

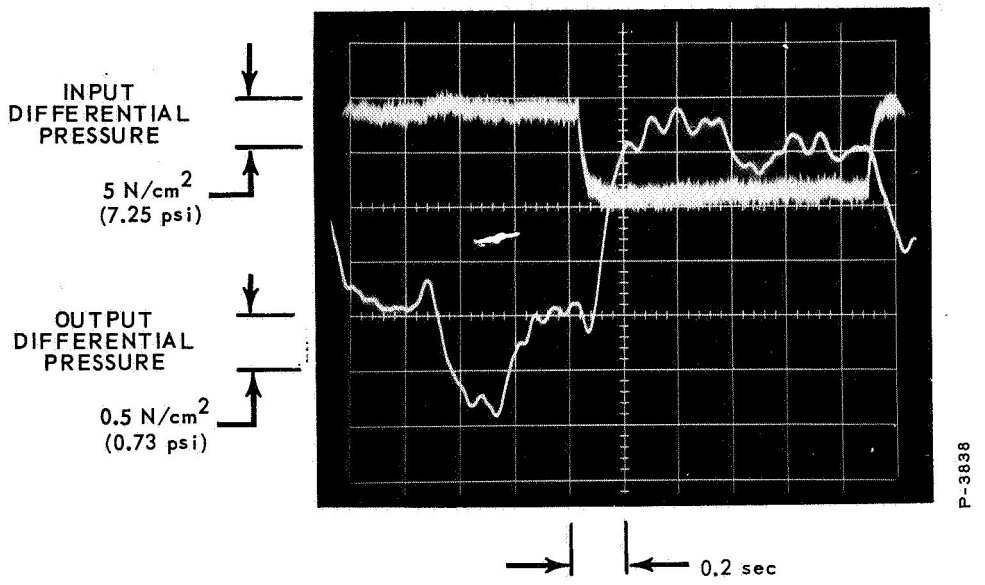

Figure 3-16 - Transient Response of Breadboard Flueric Servovalve

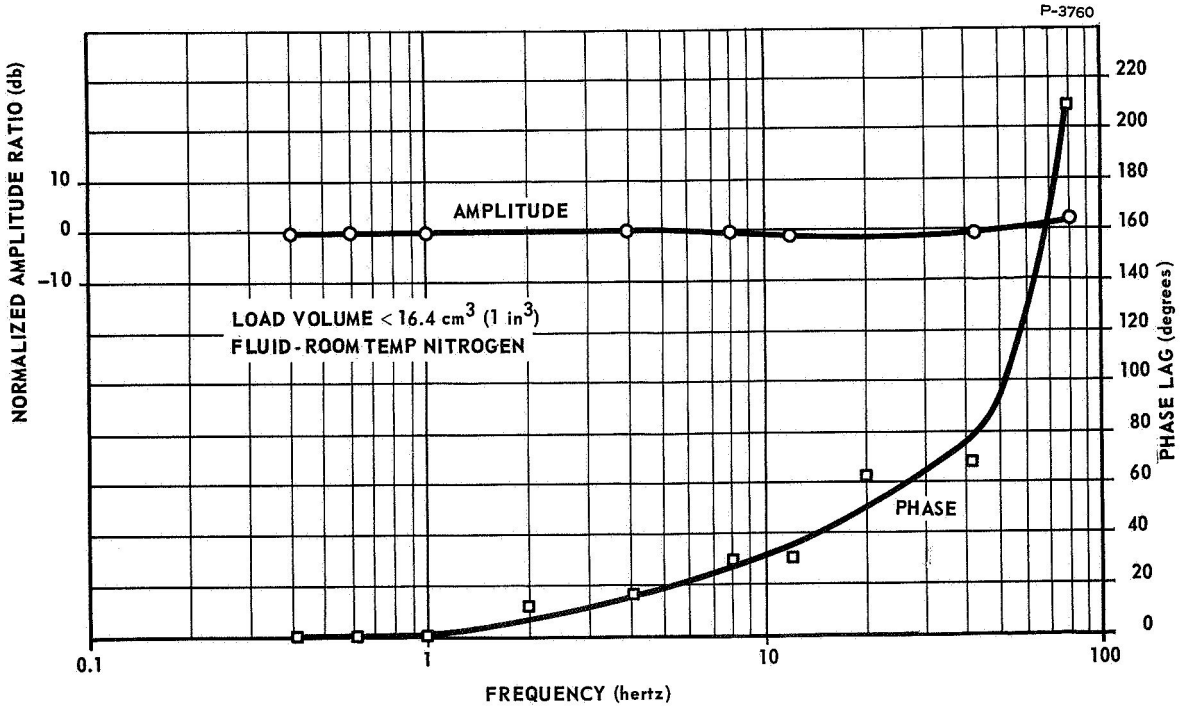

Figure 3-17 - Frequency Response of Breadboard Flueric Servovalve

Representative differential output pressure stability data are shown in Figure 3-18. The data was taken after filtering the electrical signal of the differential output pressure transducer with a $1/(0.05S + 1)^2$ filter. The upper photograph shown was taken on an average differential output pressure of 0. The maximum amplitude of oscillation in this case was 9 N/cm^2 (13.1 psi) peak-to-peak to a frequency of about 6.3 hertz. The differential output pressure was oscillatory over most of the differential input pressure range, except at near $\pm$100% rated input signal, where the output differential pressure is relatively quiet as shown in the lower photograph in Figure 3-18.

The differential output pressure versus differential control input pressure with closed load throttle is shown in Figure 3-19. The linearity and hysteresis performance was determined from this curve. The deviation from a straight line of the trace is 19% of the rated value, which exceeds the specified maximum of 10%. The maximum pressure gain is two times the average pressure gain, which is just equal to the specified limit. The curve does not pass through the origin because of the difference in gain characteristics of the two power stage vortex pressure amplifiers. These data were taken with nitrogen as the gaseous medium.

Figure 3-20 shows the servovalve pressure gain with hydrogen as the gaseous medium instead of nitrogen. The deviation from a straight line of the gain curve is 25% of the rated value, and the maximum pressure gain is 3.6 times the average gain. It is seen from comparison with the curve in Figure 3-19 that there is a large zero shift and a decrease in the maximum differential output pressure. In previous tests of individual components, it was found that the performance characteristics were almost the same with hydrogen as with nitrogen. However, because of the lack of symmetry between the two sides of the servovalve, a small gain change results in a zero shift. Identical gain characteristics of both sides of the servovalve should eliminate the zero shift. The linearity would be improved by increasing the flow capacity of the pilot stage and also by better matching of the gain characteristics of the power stage and the pilot stage individual components.

The output flow versus differential output pressure is shown in Figure 3-21. From this figure, it is seen that at rated input signal the maximum load flows were 2.85 gm/sec (0.0063 pps) in one direction and 3.3 gm/sec (0.0073 pps) in the other. The maximum differential output pressures are 65.4 N/cm^2 (95 psi) and 70.3 N/cm^2 (102 psi). The supply flow remained at 6.18 gm/sec (0.0136 pps) during the test. The two power stage vortex pressure amplifiers had different chamber exit orifice lengths, and the amplifier with the shorter orifice length had lower pressure recovery. Use of the longer exit orifice length type of vortex amplifier on both sides of the power stage would improve the pressure recovery.

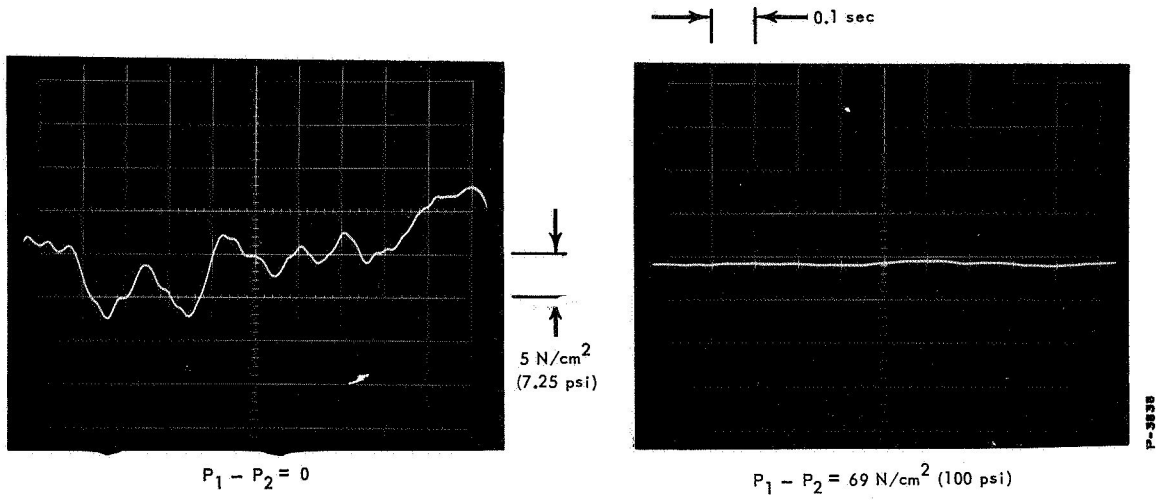

Figure 3-18 - Breadboard Flueric Servovalve Differential Output Pressure Stability

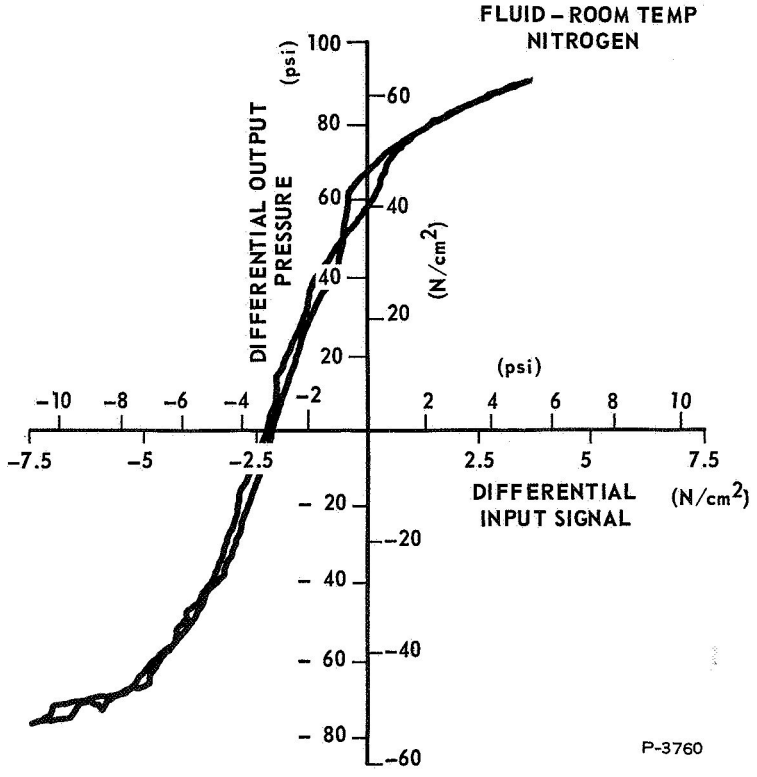

Figure 3-19 - Differential Output Pressure Versus Differential Input Signal of Breadboard Flueric Servovalve With Nitrogen

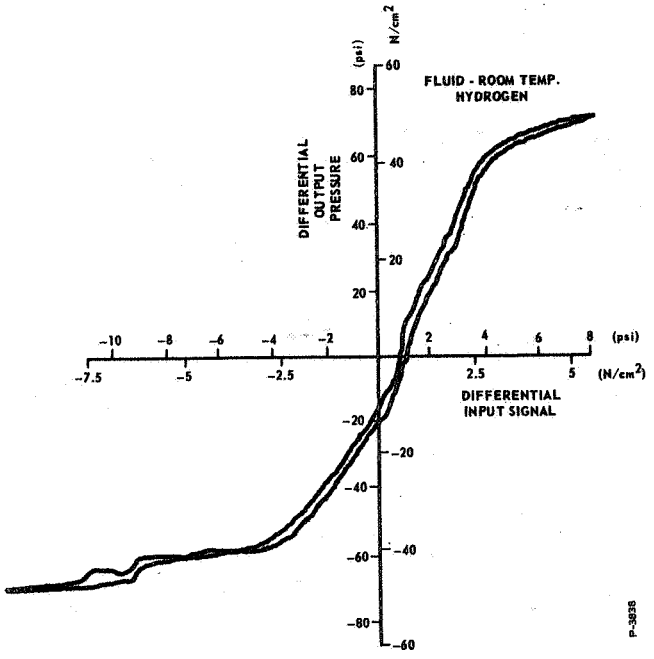

Figure 3-20 - Differential Output Pressure Versus Differential Input Signal of Breadboard Flueric Servovalve With Hydrogen

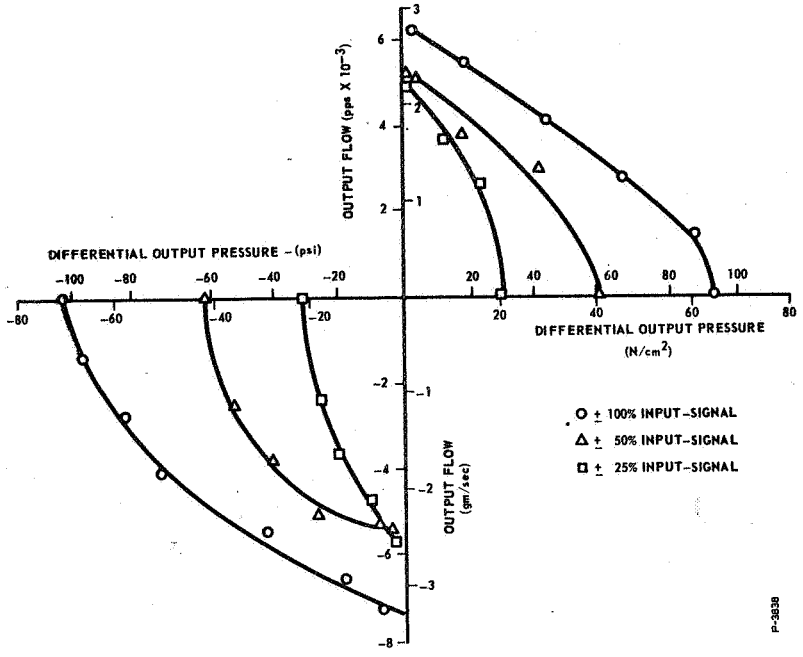

Figure 3-21 - Breadboard Flueric Servovalve Output Flow Versus Differential Pressure

3.4 POWER STAGE VORTEX PRESSURE AMPLIFIER STABILITY TESTS

Prior to the servovalve evaluation test described in Section 3.3, in a test of a power stage vortex pressure amplifier, an oscillation was found in the output pressure with blocked output pressure ranging from 52 to 72 N/cm^2 (75 to 110 psia). In the servovalve evaluation test, it was found that this power stage oscillatory characteristic caused low-frequency, high-amplitude, unsteady variation of the differential output pressure under closed load throttle conditions. After the evaluation test was completed, further tests were performed on one of the power stage vortex pressure amplifiers in order to determine the source of the oscillation. It was suspected that the oscillation might be due to a negative-resistance region in the pressure-flow characteristics of the receiver. The test results showed that this was indeed, the source of the oscillation.

Developmental tests were conducted with the objective of improving the stability of the power stage vortex pressure amplifiers used in the original servovalve circuit. Changes were made in the probe receiver entrance and vortex chamber exit orifice in an effort to eliminate the negative resistance region. A receiver configuration was found in which the negative resistance was eliminated in a single-exit amplifier. However, negative resistance was still found to be present in the dual-exit pressure amplifier.

Since the vortex amplifiers operate in push-pull, flow is positive in one amplifier (outward through the receiver toward the load) while reverse flow occurs at the other amplifier (inward through the receiver). Thus, flow in both the positive and reverse directions is of interest. The primary cause of the power stage instability was found to be a negative resistance region in the pressure-flow characteristics of the receiver. Therefore, the changes in geometry of the receiver and vortex chamber exit were evaluated by plotting the receiver output flow versus the output pressure. In most of the tests, only the reverse flow direction was plotted because it was found in earlier tests that the negative resistance region was located primarily in the reverse output flow quadrant, although the negative resistance region did cross over the zero flow axis into the positive output flow direction.

Data were taken at several constant control pressure levels in order to obtain a family of curves. A schematic of the power stage vortex pressure amplifier is shown in Figure 3-22. The vortex pressure amplifier used for the servovalve power stage is a dual-exit type with an exit orifice and receiver on each side of the vortex chamber. For most of the tests, the exit orifice and receiver were blocked off on one side of the vortex chamber.

The receiver pressure-flow characteristics of one side of the vortex pressure amplifier before any changes were made are shown in Figure 3-23. Negative resistance is seen in the P_c = 122.8 N/cm^2 and P_c = 123.1 N/cm^2 curves.

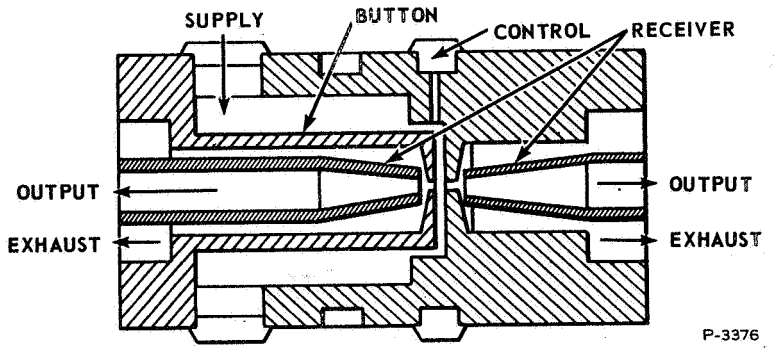

Figure 3-22 - Dual-Exit Vortex Pressure Amplifier

Several changes were made to the receiver face in an effort to eliminate the negative resistance. Figure 3-24 shows the pressure-flow characteristics for a flat-faced type of receiver. The negative resistance has been eliminated in this case but the maximum output pressure is low under the blocked output condition. The maximum blocked output pressure is 8% lower than that originally obtained. Figure 3-25 shows the effect of chamfering the receiver orifice entrance. Here again, no negative resistance is seen,but the maximum recovered pressure is even lower than before. Figure 3-26 shows the pressure-flow characteristics of a receiver with a tapered outside edge and only a very small flat at the tip. The pressure-flow characteristics for this case are about the same as for the flat-faced receiver shown in Figure 3-24.

The geometry around the vortex chamber exit orifice was also changed in an effort to improve the pressure recovery. The area around the exit orifice was undercut as shown in Figure 3-27. A flat-faced receiver was used with the undercut exit orifice. In Figure 3-27, it is seen that the maximum pressure at zero output flow was higher but the minimum pressure was also higher, so that the maximum pressure differential under blocked load condition was about the same. A small amount of negative resistance is evident and it can be seen from the pen trace that the output pressure was oscillatory in the negative resistance regions.

The above tests were performed with a single-exit vortex pressure amplifier. A dual-exit vortex pressure amplifier was tested also to determine whether there is any difference in the pressure-flow characteristics between a dual-exit and single-exit vortex pressure amplifier with the same receiver geometries. The pressure-flow characteristics of a dual-exit amplifier are shown in Figure 3-28. The configuration tested had flat-faced receivers identical to the configuration for which the test results were shown in Figure 3-24. The figure shows that the negative resistance is present, although there was no negative resistance in the single-exit configuration. The negative resistance is not as pronounced as that found in the original vortex pressure amplifier configuration but is enough to cause oscillation of the output pressure.

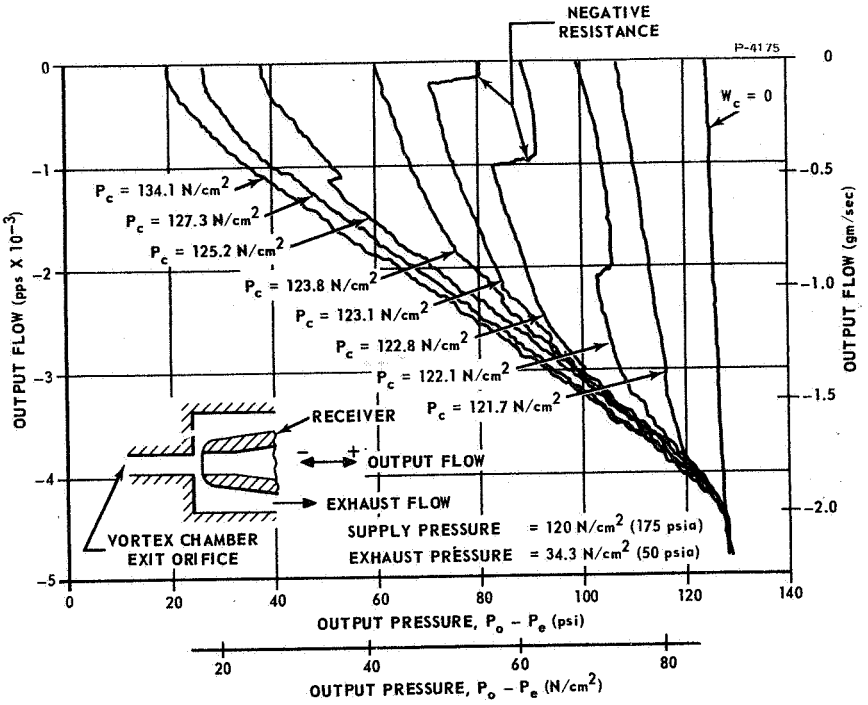

Figure 3-23 - Receiver Pressure-Flow Characteristics of Vortex Pressure Amplifier (Original Configuration)

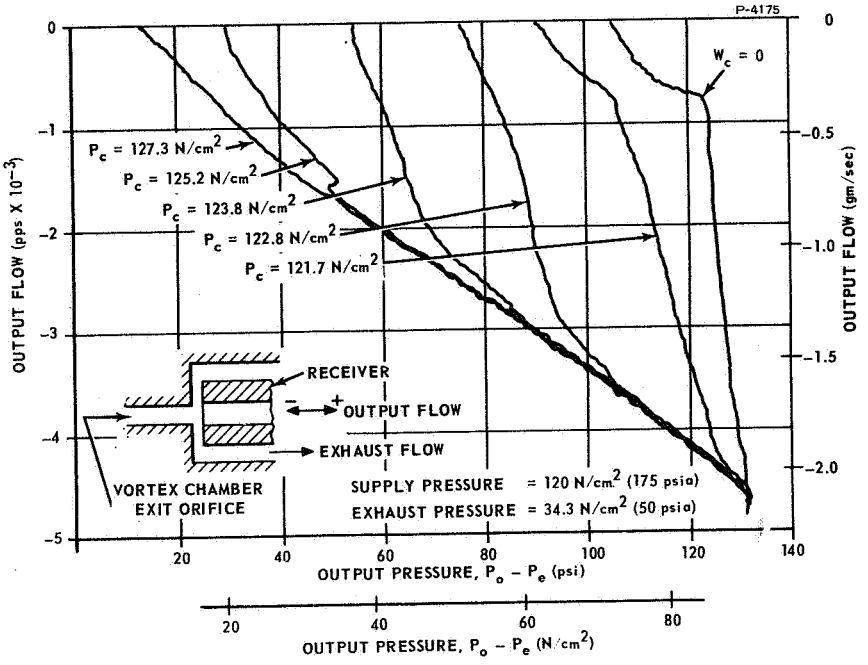

Figure 3-24 - Receiver Pressure-Flow Characteristics of Vortex Pressure Amplifier (Flat-Faced Receiver Configuration)

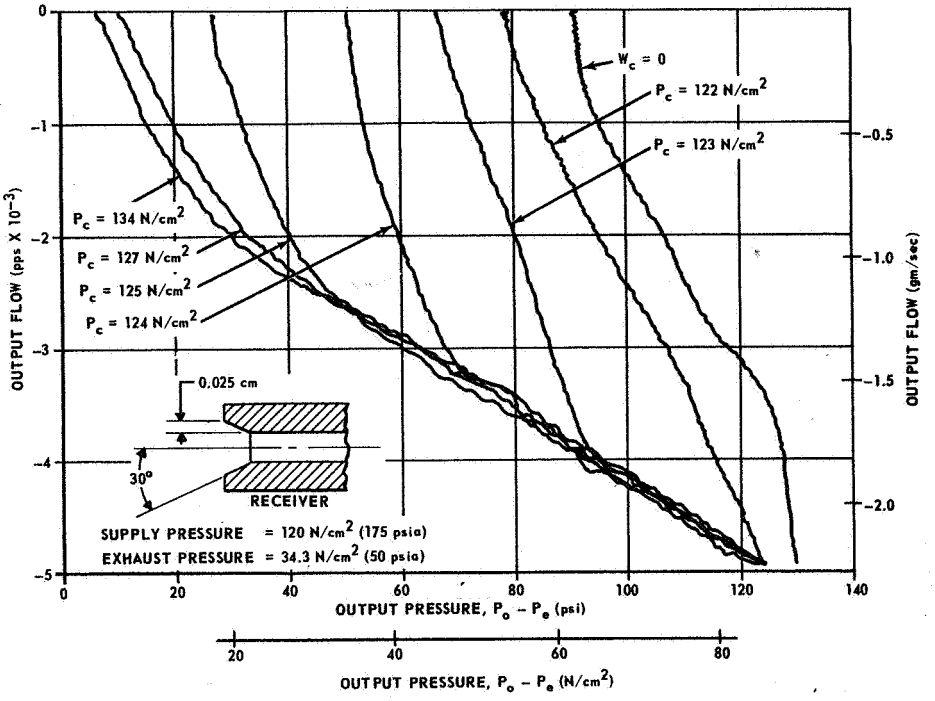

Figure 3-25 - Receiver Pressure-Flow Characteristics of Vortex Pressure Amplifier (Chamfered Receiver)

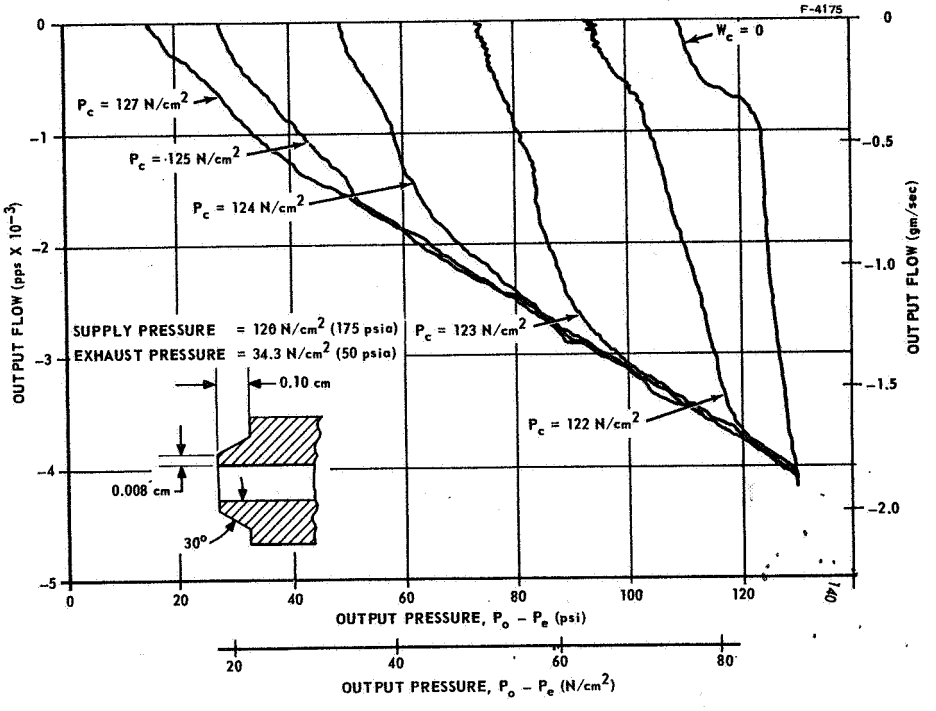

Figure 3-26 - Receiver Pressure-Flow Characteristics of Vortex Pressure Amplifier (Tapered Outer Edge)

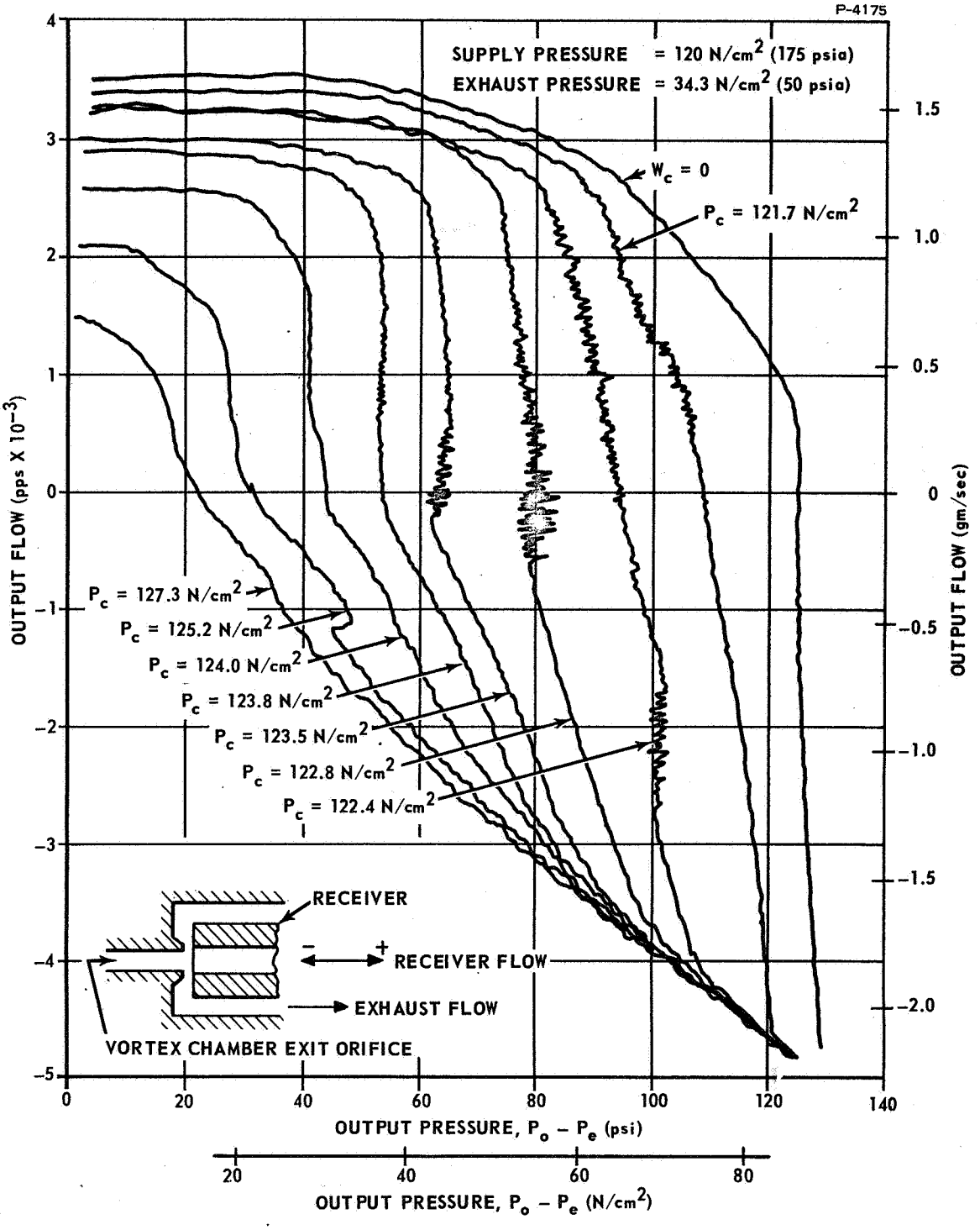

Figure 3-27 - Receiver Pressure-Flow Characteristics of Vortex Pressure Amplifier (Flat-Faced Receiver and Undercut Chamber Exit)

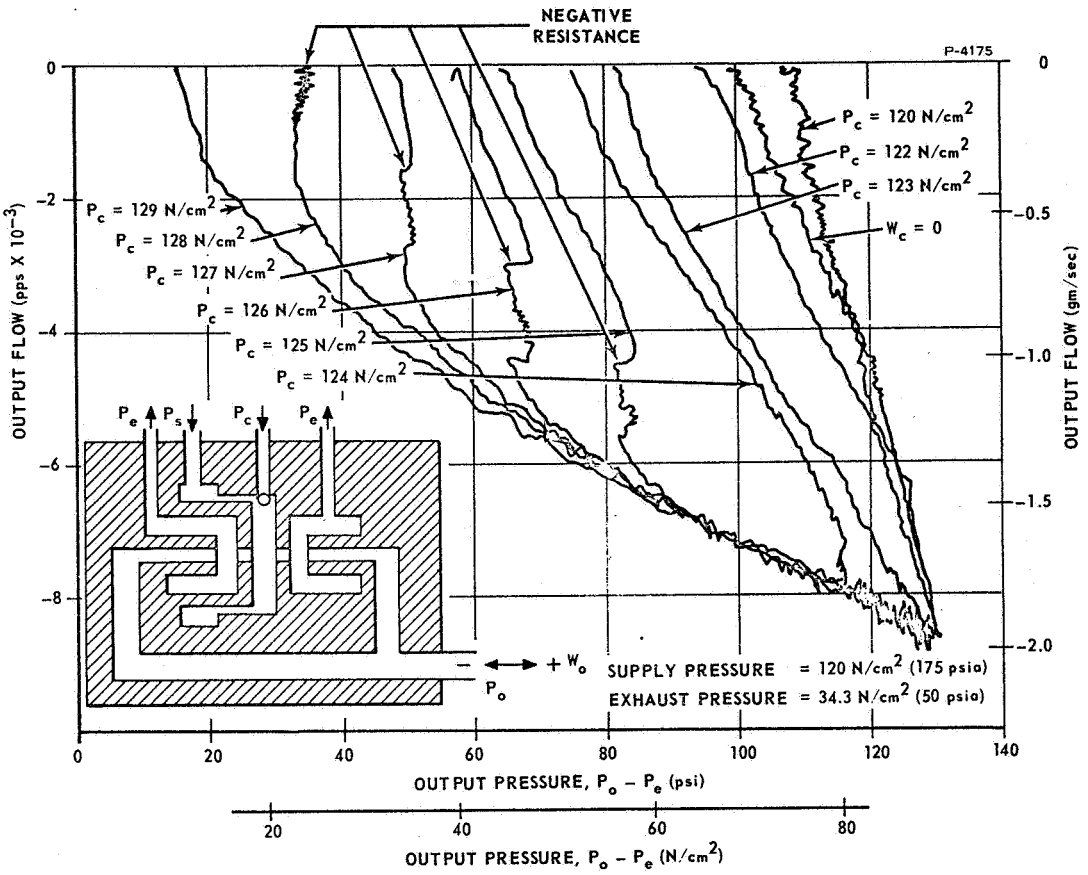

Figure 3-28 - Output Pressure-Flow Characteristics of Vortex Pressure Amplifier (Dual-Exit)

Since the tests of the vortex pressure amplifier improved but did not eliminate the instability, it was decided to pursue the alternate servovalve design incorporating a vortex valve bridge power stage. Tests on this circuit are described in Section 4.

SECTION 4

DEVELOPMENT OF VORTEX VALVE BRIDGE SERVOVALVE

The breadboard circuit of the vortex valve bridge servovalve has several significant changes from the vortex pressure amplifier servovalve. The power stage is made up of four vortex valves arranged in a bridge circuit rather than two vortex pressure amplifiers. An ejector and a jet-on-jet proportional amplifier were added to the pilot stage to improve the flow recovery. This addition also increased the power stage gain, and thus the regenerative-feedback vortex pressure amplifiers could be removed from the pilot stage.

A preliminary breadboard of the vortex valve bridge power stage was tested and showed stable, quiet output pressure characteristics. However, when the circuit was optimized to obtain good pressure and flow recovery, a stability problem recurred. The stability problem was again associated with negative resistance regions in the output pressure-flow characteristics. The power stage was stabilized at the sacrifice of some pressure and flow recovery.

The jet-on-jet proportional amplifier and ejector were tested separately and were found to have adequate performance without further development. The Venjet amplifiers and vortex summing valve which were used on the vortex pressure amplifier servovalve were used on this breadboard servovalve also.

Tests of the power stage, with the jet-on-jet proportional amplifier and ejector only, as the pilot stage, indicated that this portion of the circuit was reasonably stable and was functioning properly. However, addition of the Venjet amplifier resulted in excessive instability and further development tests were conducted on the Venjet amplifiers to decrease their noise level. Finally, an evaluation test was performed on the complete servovalve.

4.1 DESCRIPTION OF CIRCUIT

The servovalve circuit is made up of a power stage and pilot stage as shown schematically in Figure 4-1.

The power stage includes four vortex valves, as shown schematically in Figure 4-2. The control pressure to the power stage acts in a push-pull manner. Each supply vortex valve has two exit orifices located on opposite sides of the vortex chamber. The exit orifices are not equal in diameter, as shown in Figure 4-3. The larger exit orifice is connected to one side of the load and to the supply port of an exhaust vortex valve. The supply and exhaust vortex valves operate out of phase so that when the supply vortex valve is open the exhaust vortex valve is closed and

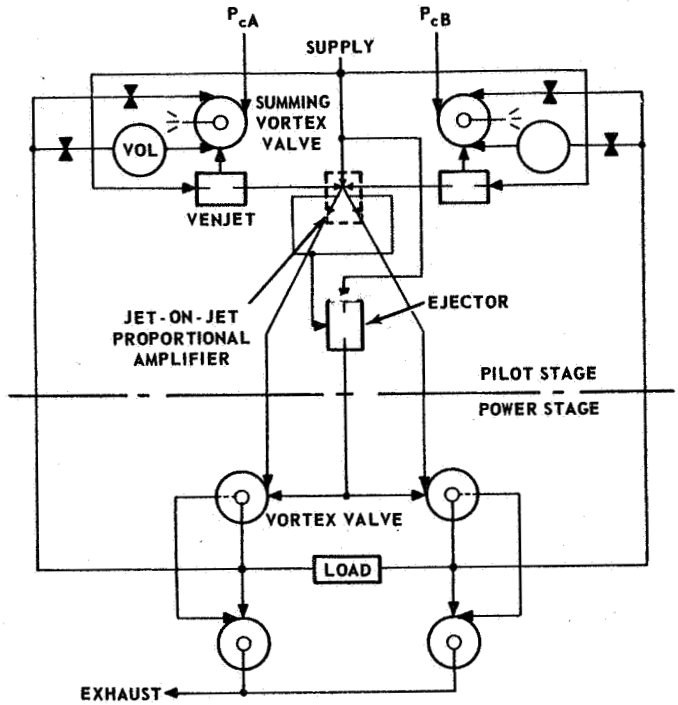

Figure 4-1 - Schematic of Flueric Servovalve With Vortex Valve Bridge Power Stage and With Jet-on-Jet Proportional Amplifier in Pilot Stage

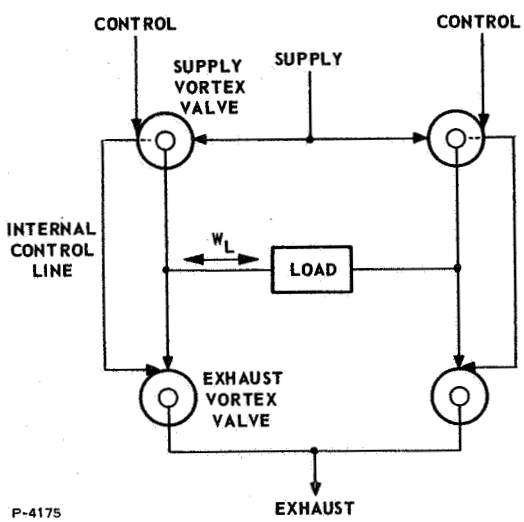

Figure 4-2 - Vortex Valve Bridge Power Stage

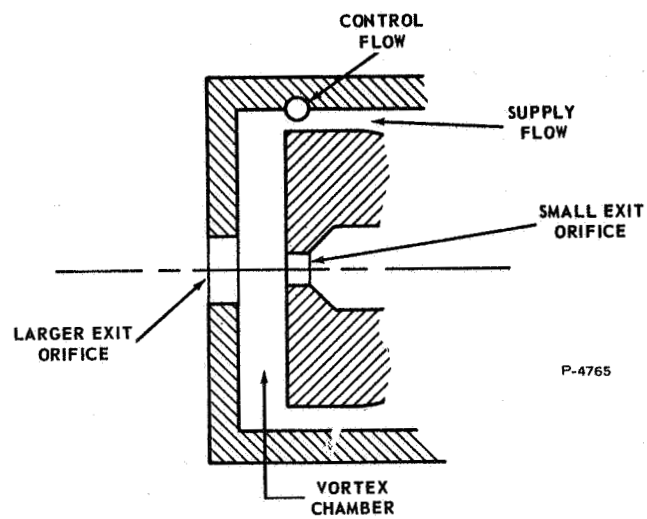

Figure 4-3 - Supply Vortex Valve

vice-versa. When the maximum control flow is applied to the supply vortex valve, the supply flow is shut off and the control flow passes through the larger exit orifice to the supply port of the exhaust vortex valve. There is a radial pressure gradient in the vortex chamber of the supply vortex valve; the pressure is lowest at the center and highest at the outer edge (equal to supply pressure). Therefore the pressure at the smaller exit orifice is slightly lower than the pressure at the larger exit orifice. Thus, the pressure in the internal control line is lower than the load pressure, and the exhaust vortex valve receives no control flow and is in the effective open condition. The combination of closed supply valve and open exhaust valve results in a low load pressure. The opposite case occurs on the opposite side of the load. When the control flow to the supply vortex valve is zero, the supply valve is in the effective open condition. There is a pressure drop across the larger exit orifice because of flow through the orifice to the exhaust vortex valve. Because of this pressure drop, the pressure in the internal control line is higher than the load pressure and control flow is introduced into the exhaust valve, which effectively closes the valve.

The exhaust valve cannot completely shut off the flow because the load pressure would then be equal to the supply pressure (and also to internal control pressure), and control flow could not be introduced into the exhaust valve. The combination of open supply valve and partly closed exhaust valve results in a high load pressure.

The pilot stage includes a jet-on-jet proportional amplifier, an ejector, two Venjet amplifiers, and two summing vortex valves.

The jet-on-jet proportional amplifier provides the differential control flow to the power stage supply vortex valves. The maximum pressure recovery of the jet-on-jet proportional amplifier is no more than 60% of the difference between the supply pressure and the amplifier vent pressure. Therefore, the vents of the jet-on-jet proportional amplifier must be back pressured in order to obtain a high enough output pressure level to control the power stage supply vortex valves. The backpressure level required is about the same as the power stage supply pressure.

Therefore, the vents of the jet-on-jet proportional amplifier are connected to the supply line of the power stage. This results in an increase in the servovalve flow recovery.

The addition of the jet-on-jet proportional amplifier resulted in the need for the addition of the ejector to the pilot stage also. Because there is a slight pressure drop from the power stage supply line to the vortex valves, the minimum power stage control pressure must be set slightly below its supply pressure in order to achieve a zero control flow condition. The output pressure of the jet-on-jet proportional amplifier cannot go below its vent pressure; therefore, the vent pressure of the jet-on-jet proportional amplifier is set slightly lower than the power stage supply and the ejector is used to entrain the exhaust flow and increase its pressure by 1.4 to 2.8 N/cm^2 (2 to 4 psi) to the power stage supply pressure level.

Two summing vortex valves are used to introduce the servovalve input signals. The input signal has a pressure bias of 44.8 N/cm^2 (65 psia). Each summing vortex valve also includes two opposing control ports which are connected to the servovalve output ports, through a frequency-sensitive pneumatic filter, to achieve dynamic load pressure feedback.

The summing vortex valves are used to control the vent flow of the Venjet amplifiers which supply the control ports of the jet-on-jet proportional amplifier. The output of the Venjet amplifier must be a minimum of 121 N/cm^2 (175 psia), which is the exhaust pressure of the jet-on-jet proportional amplifier.

4.2 COMPONENT DEVELOPMENT AND TEST RESULTS

4.2.1 Jet-on-Jet Proportional Amplifier

The objectives of the jet-on-jet proportional amplifier tests were to determine the pressure and flow recovery. The amplifier was a standard unit Model No. FD 2511-3-1321 built by Corning Glass Works, Bradford, Pennsylvania. The profile of the amplifier is shown in Figure 4-4. The supply nozzle is 0.043 cm by 0.144 cm (0.017 in. by 0.045 in.).

The output pressure and flow characteristics are shown as a function of the differential control pressure in Figure 4-5. The load orifices simulated the control input areas of the power stage. The supply and vent pressures were 141.8 N/cm^2 (215 psia) and 120 N/cm^2 (175 psia), respectively. The maximum flow recovery was 69% at an output pressure level of 126 N/cm^2 (183 psia). The control pressure bias was 122 N/cm^2 (176.5 psia).

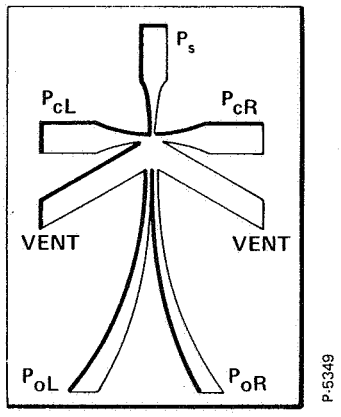

Figure 4-4 - Profile of Jet-on-Jet Proportional Amplifier

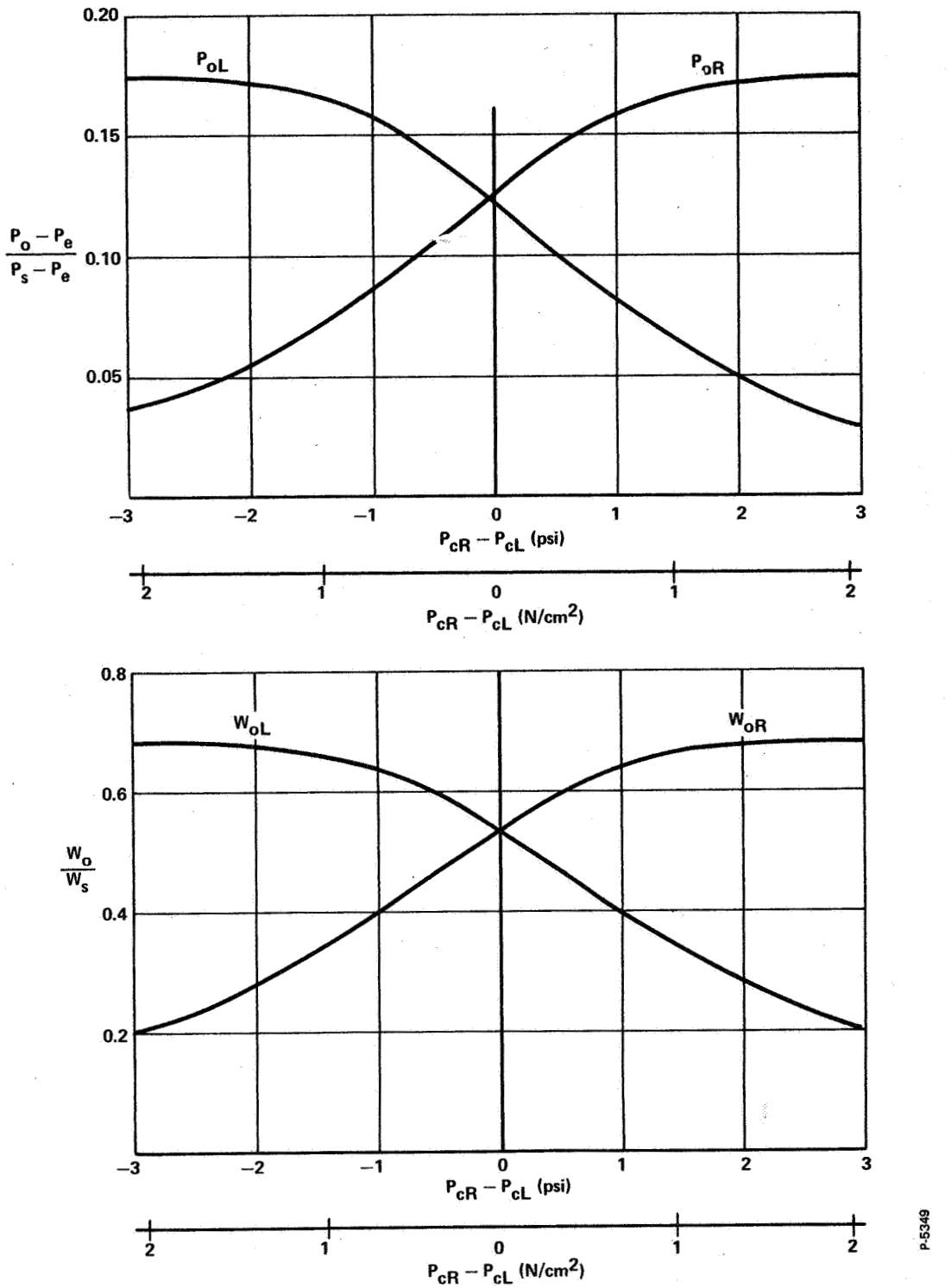

Figure 4-5 - Pressure and Flow Recovery Characteristics of Jet-on-Jet Proportional Amplifier

4.2.2 Preliminary Breadboard Vortex Valve Bridge Power Stage

Before designing a complete power stage, a preliminary breadboard circuit, consisting of two vortex valves representing one side or one-half of the power stage, was tested. The circuit was assembled from existing valves. The orifice sizes, though not optimally matched, were thought to be close enough to determine feasibility of the circuit. Figure 4-6 shows a schematic of the circuit along with the control orifice and exit orifice diameters.

The supply pressure to the test circuit was set at 79.2 N/cm^2 (115 psia) and the exhaust pressure was one atmosphere. Output flow and output pressure data were taken at several control pressure levels in order to obtain a family of curves at constant control pressure levels. The test data, shown in Figure 4-7 indicate that there is no negative resistance in the load pressure-flow characteristics. The pressure difference between the maximum and minimum output pressure at zero output flow is 45 N/cm^2(66 psi), which is equivalent to 66% pressure recovery. No noisy or unstable areas were found.

The output pressure noise was measured by photographing the oscilloscope trace of the output pressure versus time. The data was taken with zero output flow and with a load volume of 82 cm^3 (5 in^3). The data are shown in Figure 4-8. The data taken indicate that the maximum noise is about 0.07 N/cm^2 (0.1 psi) peak-to-peak.

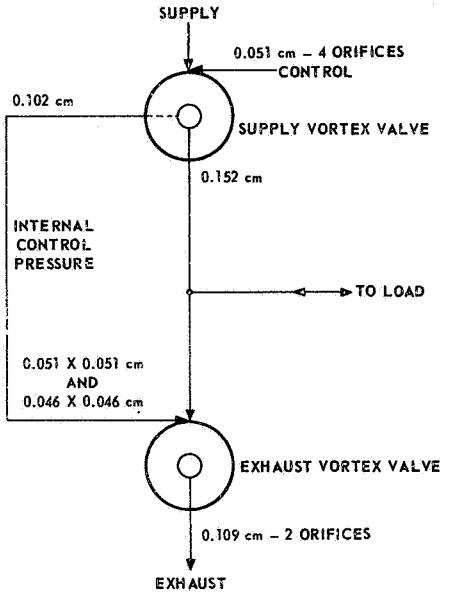

Figure 4-6 - Schematic of Preliminary Breadboard Vortex Valve Bridge Power Stage (One Side) Showing Orifice Diameters

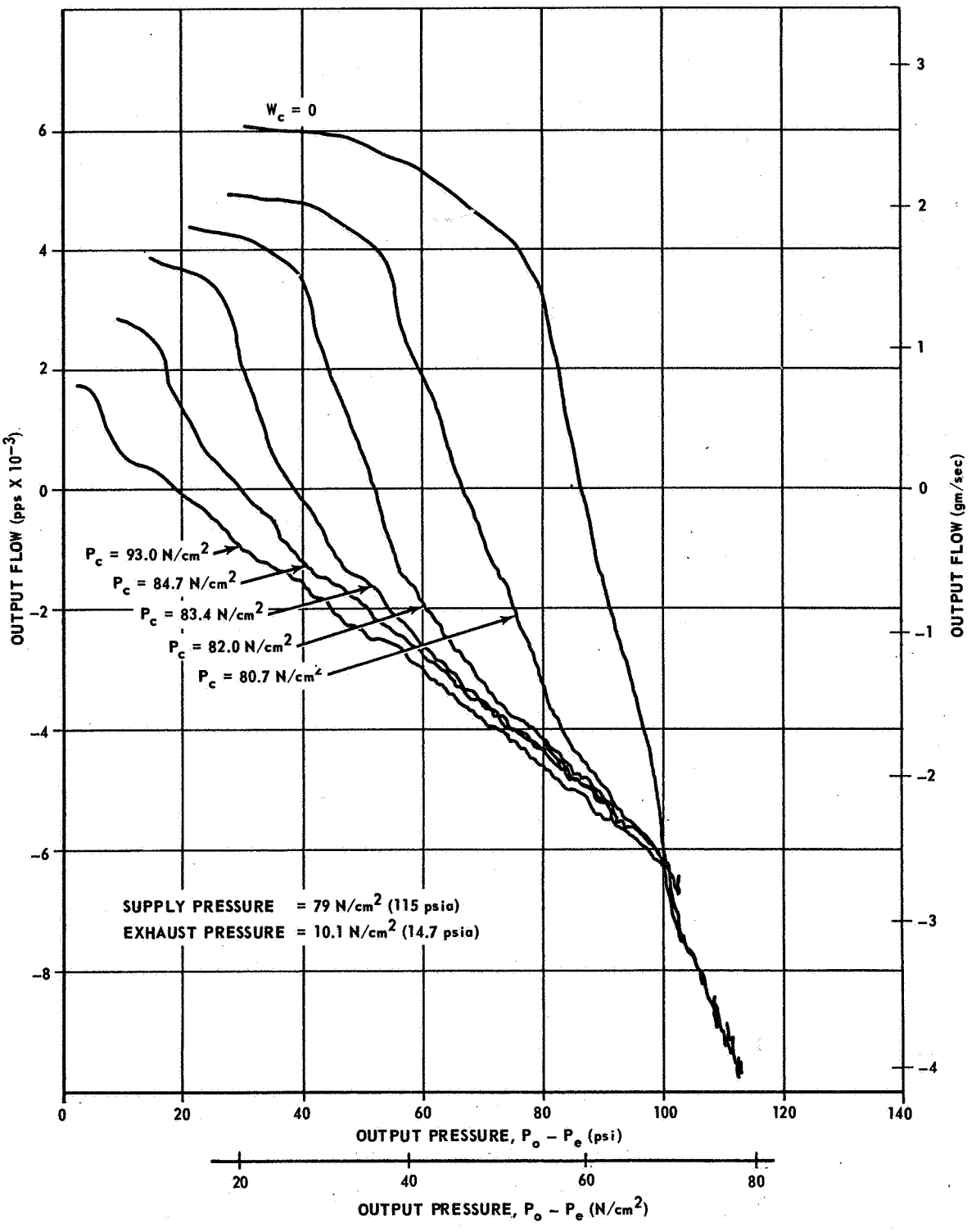

Figure 4-7 - Output Pressure-Flow Characteristics of Vortex Valve Circuit

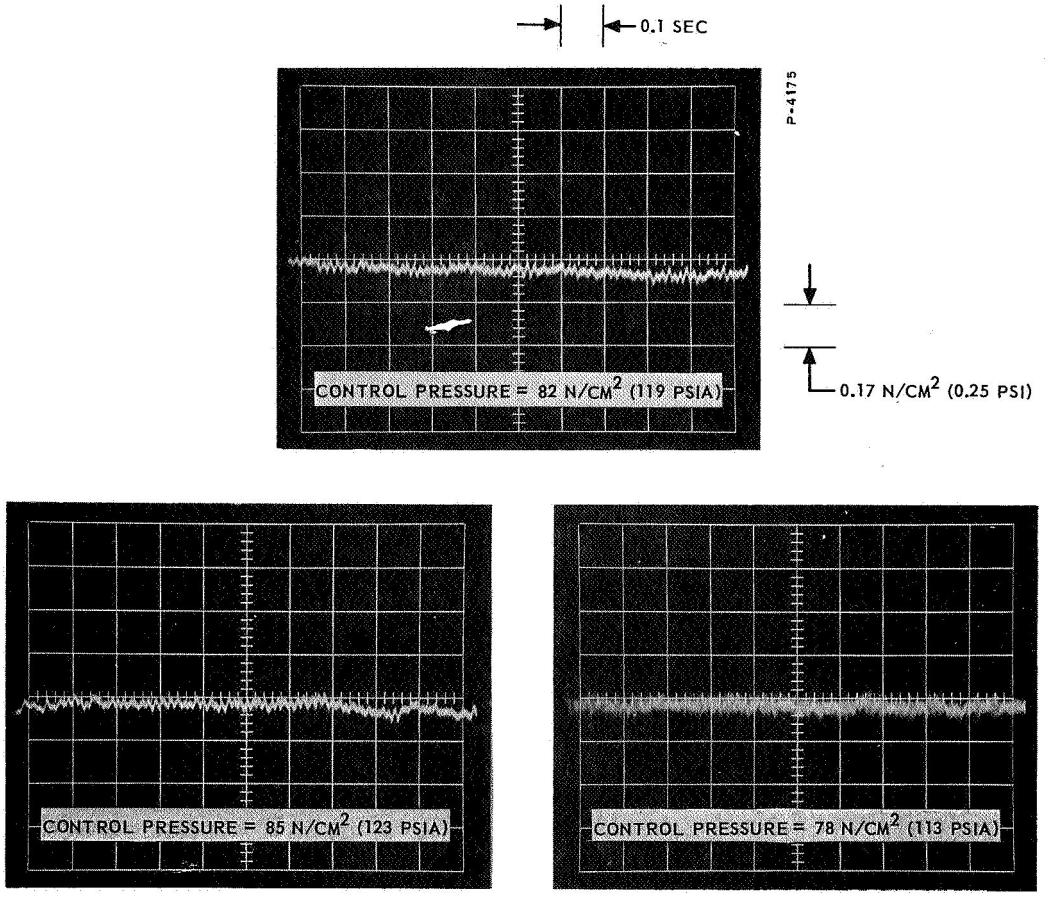

Figure 4-8 - Vortex Valve Circuit Noise

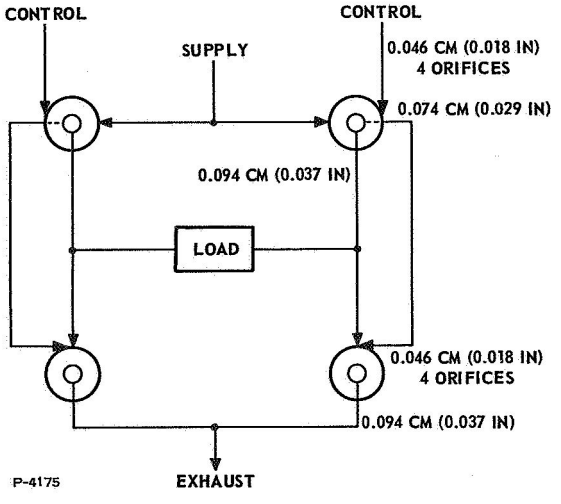

Figure 4-9 - Schematic of Breadboard Vortex Valve Bridge Power Stage Showing Orifice Diameters

It was concluded from this test that the vortex bridge type of power stage appears feasible and has stable, quiet output pressure characteristics. The pressure recovery of this circuit was low, only 66%, but it was thought that this could be improved by optimizing the orifice sizes.

4.2.3 Final Vortex Valve Bridge

A new vortex valve bridge circuit was designed and fabricated with the design intended to provide better pressure and flow recovery than was obtained from the preliminary breadboard bridge circuit. A schematic of the circuit is shown in Figure 4-9 along with the sizes of the control orifices and chamber exit orifices.

Preliminary evaluation tests were performed to determine the stability, pressure recovery, and flow recovery of the vortex valve bridge power stage. The pressure recovery was about the same as that obtained with the vortex pressure amplifier power stage. However, the flow recovery was considerably lower because the vortex bridge circuit required about twice as much control flow for the same no-load output flow. The new power stage was not as stable as the preliminary breadboard vortex pressure amplifier power stage.

Development tests were conducted with the objective of improving the stability of the vortex valve bridge power stage. These tests revealed that the output pressure oscillation of the power stage was caused by a negative resistance region in the output pressure-flow characteristics. The oscillation was eliminated by changing some of the control and exit orifice areas of the vortex valves which make up the power stage. Stability, linearity, and output pressure-flow characteristic tests were then performed on the breadboard vortex valve bridge power stage combined with a jet-on-jet proportional amplifier pilot stage.

(1) Preliminary Evaluation Tests

Tests were performed on the complete vortex bridge power stage. The power stage was controlled by a pilot stage consisting of a jet-on-jet proportional amplifier and an ejector. The supply pressure to the pilot stage was 148 N/cm^2(215 psia), and the exhaust pressure of the power stage was 34.5 N/cm^2(50 psia).

The performance of the amplifier and ejector were satisfactory. The output flow versus output pressure characteristics are shown in Figure 4-10. The data indicate that the maximum load flow is 1.41 gm/sec (0.0031 lb/sec) and the maximum differential output pressure is 69.7 N/cm^2 (101 psi). Negative resistance areas and unsteady output pressures are evident in the reverse pressure and flow quadrant. The output pressure noise was measured and a 9 hertz, 6.9 N/cm^2 (10 psi) peak-to-peak oscillation was found at about zero differential pressure.

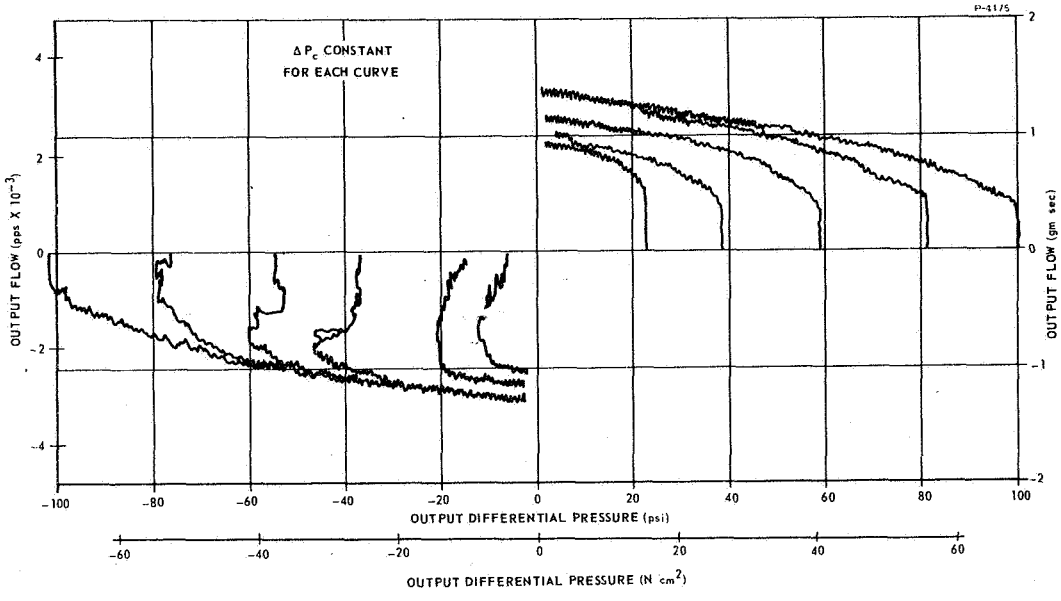

Figure 4-10 - Output Pressure-Flow Characteristics of Vortex Valve Bridge Power Stage

(2) Development Tests to Improve Stability

Various changes were made in the power stage in order to eliminate the oscillation of the output pressure. Most of the tests were performed on only one side of the power stage. The changes were evaluated by measuring the output pressure as a function of time or by plotting the output pressure versus output flow. The output pressure-flow data were taken at several constant control pressure levels in order to obtain a family of curves.

The first modification that was made to improve the stability of the vortex valve bridge power stage was to change the exhaust vortex valves from dual-exit to single-exit type. This has the effect of decreasing the flow gain of the exhaust vortex valve. Although the oscillation was not eliminated, the amplitude was decreased, and the output pressure range over which the oscillation occurred also was decreased.

The output pressure-flow characteristics of one side of the power stage with single-exit exhaust valves were then measured to determine whether the oscillation was caused by negative resistance. The data are shown in Figure 4-11. The figure shows that negative resistance is present at a control pressure level of 122 N/cm^2 (177 psia), which accounts for the output pressure oscillation. The figure also shows that the maximum output differential pressure is 68 N/cm^2 (99 psi) at zero output flow.

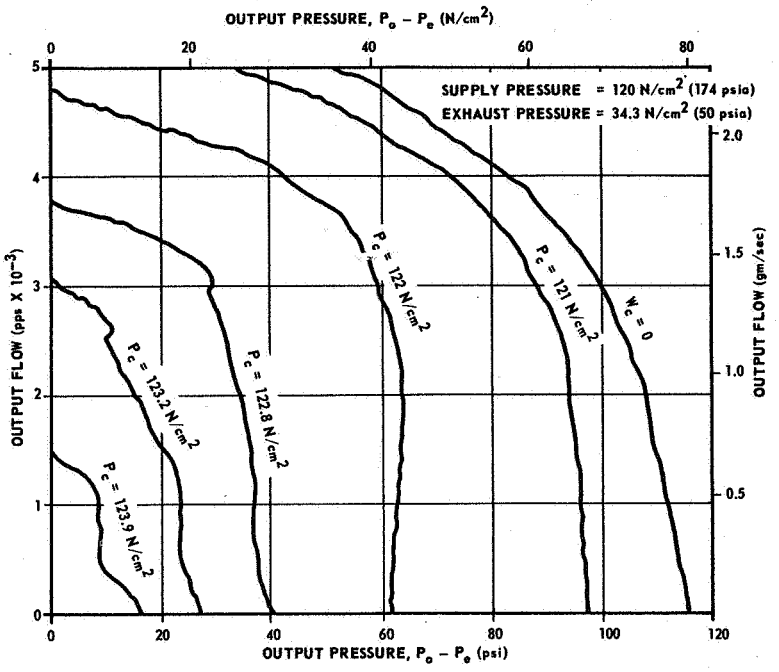

Figure 4-11 - Output Pressure-Flow Characteristics of One Side of Vortex Valve Bridge Power Stage

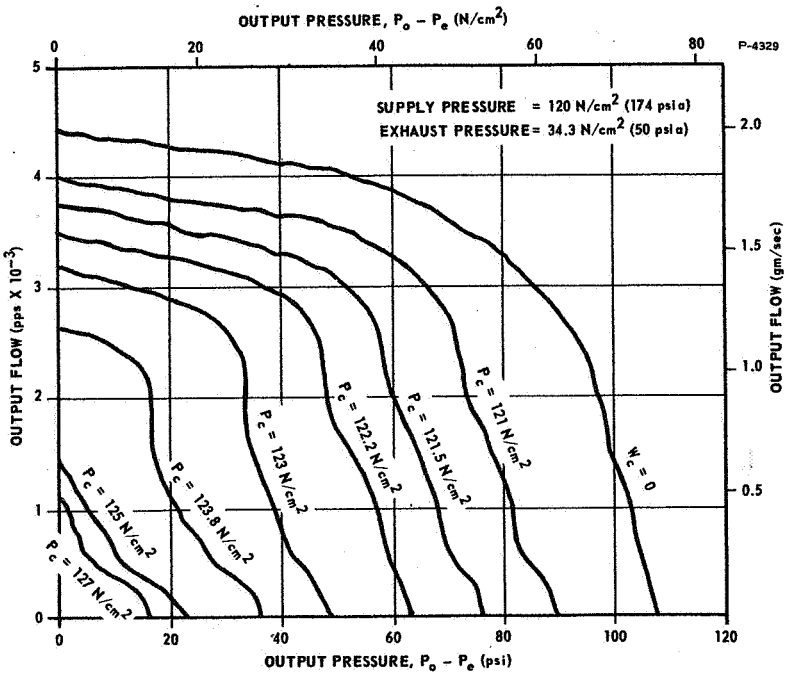

Figure 4-12 - Output Pressure-Flow Characteristics of One Side of Vortex Valve Bridge Power Stage (Final Configuration)

The negative resistance, and hence the output pressure oscillation, was eliminated by decreasing the amount of control flow to the exhaust vortex valve. This was accomplished by decreasing the size of the supply vortex valve. Various combinations of exit orifice and control orifice sizes were tested before the final combination was chosen. Figure 4-12 shows the output pressure-flow characteristics of one side of the modified power stage with a combination of orifice size which resulted in a stable output pressure with the least degradation in maximum differential output pressure. The figure shows that the negative resistance has been eliminated. The maximum differential output pressure is 62.7 N/cm^2 (91 psi). The final combination of orifice sizes is shown in Figure 4-13.

The complete modified power stage was then tested together with a jet-on-jet proportional amplifier and an ejector. The tests included stability, linearity and pressure-flow characteristics. The output pressure stability was tested with closed load throttle and with equal load volumes of 82 cm^3 (5 in^3) on each side of the load throttle. The maximum output pressure ripple was 2 N/cm^2 (2.9 psi) peak-to-peak as compared with the required value of 0.4 N/cm^2 (0.6 psi). A photograph of the output pressure trace is shown in Figure 4-14.

The differential output pressure versus differential input pressure is shown in Figure 4-15. The linearity is good over most of the curve, except that the gain tapers off near the ends. The pressure gain in the center portion of the curve is about 60 to 1. The output flow versus differential output pressure characteristics are shown in Figure 4-16.

4.2.4 Venjet Amplifier

After the vortex valve bridge power stage combined with the jet-on-jet proportional amplifier pilot stage had been tested, the Venjet amplifiers and the vortex summing valves were added to the pilot stage and the complete servovalve was tested. It was found that the servovalve output pressure was excessively noisy. In tracing the source of the noise, it was found that the output pressures of the Venjet amplifiers were unstable. Development tests were performed on the Venjet amplifier in which the receiver entrance geometry, the receiver diameter, and the distance between the nozzle and receiver were modified to improve the stability of the output pressure. The effects of the changes were evaluated by measuring the stability and pressure gain. The noise was decreased in amplitude from 2.8 N/cm^2 (4 psi) down to 0.83 N/cm^2 (1.2 psi) peak-to-peak by decreasing the distance between the nozzle and receiver and by reducing the receiver diameter. The other Venjet amplifier was then modified the same as the first one, and tested. It was found that the pressure gain was quite different from that of the first Venjet amplifier. The Venjet amplifiers were redesigned to make it easier to achieve the required dimensional accuracy. New ports were fabricated or old ports were reworked and the redesigned Venjets were tested. The test data indicates that the gain characteristics were adequately matched after the rework.

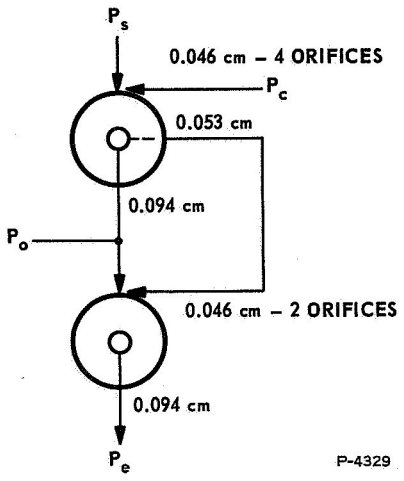

Figure 4-13 - Schematic of One Side of Vortex Valve Bridge Power Stage Showing Orifice Diameters

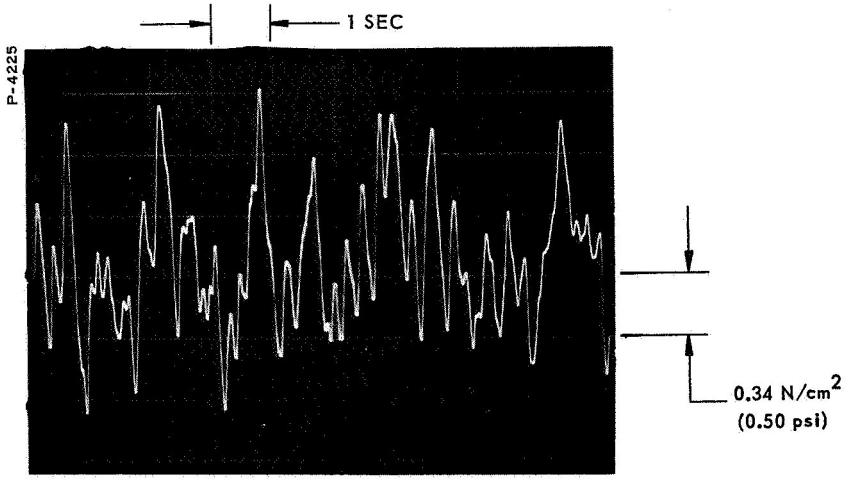

Figure 4-14 - Stability of Vortex Valve Bridge Power Stage With Jet-on-Jet Proportional Amplifier Pilot Stage

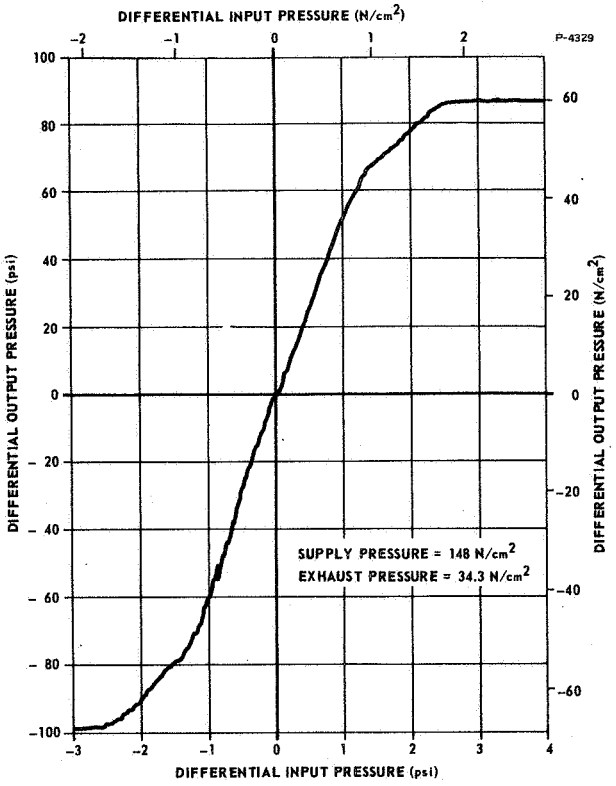

Figure 4-15 - Pressure Gain of Vortex Valve Bridge Power Stage With Jet-on-Jet Proportional Amplifier Pilot Stage

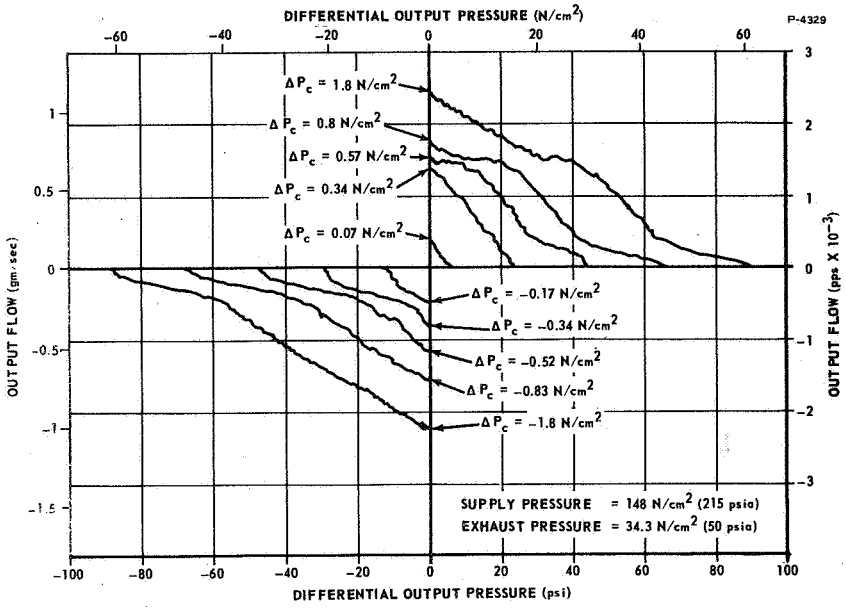

Figure 4-16 - Output Flow Versus Output Pressure of Vortex Valve Bridge Power Stage With Jet-on-Jet Proportional Amplifier Pilot Stage

The output pressure versus Venjet chamber pressure data were taken with a supply pressure of 148 N/cm^2 (215 psia) and with two different load conditions on the output pressure. (The chamber pressure is the pressure in the area around the nozzle and receiver.) The output was either blocked so that there was zero output flow, or it was loaded with a control orifice of the jet-on-jet proportional amplifier. The exhaust pressure of the jet-on-jet proportional amplifier was set at 124 N/cm^2 (180 psia). The stability was measured by photographing the output pressure trace on an oscilloscope.

The gain characteristics of the Venjet amplifier before modification are shown in Figure 4-17, in which the output pressure versus the Venjet chamber pressure is plotted. The output pressure port was loaded with an orifice simulating the area of the jet-on-jet proportional amplifier control orifice. A rough conception of the noise amplitude and the locations of the noise regions can be seen from the variations of the pen trace excursions. A typical photograph of the oscilloscope traces of the output pressure and chamber pressure is shown in Figure 4-18. The data show that the output pressure is oscillatory with varying amplitude. The maximum amplitude is 2.8 N/cm^2 (4 psi) peak-to-peak at a frequency of about 100 hertz.

Several modifications were made to the Venjet amplifier, and the effects of the modification were evaluated. First, the geometry around the receiver entrance was modified. The pressure gain characteristics of the Venjet with a chamfered receiver are shown in Figure 4-19. Data were taken both with blocked output (zero output flow) and with a control orifice of the jet-on-jet proportional amplifier as a load. It was found that the chamfer had little effect.

The effect of using a receiver with a sharp tip is shown in Figure 4-20. The sharp tip has the effect of improving the linearity of the output pressure versus chamber pressure curve, but the noise level is about the same as the original configuration.

The effects of increasing and decreasing the distance between the nozzle and receiver are shown in Figures 4-21 and 4-22, respectively. The amplitude of the noise is slightly smaller at the shorter distance between the nozzle and the receiver. The pressure gain, however, increases as the distance between the nozzle and receiver is increased, at least for the range of distances tested. It is known from other Venjet amplifier tests that, as the distance between the nozzle and receiver is increased still further, a point is reached where the gain again decreases.

The effect of changing the receiver diameter was also investigated. Figure 4-23 shows the gain characteristics of the Venjet with 29% larger receiver orifice diameter. This configuration shows good pressure gain but poor stability. The effect of decreasing the receiver orifice diameter by 16% is shown in Figure 4-24. The gain is lower in this case, but the stability is increased considerably.

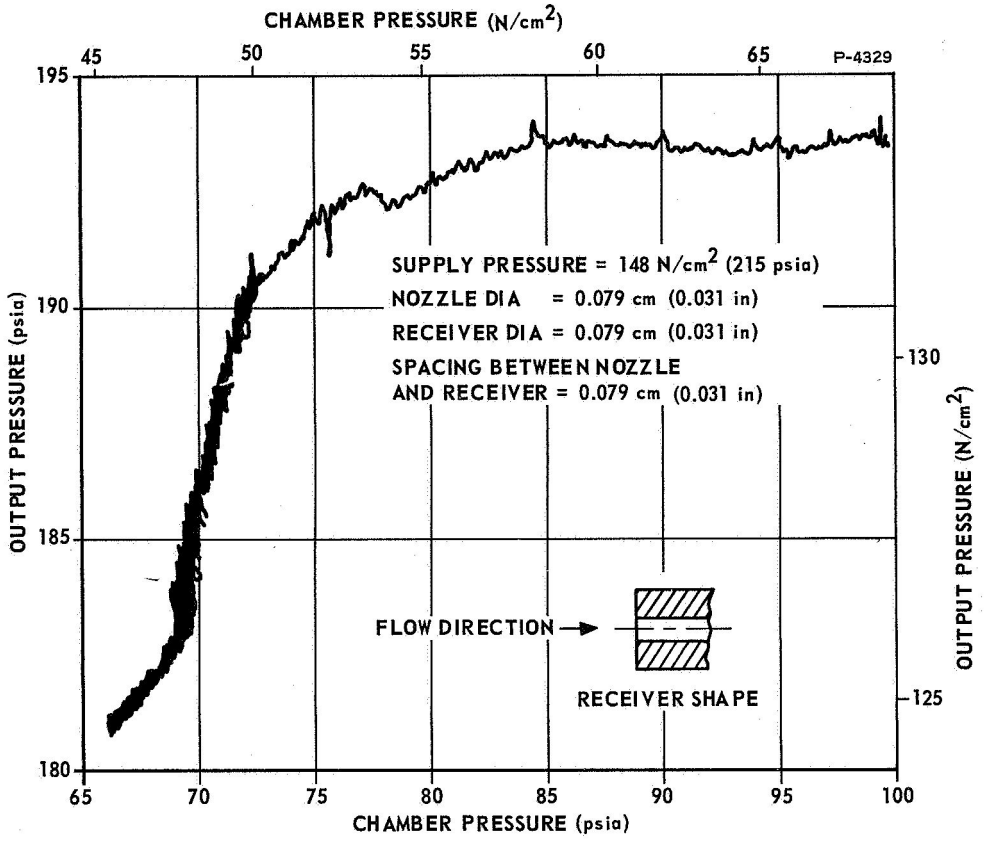

Figure 4-17 - Venjet Amplifier Gain Characteristics (Original Configuration,

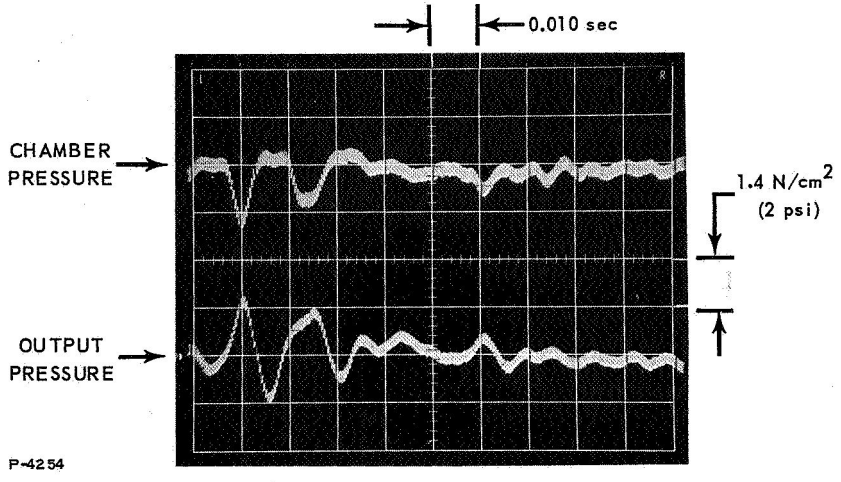

Figure 4-18 - Stability of Venjet Amplifier (Original Configuration)

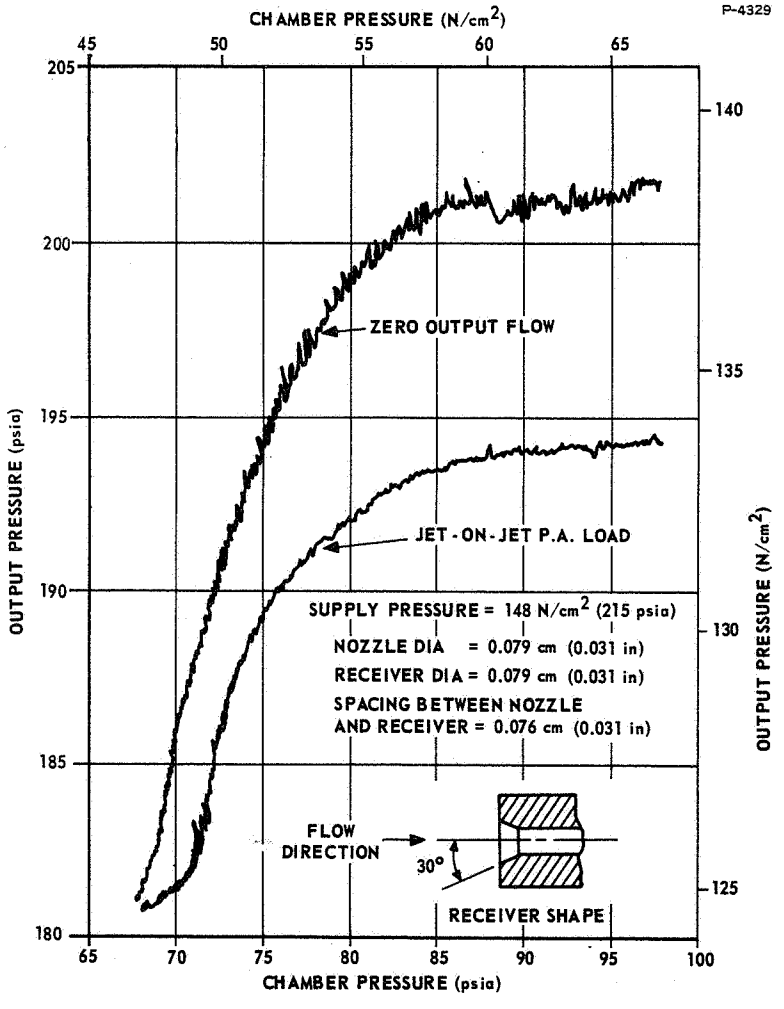

Figure 4-19 - Venjet Amplifier Gain Characteristics With Chamfered Receiver

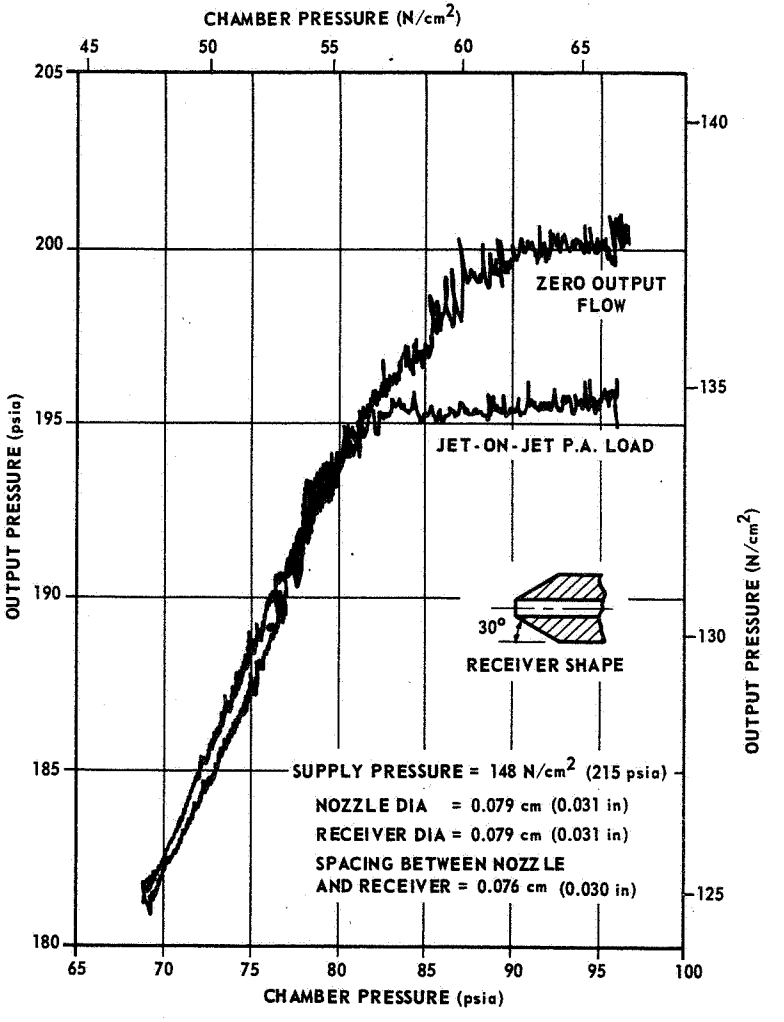

Figure 4-20 - Venjet Amplifier Gain Characteristics With Sharp-Tip Receiver

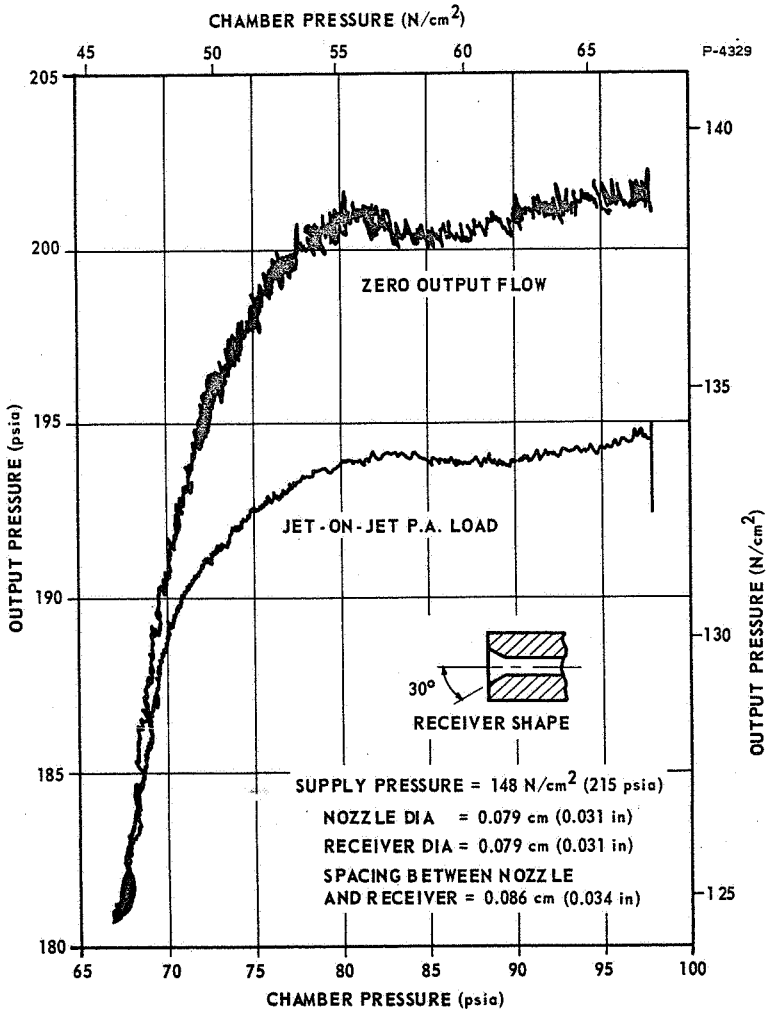

Figure 4-21 - Venjet Amplifier Gain Characteristics With Chamfered Receiver and Increased Spacing Between Nozzle and Receiver

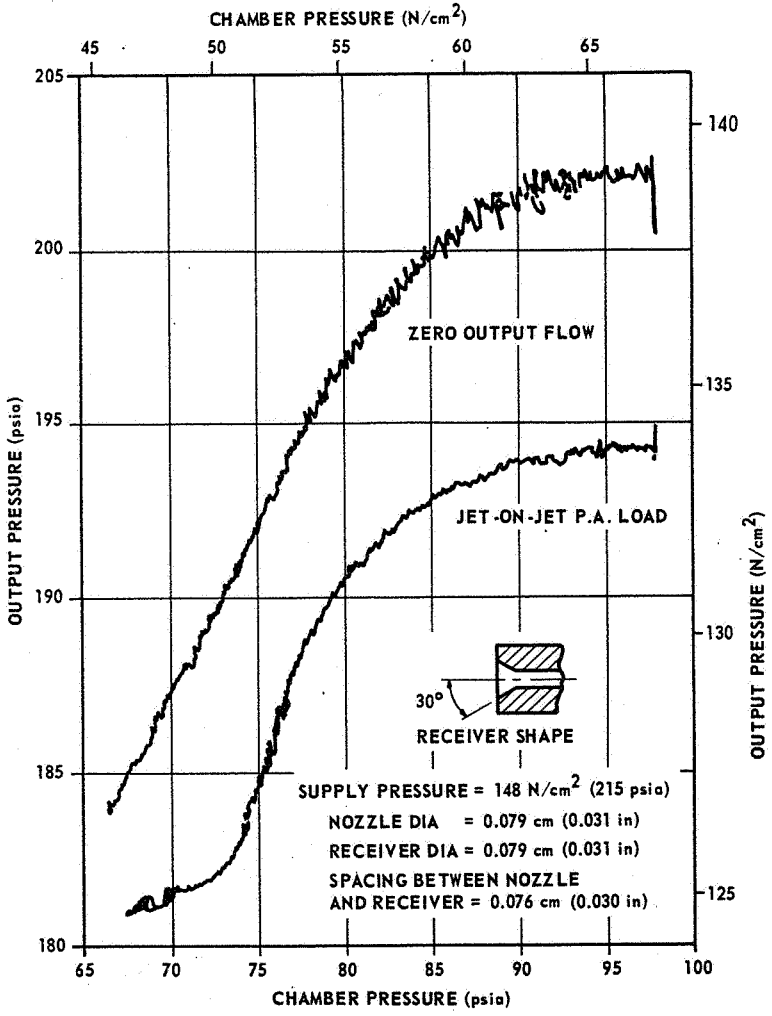

Figure 4-22 - Venjet Amplifier Gain Characteristics With Chamfered Receiver and Decreased Spacing Between Nozzle and Receiver

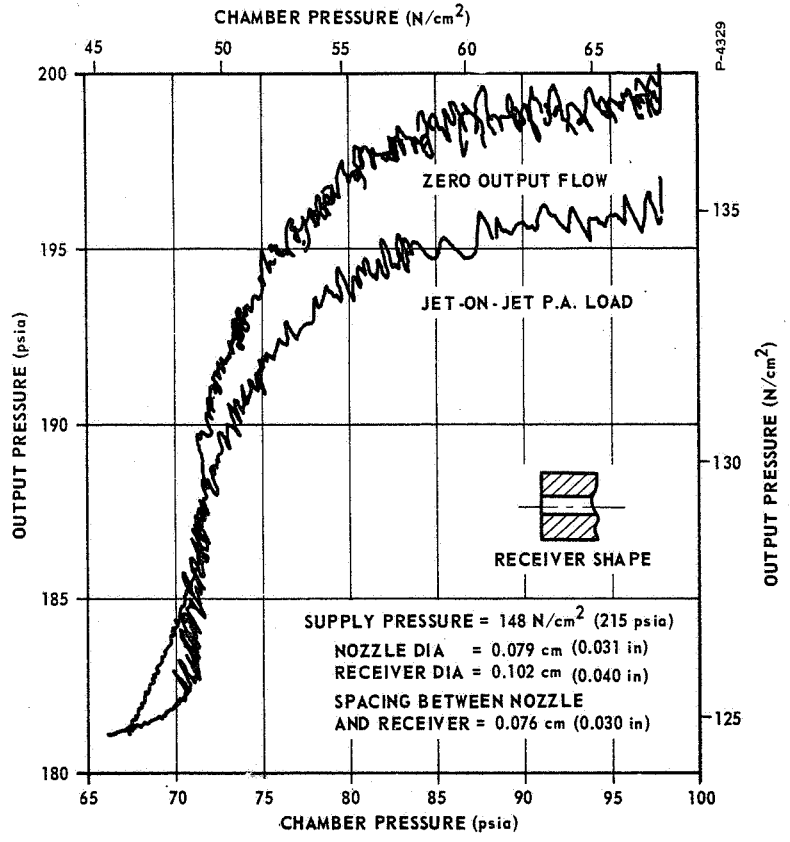

Figure 4-23 - Venjet Amplifier Gain Characteristics With Larger Receiver Orifice Diameter

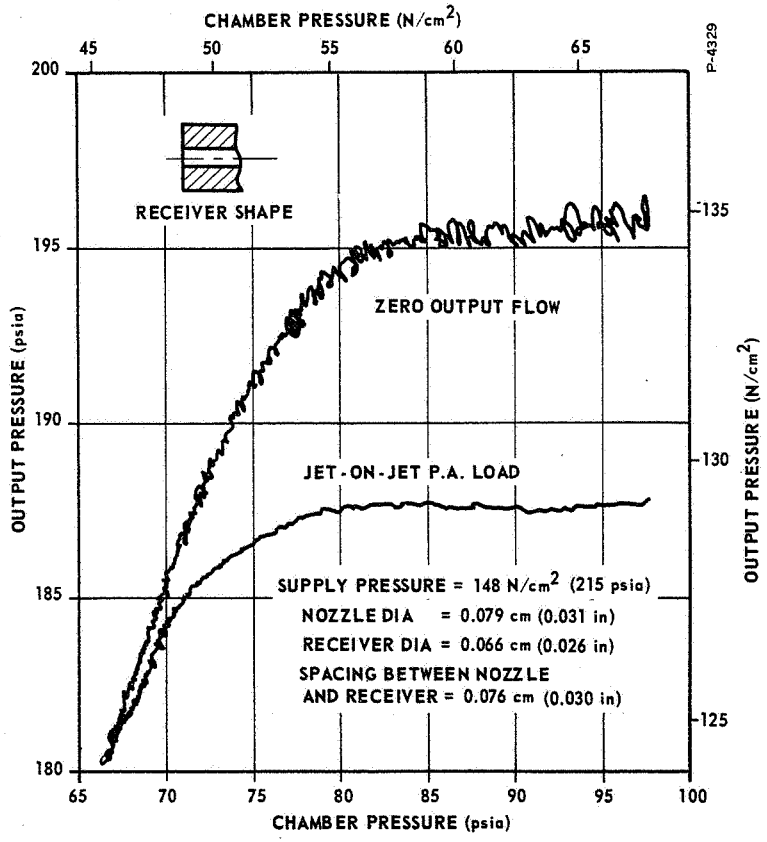

Figure 4-24 - Venjet Amplifier Gain Characteristics With Decreased Receiver Orifice Diameter

The next step was to test the smaller-diameter receiver orifice with a shorter distance between the nozzle and receiver. The results are shown in Figure 4-25. The figure shows that the pressure gain is slightly lower than originally obtained, but the output pressure appears to be stable with the jet-on-jet proportional amplifier load. A photograph of the oscilloscope trace of the output pressure with the jet-on-jet proportional amplifier load is shown in Figure 4-26. The data show that the maximum amplitude is 0.83 N/cm^2 (1.2 psi) peak-to-peak at a frequency of about 110 hertz. This configuration had the best performance of the various configurations tested. The distance between the nozzle and receiver were decreased further but no increase in stability was found and the pressure gain dropped off considerably.

The dimensions of the second Venjet amplifier were modified to match the first Venjet whose performance was shown in Figures 4-24 and 4-25. The gain characteristics of the second Venjet are shown in Figure 4-27. It is seen that there is a discontinuity in the gain curve at a chamber pressure of 41.3 N/cm^2 (60 psia). When the second Venjet amplifier was tested with a different receiver, the discontinuity was eliminated. However, there was still a considerable difference in the gain characteristics between the two Venjets. To match the gain characteristics of the two Venjets, it will be necessary to match the nozzles as well as the receivers. The original design of the Venjet amplifier was such that it was not possible to inspect the nozzle length, nozzle entrance surface finish, or nozzle entrance geometry after the assembly was brazed together. It was also difficult to maintain the required accuracy of the nozzle entrance geometry and the concentricity of the nozzle orifice with the receiver orifice during manufacture. Therefore, the Venjets were redesigned to make it easier to achieve the required dimensional accuracy of the Venjet parts. The redesigned Venjet amplifiers were fabricated and tested. The test data indicate that the gain characteristics are fairly well matched as shown in Figures 4-28 and 4-29.

4.3 BREADBOARD SERVOVALVE EVALUATION TEST

The objectives of the evaluation test were to determine how well the servovalve would perform and how its performance would compare with the vortex pressure amplifier type power stage and with the specified performance.

The pressure recovery, flow recovery, input power, linearity, stability, frequency response, and transient response were measured using both nitrogen and hydrogen as the gaseous medium.

The vortex bridge-type servovalve had better linearity and stability than the vortex pressure amplifier type servovalve but the flow recovery and power gain were not so high. The major deficiencies in performance as compared to the specified performance were in stability and power recovery.

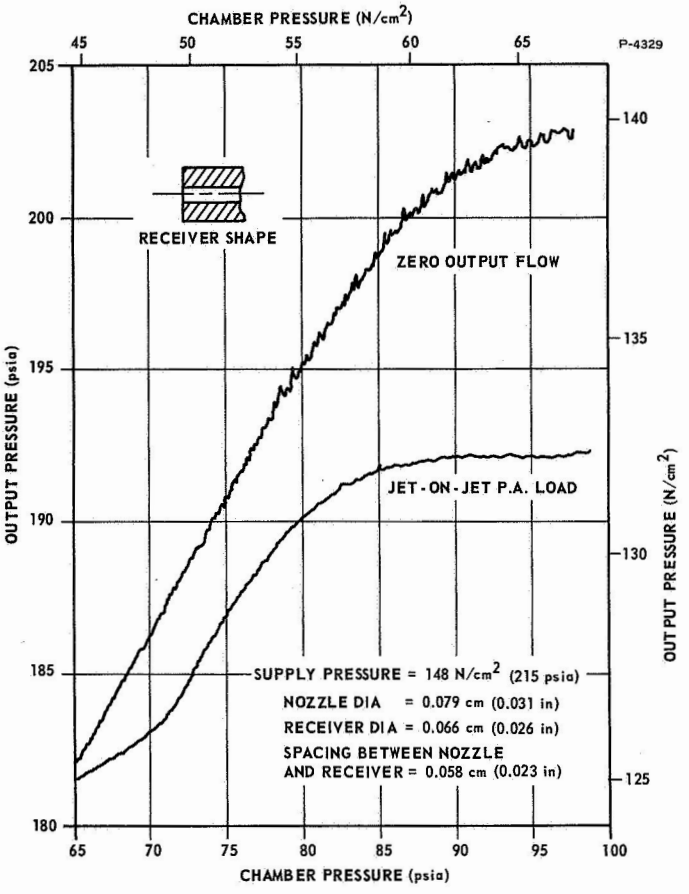

Figure 4-25 - Venjet Amplifier Gain Characteristics With Decreased Receiver Diameter and Decreased Spacing Between Nozzle and Receiver

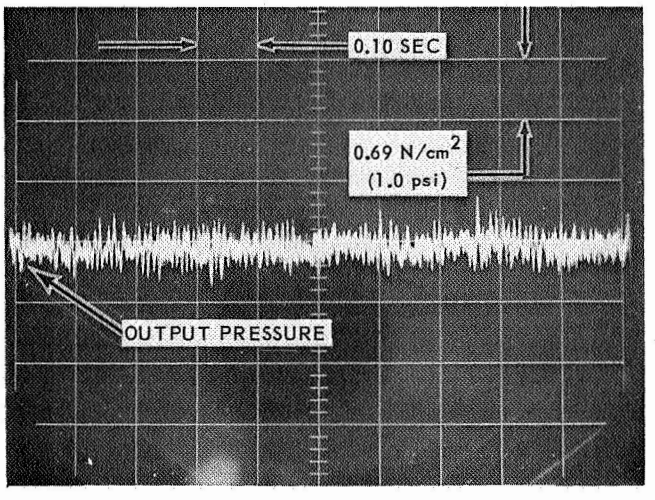

Figure 4-26 - Venjet Amplifier Stability With Decreased Receiver Diameter and Decreased Spacing Between Nozzle and Receiver

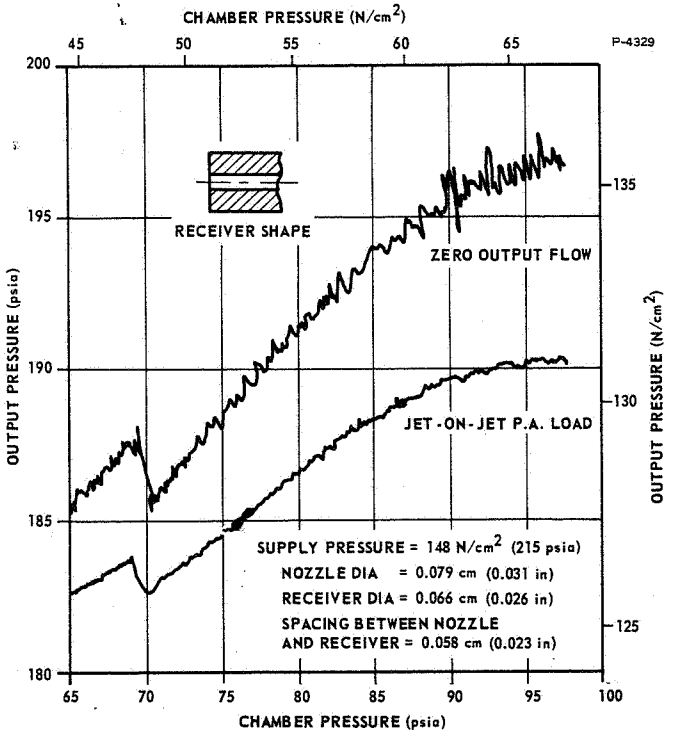

Figure 4-27 - Venjet Amplifier Gain Characteristics With Decreased Receiver Diameter and Decreased Spacing Between Nozzle and Receiver (Second Venjet)

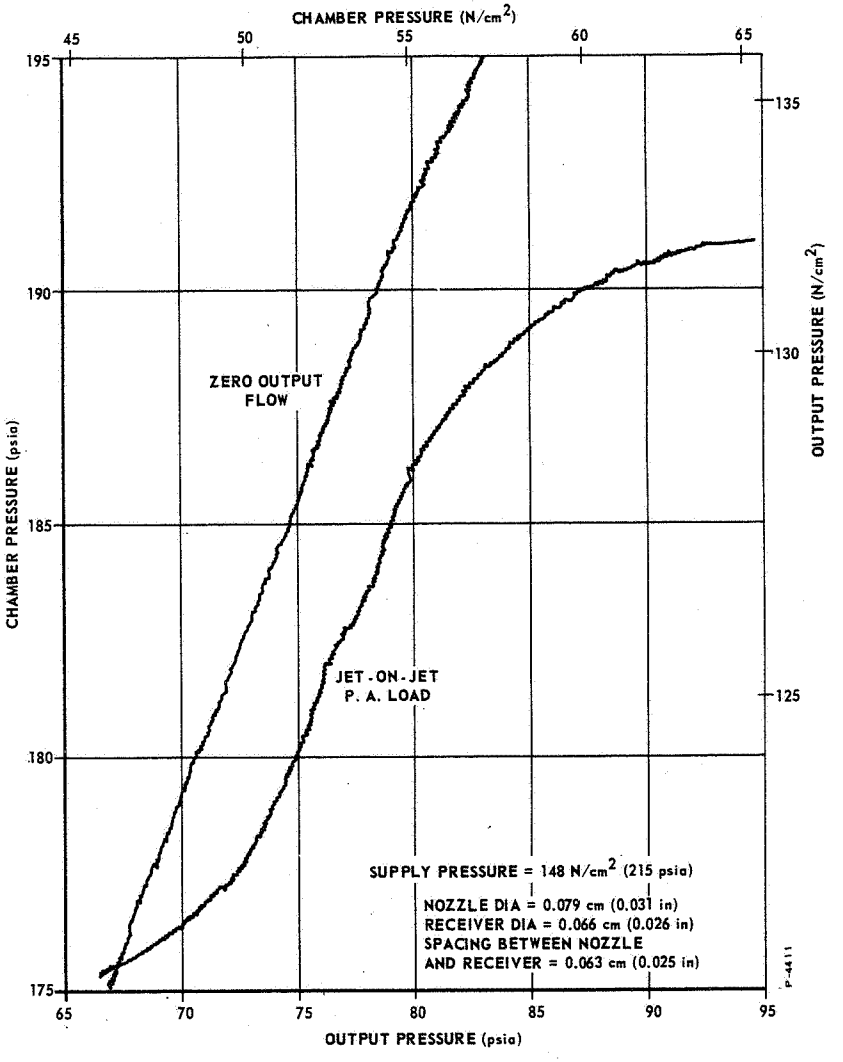

Figure 4-28 - No. 1 Venjet Gain Characteristics (Final Configuration)

The breadboard servovalve test performance is compared with the specified requirements in Table 4-1.

The transient response rise time was slow,using nitrogen, but faster than the required rise time for hydrogen. The transient response data with hydrogen as the gaseous medium is shown in Figure 4-30. For an output pressure step amplitude of 9.6 N/cm^2 (14 psi), the time required to reach 62.5% of the final value is 0.045 second versus the specified value of 0.055 second.

The frequency response of the servovalve was measured both with and without the dynamic load pressure feedback. The effect of the load pressure feedback on the frequency response of the servovalve operating on nitrogen is shown in Figure 4-31. The data indicate that the circuit functions, although the feedback gain and corner (break) frequency need to be adjusted slightly. The frequency response of the servovalve with dynamic pressure feedback and using hydrogen as the gaseous medium is shown in Figure 4-32. Previous tests of the vortex pressure amplifier breadboard servovalve, which was more compact than this breadboard model, have indicated that the frequency response would be adequate if the excessive line volumes were eliminated.

The differential output pressure versus differential input pressure curves for both nitrogen and hydrogen are shown in Figure 4-33. The gain curves show good linearity through the central two-thirds of the curve with a small decrease of gain at both end regions. The hydrogen and nitrogen curves almost coincide, except at the end regions. The maximum differential output pressure is 61.3 N/cm^2 (89 psi) using nitrogen and 59.2 N/cm^2 (86 psi) using hydrogen.

Representative differential output pressure stability is shown in Figures 4-34 and 4-35. The data was taken after filtering the electrical signal of the differential output transducer with a $1/(0.05S + 1)^2$ filter. The maximum amplitude of oscillation was 7.9 N/cm^2 (11.4 psi) peak-to-peak with nitrogen. The stability was improved when operating on hydrogen where the maximum amplitude of oscillation was 4.1 N/cm^2 (6.0 psi) peak-to-peak. As can be seen from the figures, the oscillation did not occur at any regular frequency but was rather random. Similarly to the vortex pressure amplifier servovalve, the differential output pressure range, except at near $\pm$100% rated input signal, where the output differential pressure is relatively quiet.

The output flow versus differential output pressure with nitrogen is shown in Figure 4-36. As seen from the figure, the maximum load flow is 1.0 gm/sec (0.0022 pps) at rated input signal.

Table 4-1 - Breadboard Flueric Servovalve Performance

Item		Specified	Measured (N_2)	Measured (H_2)
3.1.5	Supply Flow	1.82 rated no-load output flow max.	5.1	5.1*
5.2	Rated Input Signal	7 N/cm^2 (10 psi) max.	4.8 N/cm^2 (5.6 psi) max.	4.8 N/cm^2 (5.6 psi)
5.3	Input Signal Pressure Bias	45 N/cm^2 (65.3 psia)	49.3 N/cm^2 (71.7 psia)	49.3 N/cm^2 (71.7 psia)
5.5	Total Input Power	2.1 watts max. N_2 @ 530°R 7.7 watts max. H_2 @ 530°R	7.8 watts	24 watts
6.2	Rated No-Load Flow	2.76 gm/sec (0.0063 pps) N_2 @ 530°R 0.782 gm/sec (0.00173 pps) H_2 @ 530°R	1.0 gm/sec (0.0022 pps) N_2 @ 530°R	0.263 gm/sec (0.00058 pps)
6.3	Pressure Recovery	82 N/cm^2 (119 psi)	61.2 N/cm^2 (89 psi)	58.5 N/cm^2 (85 psi)
6.4	Flow $\geq \dot{m}_o (1 - P/P_o)$		No	No
6.5	Linearity-Deviation Gain Variation	10% max. 2 times average max.	16% 1.7 times	16% 1.8 times
6.7	Stability	0.4 N/cm^2 (0.58 psi) p-p	7.9 N/cm^2 (11.4 psi) p-p	4.1 N/cm^2 (6.0 psi)
6.8	Transient Response	62.5% F.V. in 0.055 sec 90.0% F.V. in 0.210 sec	0.14 sec 0.29 sec	0.045 sec 0.052 sec
6.9	Frequency Response Phase Shift and Amplitude Ratio	20° max. @ 6 hertz 90° max. @ 60 hertz ±2 db max. @ 0-60 hertz	1.9 hertz 10 hertz 0-8 hertz	3 hertz 35 hertz 0-9 hertz
6.10	Threshold	0.5% max.	-	-
6.11	Hysteresis	3% max.	10%	4%

P-5349

*Calculated

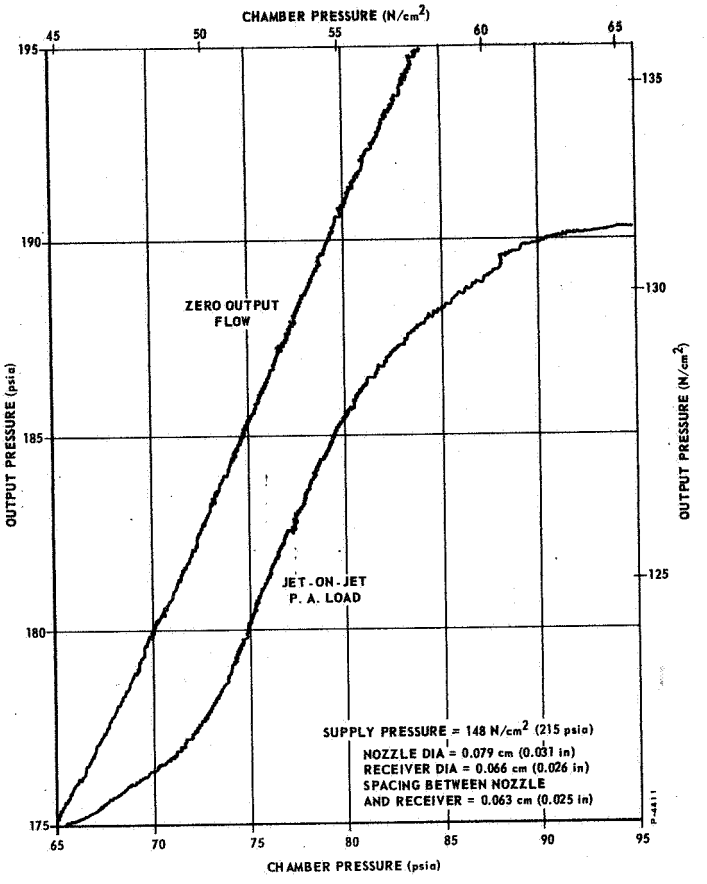

Figure 4-29 - No. 2 Venjet Gain Characteristics (Final Configuration)

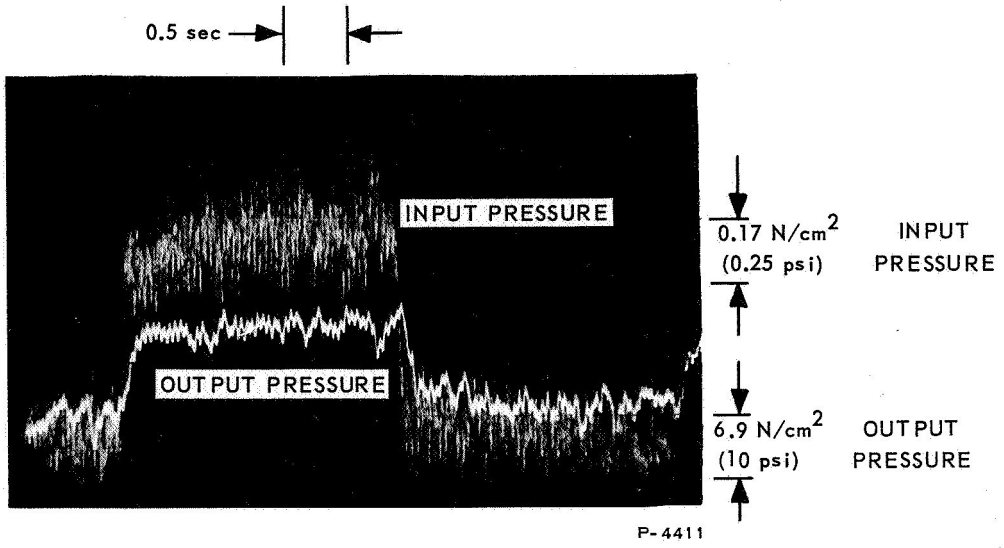

Figure 4-30 - Transient Response of Breadboard Servovalve on Hydrogen

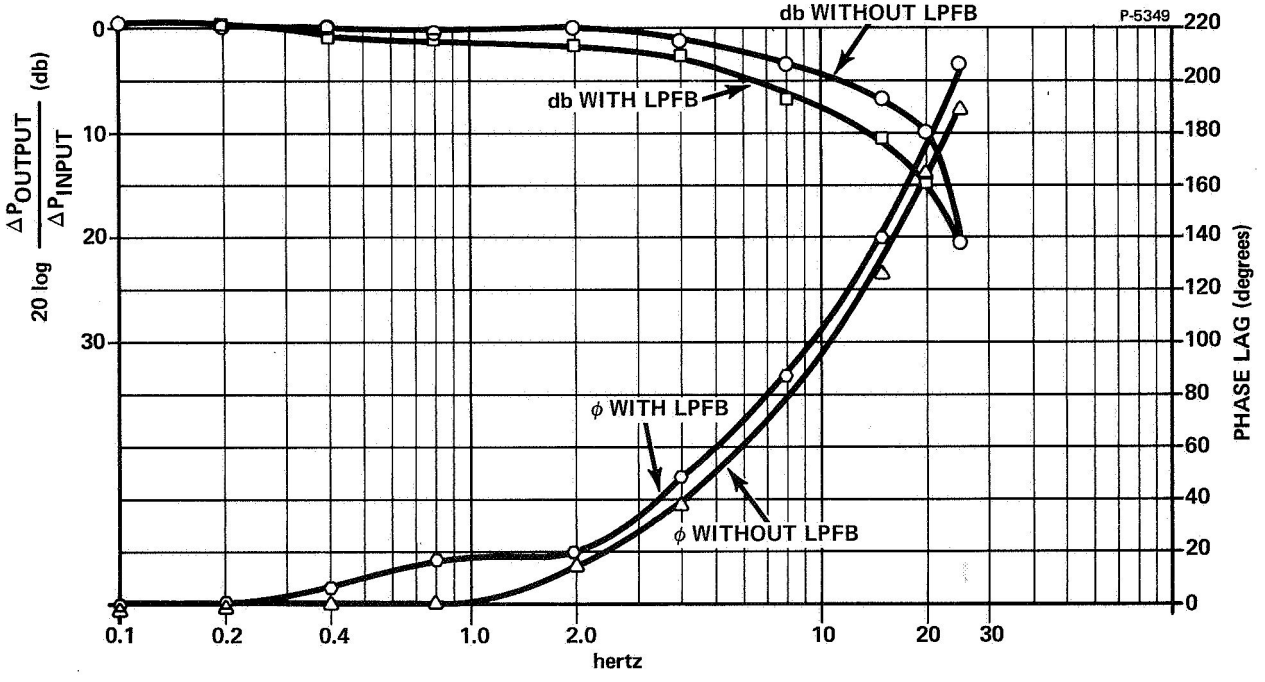

Figure 4-31 - Breadboard Servovalve Frequency Response With and Without Dynamic Load Pressure Feedback (Gaseous Medium Nitrogen)

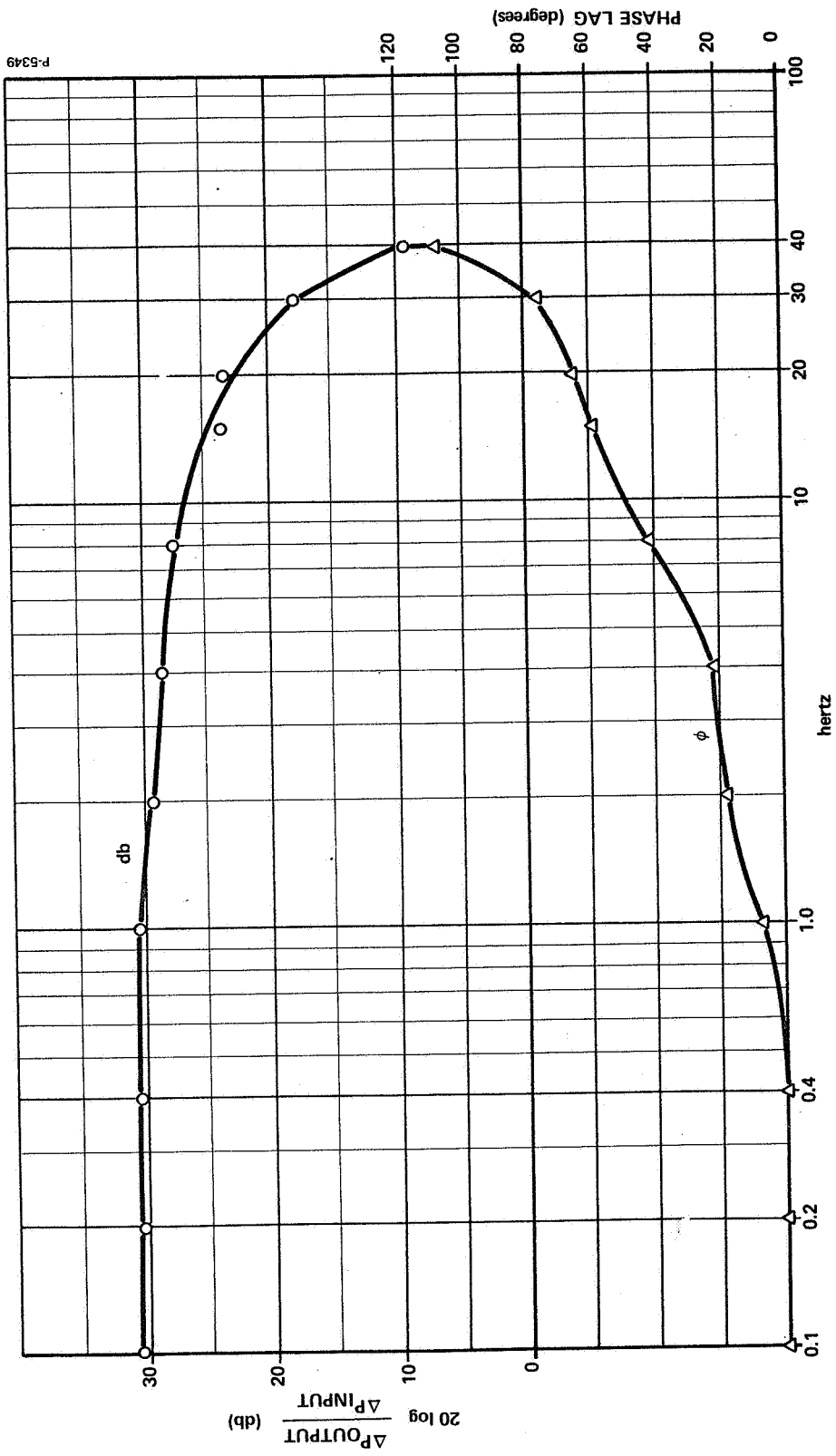

Figure 4-32 - Breadboard Servovalve Frequency Response With Load Pressure Feedback (Gaseous Medium Hydrogen)

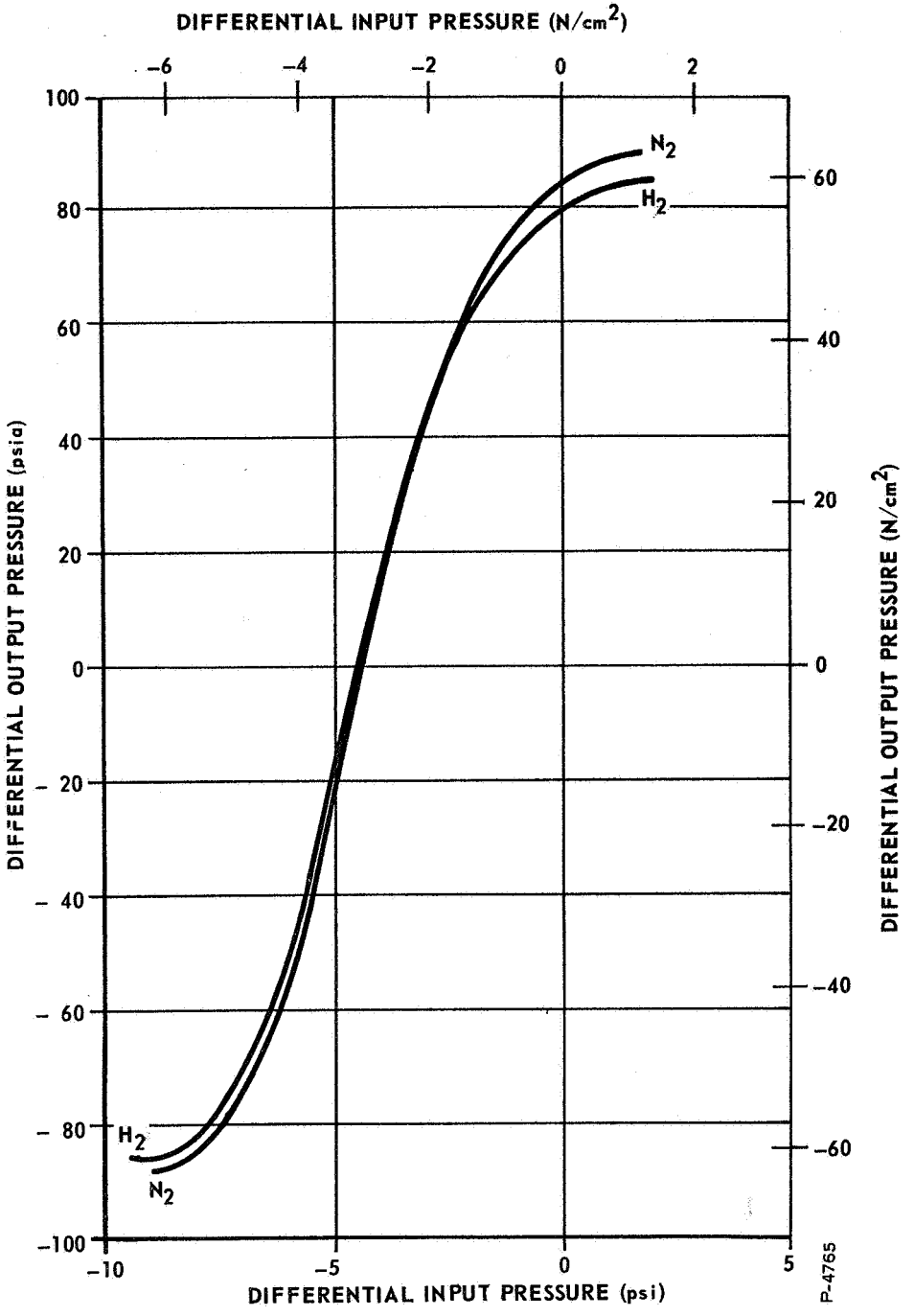

Figure 4-33 - Differential Output Pressure Versus Differential Input Pressure

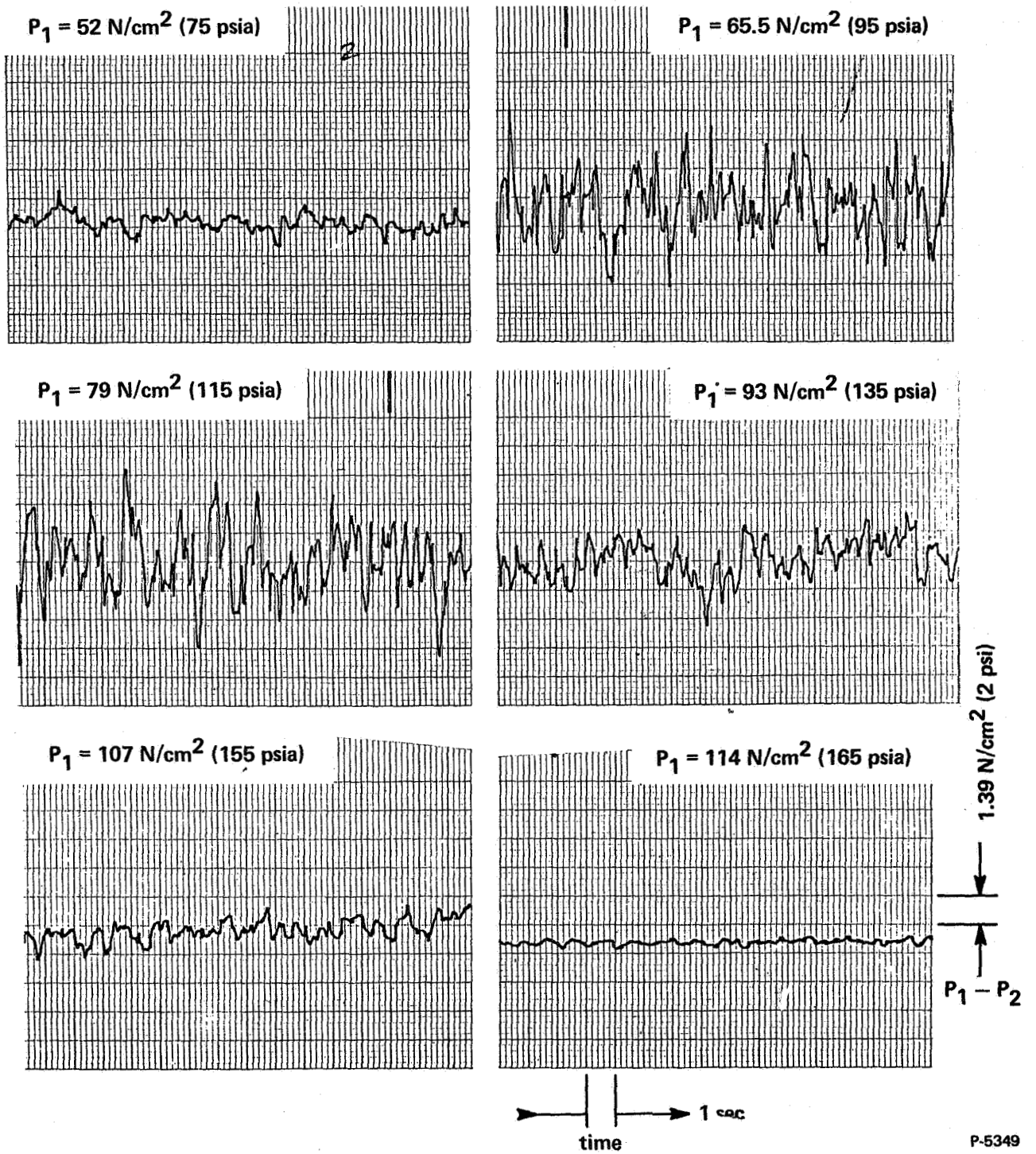

Figure 4-34 - Stability of Vortex Valve Bridge Servovalve
(Differential Output Pressure Versus Time)
(Gaseous Medium Nitrogen)

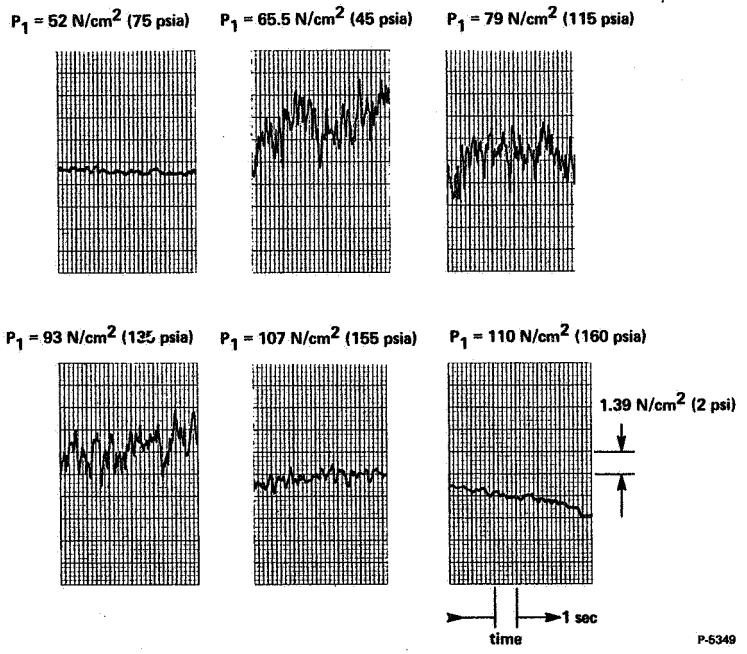

Figure 4-35 - Stability of Vortex Valve Bridge Servovalve (Differential Output Pressure Versus Time) (Gaseous Medium Hydrogen)

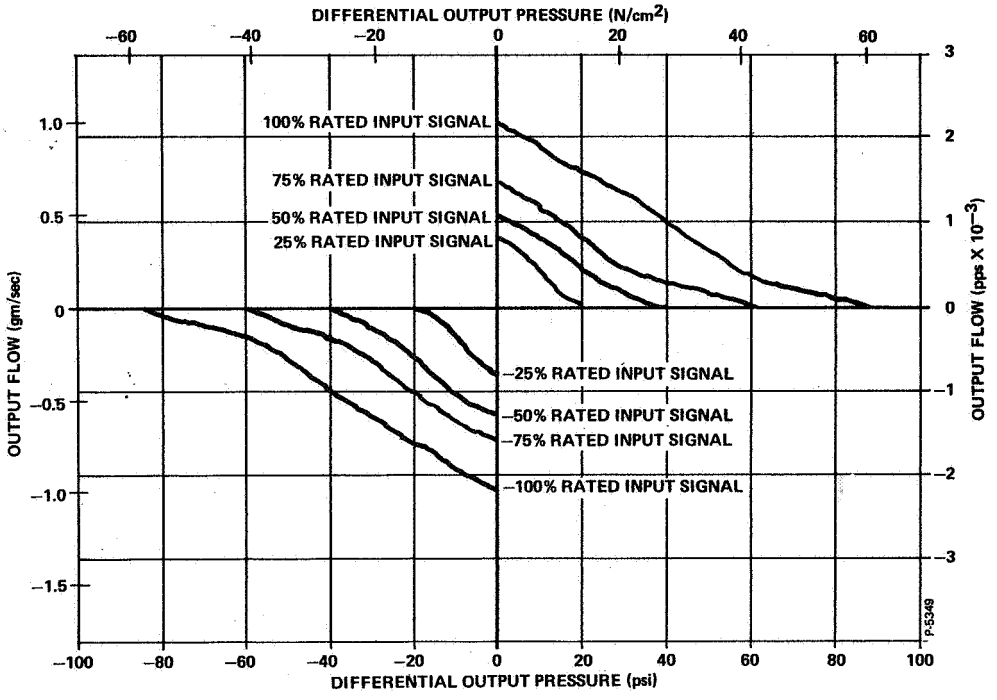

Figure 4-36 - Vortex Bridge Servovalve Output Flow Versus Output Pressure (Gaseous Medium Nitrogen)

SECTION 5

CONCLUSIONS AND RECOMMENDATIONS

It has been established that a flueric servovalve with performance capabilities comparable to a flapper-nozzle type servovalve can be built. A problem with stability still exists. All techniques evaluated thus far, to improve stability, have resulted in reduction of pressure and flow recovery. In the case of the vortex bridge servovalve, a severe loss in flow recovery resulted. If the full potential of this type of servovalve is to be realized, it will be necessary to develop techniques for stabilization that do not result in severe losses in performance.

The following conclusions can be drawn from this research project:

(1) Of the two power stage concepts evaluated, the power stage using the two vortex pressure amplifiers has demonstrated much higher flow recovery and power efficiency.

(2) The vortex bridge power stage is more stable than the vortex pressure amplifier power stage. The regions of instability of the output pressure-flow are more limited and the amplitude of oscillations are lower.

(3) Operation of both power stages with steep slopes or slope reversals in output pressure-flow characteristic curves result in low-frequency output pressure oscillations.

(4) During the development effort, geometric changes that reduced the slope or eliminated slope reversals in the pressure-flow characteristics resulted in lower pressure and flow recovery.

(5) The present vortex bridge power stage, operating with the pilot stage incorporating Venjets, exhibits a low-frequency output instability which does not correlate with the high-frequency noise in the Venjet output.

Since the flueric servovalve has demonstrated good performance capabilities, excluding stability, and offers important advantages in reliability and maintenance, it is recommended that further development effort be carried on to improve stability. The objectives of the next effort should be:

(1) To study the compressible flow phenomena and to establish, by test and supporting analysis, the specific sources of instability in fluidic devices and circuits.

(2) To formulate comprehensive mathematical models for fluidic elements and interconnecting transmission lines so that circuits may be analyzed and optimized on the digital computer, where tradeoffs between performance and stability may be made without resorting to expensive hardware programs.

(3) To formulate a design criterion to provide guidelines for designing stable circuits with optimum performance. These guidelines would be compiled from the results of computer simulations of components integrated into typical circuit applications.

The instability in fluidic systems is apparently caused by one or both of the following forms of energy interchange:

(1) between two or more pneumatic energy storage mechanisms. These mechanisms are fluid inertance, i.e., fluid inertia whose electrical analog is inductance; fluid capacitance, i.e., fluid accumulation whose electrical analog is capacitance; or various series-parallel combinations of either. Tuning of transmission lines to eliminate resonances which low noise levels trigger into large-scale instabilities, is a common illustration of this phenomenon.

(2) between a single pneumatic energy storage mechanism and a multivalue nonlinearity such as negative resistance, as in a vortex device, or the hysteresis associated with wall attachment of a free jet.

Observations on causes of instability point out necessary areas of investigation which will require study to eliminate instability from the vortex pressure amplifier power stage. For example, the vortex action within the chamber of the amplifier must be free of negative resistance. Techniques to eliminate this negative resistance are presently available. Also, geometries which might cause wall attachment of the vortex conical jet in the region of the chamber exit and probe tip must be identified and modified accordingly to minimize this effect. Finally, accumulated volumes, orifices, and line segments which cause energy interchange, either among each other or in conjunction with a multivalued nonlinearity, must be identified, then modified to eliminate the instability.

APPENDIX A

DESIGN SPECIFICATIONS FOR FLUERIC SERVOVALVE

1. SCOPE

The specification covers a valve to be designed to meet the requirements of NASA Contract Number NAS 3-7980, entitled "Design, Fabrication and Test of a Flueric Servovalve."

2. DESCRIPTION

The servovalve shall be a four-way valve with dynamic negative feedback of the output pressure. The servovalve shall contain no moving mechanical parts such as bellows, variable orifices, and jet-pipes. The principle of operation shall be the interaction of fluid streams.

3. SUPPLY AND EXHAUST SPECIFICATIONS

3.1 Phase 1 - Breadboard Model

3.1.1 Working Fluid: The working fluid shall be both nitrogen and hydrogen gas.

3.1.2 Temperature: Supply gas shall be room temperature.

3.1.3 Supply Pressure: The supply pressure shall be 148 $\pm$7 newtons per square centimeter, absolute (215 $\pm$ 10 psia).

3.1.4 Exhaust Pressure: The exhaust pressure shall be 34.5 $\pm$ 3.5 N/cm^2a (50 $\pm$ 5 psia).

3.1.5 Supply Flow: Under all operating conditions, the flow through the supply port shall be less than 1.82 times the rated no-load output flow, where "rated no-load output flow" is defined here as the mass flow through the wide open load-throttle for rated input-signal. "Rated input-signal" is defined in paragraph 5.2.

3.2 Phase II - Breadboard Model and Prototype Servovalve

3.2.1 Working Fluid: The working fluid shall be dry hydrogen.

3.2.2 Temperature: Supply gas temperature shall be variable from 56 to 333 degrees Kelvin (100 to 600°R).

3.2.3 Supply Pressure: The supply pressure shall be 148 $\pm$ 7 N/cm^2a (215 $\pm$ 10 psia).

3.2.4 Exhaust Pressure: The exhaust pressure shall be 34.5 ± 3.5 N/cm^{2}a (50 ± 5 psia).

3.2.5 Supply Flow: Under all operating conditions, the flow through the supply port shall be less than 1.82 times the rated no-load output flow.

4. LOAD SPECIFICATION

The two output ports shall be connected to a load consisting of a series arrangement of a volume-throttle-volume combination. The load shall contain no vents. The load volumes shall be adjustable to the extent that the difference between the two volumes can vary between plus and minus 115 cubic centimeters (7 in^3). The total of the two volumes shall remain equal to 164 cm^3 (10 in^3). The load-throttle shall be a two-way valve adjustable from closed to wide open passageway. With wide open load throttle, the differential output pressure shall be less than 5 N/cm^2 (7 psi).

5. INPUT-SIGNAL SPECIFICATIONS

5.1 Input-Signal: The input-signal shall be a two-port differential pneumatic signal. The working fluid shall be the same as the supply gas for the servovalve. "Input-signal pressure" is defined here as the pressure difference between the two input ports.

5.2 Rated Pressure: The rated input-signal pressure shall be less than 7 N/cm^2 (10.2 psi) for flow in both directions through the load-throttle. "Rated input-signal" is defined here as the input-signal that produces the rated no-load flow specified in Paragraph 6.2.

5.3 Quiescent Pressure: For zero input-signal, the pressure bias of the input-signal shall be less than 45 N/cm^{2}a (65.3 psia); where "pressure bias" is defined here as the average pressure of two lines.

5.4 Admittance: Variation in the admittance of each input port, resulting from changes in the load-throttle, shall be less than 10% of the maximum input admittance for the complete range from closed to wide open load-throttle; where "admittance" is defined here as the mathematical derivative of volumetric flow with respect to the absolute pressure in the input port. No specification is placed upon variation in the input admittance as a function of the input-signal.

5.5 Power: Under all operating conditions with dry hydrogen at 56°K (100°R), the combined power delivered to the input ports shall be less than 4 watts; where "power" is defined here as the product of the gage pressure (i.e., pressure relative to the exhaust pressure) and volumetric flow.

6. OUTPUT SPECIFICATIONS

6.1 Output: The servovalve shall have two output ports. "Differential output pressure" is defined here as the pressure difference between the output ports. "Output flow" is defined here as the mass flow through the load-throttle.

6.2 Rated No-Load Flow: With wide open load-throttle, the output flow of dry hydrogen at 56°K (100°R) shall be 2.1 grams per second (0.00463 lb/sec) for the rated input-signal.

6.3 Pressure Recovery: With closed load-throttle, the differential output pressure shall be greater than 82 N/cm^2 (119 psi); i.e., 73% pressure recovery.

6.4 Pressure-Flow Characteristics: For all values of constant input-signal, the output flow shall be equal to or greater than

$$\dot{m}_o \left(1 - \frac{p}{P_o}\right)$$

where quantity $\dot{m}_o$ is a constant and equals the output flow for the given input-signal with wide open load-throttle; p_o is a constant and equals the differential output pressure for the given input-signal with closed load-throttle; and p is a variable term equal to the differential output pressure for the given input-signal and is a function of the load-throttle setting.

6.5 Linearity: Deviation from a straight line of input-signal pressure versus differential output pressure for closed load-throttle shall be less than 10% of the rated values. The pressure gain for all values of input-signal shall be less than two (2) times the average pressure gain, where "pressure gain" is defined here as the mathematical derivative of the differential output pressure with respect to the input-signal pressure during steady operating conditions with closed load-throttle.

6.6 Pressure Feedback: Dynamic negative feedback of the pressure of each output port shall be an integral part of the servovalve. The feedback gain at zero frequency shall be less than 1% of the rated input-signal. The feedback gain at the corner (break) frequency of 5 hertz shall be 8 $\pm$ 1% of the rated input-signal. Construction of the servovalve shall allow easy exchange of components for changing the pressure feedback characteristics.

6.7 Stability: Peak-to-peak ripple of frequencies above 3 hertz shall be less than 0.4 N/cm^2 (0.58 psi) measured after filtering an electrical signal of the differential output pressure with a $1/(0.05S + 1)^2$ filter, for various load-volume settings and for all values of input-signal with closed load-throttle.

6.8 Transient Response: From any initial value and for step input-signals that produce a 20 N/cm^2 (29 psi) change in the differential output pressure, the differential output pressure shall reach 62.5% of the step in a time period of less than 0.055 second and shall settle within 2 N/cm^2 (2.9 psi) of the final value in a time period of less than 0.210 second when tested with closed load-throttle and with equal load-volumes.

6.9 Frequency Response: With zero load-volumes and blocked output ports, the phase shift of the differential output pressure for a 2% rated input-signal at 6 hertz shall be less than 20 degrees, and at 60 hertz the phase shift shall be less than 90 degrees. The differential output pressure amplitude variation for a constant input-signal shall be less than ± 2 db from 0 to 60 hertz.

6.10 Threshold: For all values of input-signal, the increment of input-signal required to produce a change in the output shall be less than 0.5% of the rated input-signal.

6.11 Hysteresis: The difference in the input-signal required to produce the same output during a single input cycle shall be less than 3% of the rated input-signal.

7. ENVIRONMENT SPECIFICATIONS

Items 7.2, 7.3, and 7.4 shall not apply to the breadboard model of the servovalve.

7.1 Ambient Temperature: The servovalve shall be capable of operation under ambient temperatures that vary between 56°K and 333°K (100°R and 600°R).

7.2 Vibration: The servovalve shall be operational when subjected to 6 g's amplitude from 0 to 20 hertz and then linear amplitude to 20 g's at 200 hertz and then constant at 20 g's to 2000 hertz along any axis.

7.3 Shock and Acceleration: The servovalve shall operate after a 6-g shock and/or an 8-g acceleration along any axis.

7.4 Radiation Field: The servovalve shall be operational under a total dose of 6×10^6 rads (ethylene) 1 hour; a fast neutron flux rate ($E > 1.0$ nev) of 3×10^{11} neutrons/cm^2-sec; a thermal neutron flux ($E < 1.86$ EV) of 1×10^{10} neutrons/cm^2-sec; and a gamma heating equivalent to 770 watts/kilogram aluminum (350 watts/lbm aluminum).

APPENDIX B

DESCRIPTION OF FLUERIC COMPONENTS

1. VORTEX VALVE

A vortex valve is essentially a throttling device. The basic vortex valve consists of a cylindrical chamber with supply flow and control flow inlets and an outlet orifice as illustrated in Figure B-1. The supply flow of gas enters the chamber and, in the absence of control flow, proceeds radially inward without resistance and then flows out of the inlet orifice. In the absence of control flow the maximum total flow through the valve is achieved, with the main pressure drop occurring across the outlet orifice. The chamber pressure is slightly less than the supply pressure. Control flow, caused by the control pressure being above the chamber pressure, is injected tangentially into the chamber. The tangential control flow imparts a rotational component to the supply flow. The centrifugal force due to the fluid rotation results in a radial pressure gradient. For a constant supply pressure, this drop in pressure across the chamber reduces the pressure differential across the outlet orifice, and thus reduces the outlet flow.

If sufficient control flow is introduced, the flow from constant pressure supply can be completely shut off, and thus the supply flow can be modulated from full flow to zero. The outlet flow can be modulated from full outlet flow, when the control flow is zero, down to 10% to 30% of the full outlet flow, when the supply flow is zero and only control flow enters the chamber. The ratio between the full or maximum outlet flow and minimum outlet flow is called the turndown ratio. Typical throttling characteristics of the vortex valve are shown in Figure B-2.

The vortex valve shown in Figure B-1 has an outlet orifice on only one side of the vortex chamber, but vortex valves are also made with an outlet orifice on both sides of the vortex chamber. With two outlet orifices of equal size, the maximum outlet flow is almost double that obtained with a vortex valve with a single outlet orifice. However, the minimum outlet flow is only slightly higher with two outlet holes than with one. Thus, the turndown ratio of a vortex valve with two outlet orifices is higher than a similar vortex valve with a single outlet orifice by a factor of 1.7 to 1.9.

Vortex Pressure Amplifier

The vortex pressure amplifier is a power amplifier. The output power can be modulated from maximum to zero, and the vortex chamber is insensitive to back pressure because the vortex pressure amplifier has a vent. A vortex pressure amplifier is similar to a vortex valve with

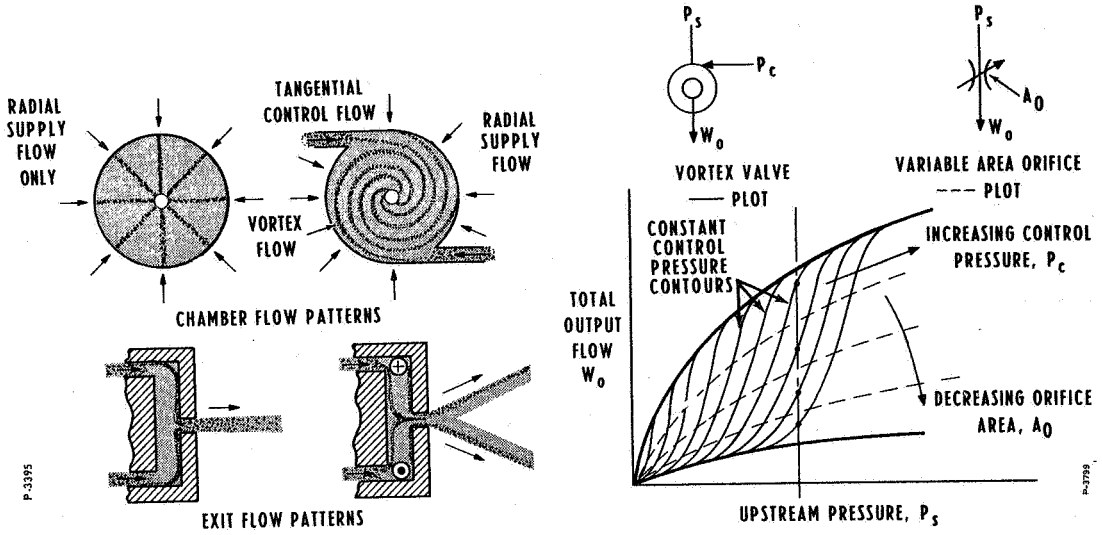

Figure B-1 - Vortex Valve

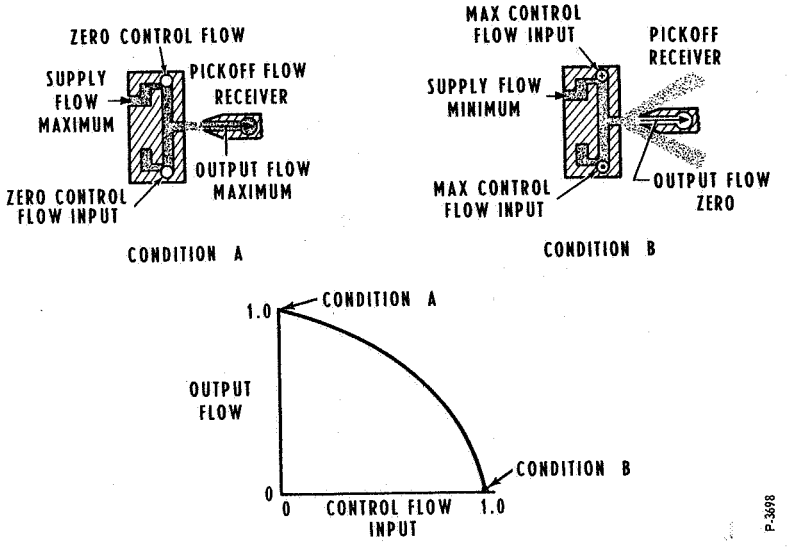

Figure B-2 - Vortex Amplifier

the exception that a pickoff or receiver is placed in the gas stream of the outlet orifice; the pickoff acts in much the same manner as a pitot tube. The receiver pressure and flow is the output of the device. When there is no control flow, the flow out of the outlet orifice is directed into the receiver, Figure B-2, Condition A, and the pressure and flow recovered under the condition is at a maximum. As control flow is added, the exit flow fans out as shown in Figure B-2, Condition B, and the recovered pressure decreases. Hence, the vortex pressure amplifier uses the combined effects of the vortex valve and flow diversion for obtaining amplification.

Both the vortex valve and vortex pressure amplifier can be used as summing devices by incorporating a number of positive and negative control input ports.

Venjet Amplifier

The Venjet amplifier is used primarily to boost a pressure signal from a low pressure level to a high pressure level. It has good pressure and flow recovery and the pressure gain varies from less than 1 up to 5 or sometimes even higher. The Venjet amplifier consists of a nozzle and receiver enclosed in a chamber, as illustrated in Figure B-3. The flow in the supply nozzle is sonic throughout the useful operating range. The output pressure is modulated by changing the ambient pressure around the free jet which issues from the receiver and impinges on the receiver. To control this ambient pressure, the jet is enclosed in a chamber as shown and the flow rate of the gas vented from the chamber is controlled. Restricting the flow vented from the chamber increases the ambient chamber pressure causing an increase in output pressure. Typical performance data is shown in Figure B-3 also.

2. JET-ON-JET PROPORTIONAL AMPLIFIER

The jet-on-jet proportional amplifier operates on the momentum exchange properties of two intersecting fluid jets. A primary fluid jet converts pressure head into velocity head. A control jet is located at right angles to this supply jet and the control fluid momentum is mixed with the supply jet, resulting in a deflection while maintaining a coherent jet of mixed supply and control fluid. The resulting jet of fluid is divided between two flow receivers as shown in Figure B-4. The jet momentum can then be converted back to pressure head and flow, depending on the nature of the load requirements. Typical amplifier pressure gain characteristics are also shown in Figure B-4. The physical size of the element is set by the area of the supply jet. Most of the devices being used today have rectangular porting. These devices are limited in a pressure recovery to approximately 60% of supply pressure and demand a constant flow, only acting as a flow divider.

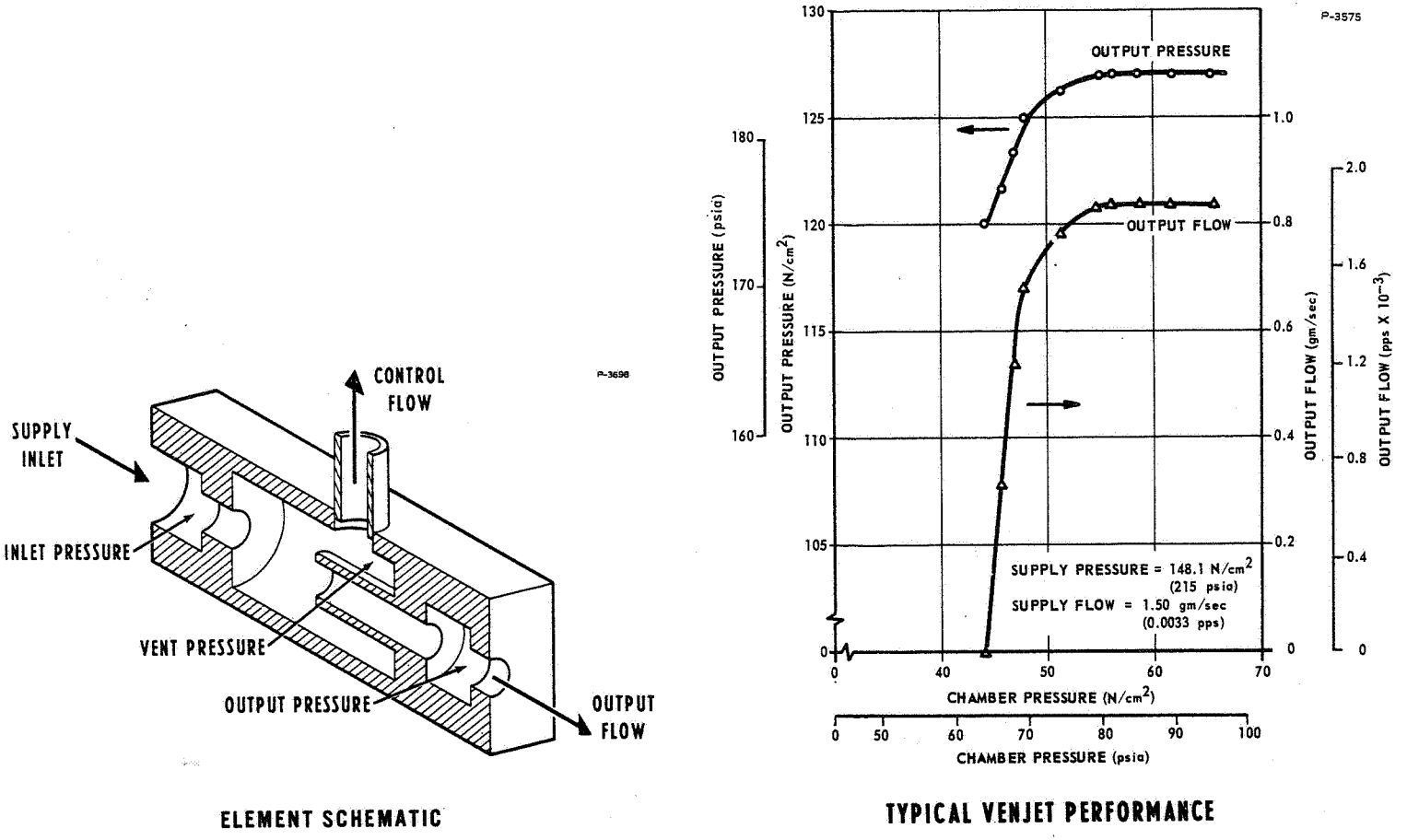

Figure B-3 - Venjet Amplifier

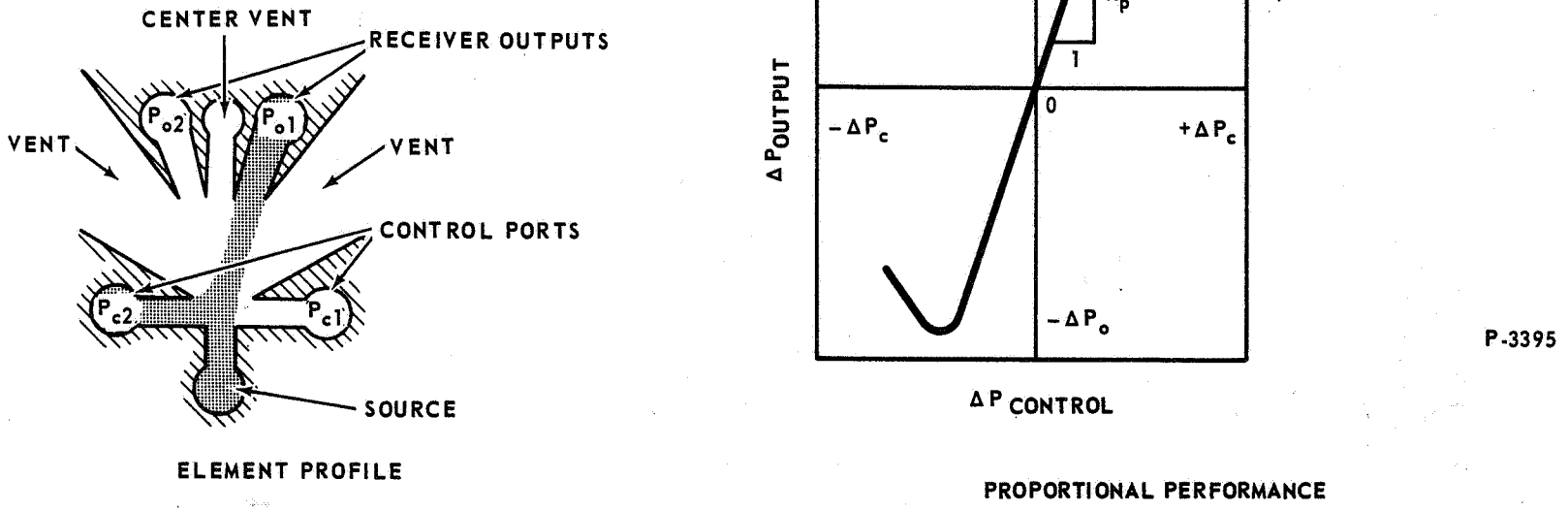

Figure B-4 - Jet-on-Jet Proportional Amplifier

3. EJECTOR

An ejector is a pump with no moving parts. In the ejector, a jet entrains fluid from a low pressure region and delivers it to a higher-pressure region. The ejector consists of a nozzle and diffuser and surrounding chamber as shown schematically in Figure B-5. The low-pressure high-velocity jet acts to entrain the fluid in the surrounding chamber, thereby enabling the device to withdraw fluid from a region that is at the same pressure as the ejector chamber. The deceleration in the diffuser of the resulting mixture made up of the supply jet and the entrained fluid results in higher pressure and lower velocity at the outlet of the ejector. Typical performance characteristics are also shown in Figure B-5.

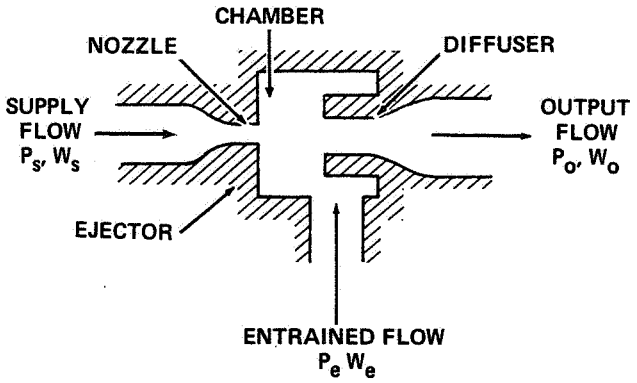

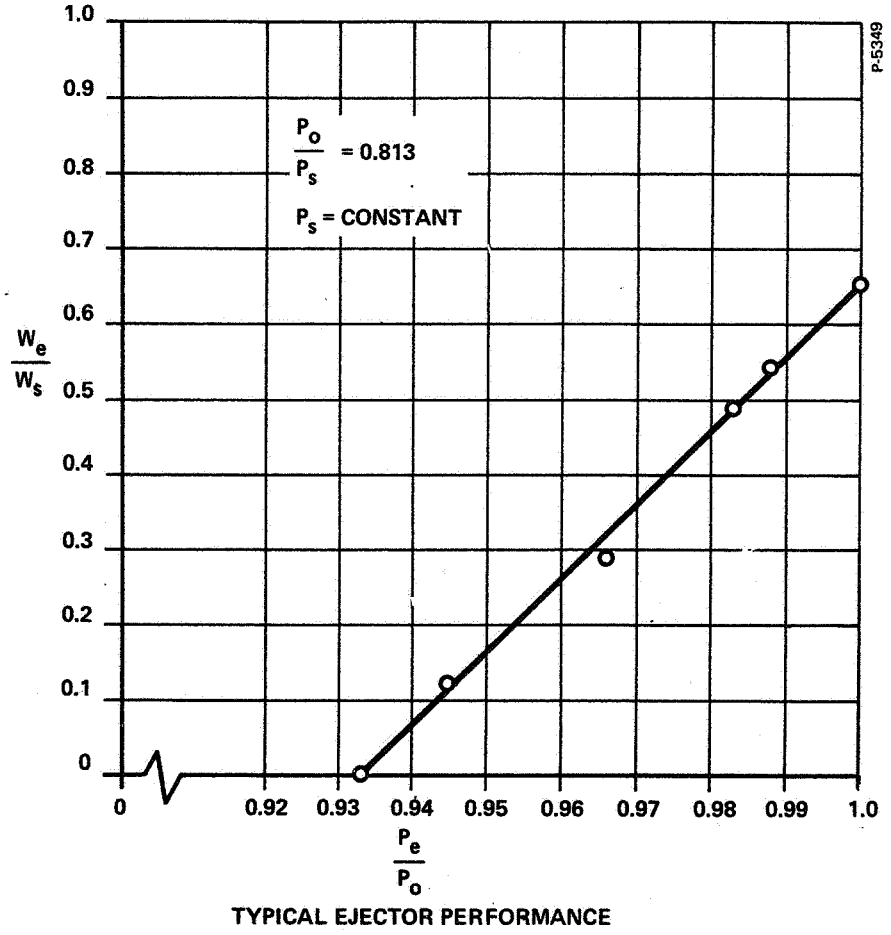

Figure B-5 - Ejector

APPENDIX C

SYMBOLS AND TERMS

pps	=	pounds per second
P_{cA}, P_{cB}	=	control pressure to the pilot stage
P_c	=	control pressure
$P_{CHAMBER}$	=	chamber pressure
ΔP_c	=	differential control pressure
ΔP_o	=	differential output pressure
P_e	=	exhaust pressure
P_o	=	output pressure
P_s	=	supply pressure
P.T.	=	pressure transducer
P_1, P_2	=	pressure on either side of load
Q_c	=	control volume flow
Q_e	=	exhaust volume flow
Q_o	=	output volume flow
Q_s	=	supply volume flow
W_c	=	control weight flow
W_e	=	exhaust weight flow
W_L	=	weight flow across the load
W_o	=	output weight flow
W_s	=	supply weight flow

Terms

Turndown Ratio: Ratio of the output flow of a vortex valve with no input control flow to the output flow with the supply flow equal to zero when the supply is a constant pressure source.

Negative Resistance: A flueric device is said to have negative resistance when a portion of its output pressure-flow curve indicates increasing output flow with increasing output pressure rather than decreasing output pressure.

Pressure Recovery:	Either the output pressure differential of a servovalve with a given supply pressure or the output pressure differential of a servovalve divided by the difference between supply and exhaust pressures.
Flow Recovery:	The ratio of the output weight flow to the input weight flow of a valve.
Push-Pull Output Amplifier:	An amplifier with two outputs such that as one output increases, the other output decreases and vice versa.
Receiver:	A cavity or tube positioned in the path of a fluid jet for the purpose of receiving or recovering some portion of the jet's total pressure or energy.
Pressure Bias:	The average pressure of two control signal lines.

Orifice 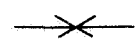 or 

Valve 

Pressure Regulator 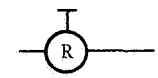

Pressure Gauge 

Float-Type Flowmeter 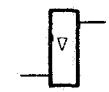

Pressure Transducer 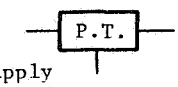

Vortex Valve 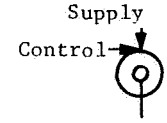

Vortex Pressure Amplifier 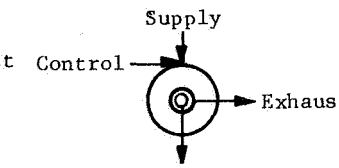

Venjet Amplifier or Ejector 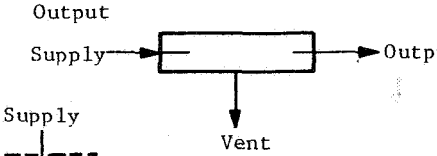

Jet-on-Jet Pressure Amplifier 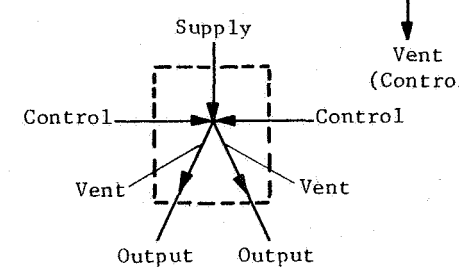

APPENDIX D

DIMENSIONS OF COMPONENTS

Following are a drawing, a photograph, and dimensions not shown in the text of the servovalve components.

1. VORTEX PRESSURE AMPLIFIER SERVOVALVE

A layout assembly drawing of the vortex pressure amplifier servovalve is shown in Figure D-1 and a photograph showing an exploded view of the servovalve is shown in Figure D-2.

The significant dimensions of the power stage vortex pressure amplifiers are as follows:

Vortex Chamber Diameter	1.112 cm (0.438 in.)
Vortex Chamber Length	0.094 cm (0.037 in.)
Button Diameter	1.062 cm (0.418 in.)
Exit Orifice Diameter (two orifices)	0.094 cm (0.037 in.)
Control Orifice Diameter (four orifices)	0.046 cm (0.018 in.)
Receiver Diameter	0.104 cm (0.041 in.)
Distance Between Exit Orifice and Receiver	0.028 cm (0.011 in.)

The significant dimensions of the summing vortex amplifiers are as follows:

Vortex Chamber Diameter	1.12 cm	(0.441 in.)
Vortex Chamber Length	0.16 cm	(0.063 in.)
Button Diameter	1.05 cm	(0.412 in.)
Exit Orifice Diameter (Two Orifices)	0.16 cm	(0.063 in.)
Control Orifice Area:		
No. 1 (Input Signal)	2.58×10^{-3} cm^2	(4.0×10^{-4} in^2)
No. 2 (Regenerative Feedback)	0.93×10^{-3} cm^2	(3.0×10^{-4} in^2)
No. 3 and No. 4 (Dynamic Pressure Feedback)	0.26×10^{-3} cm^2	(0.4×10^{-4} in^2)

2	D	2158268	BODY, POWER STAGE	416 CRES	14
AR	B	2158269-1-2-3	SPACER, POWER STAGE	CRES SHIM STOCK	13
2	D	2158266-2	NOZZLE, POWER STAGE	416 CRES	12
1	D	2158841	MANIFOLD, LOWER	416 CRES	11
4			SOCKET HEAD CAP SCREW	#6-32UNC-3A x .38 LG.	10
4			SOCKET HEAD CAP SCREW	#6-32UNC-3A x 1.38 LG.	9
4			SOCKET HEAD CAP SCREW	#6-32UNC-3A x 1.62 LG.	8
38			"O" RING SEAL	SIZE AS REQ'D.	7
2	D	2158710	HOUSING, VENJET	416 CRES	6
AR	B	2158712-1-2-3	SHIM, VENJET	CRES SHIM STOCK	5
2	B	2158711-1-2	NOZZLE, VENJET	416 CRES	4
4			SOCKET HEAD CAP SCREW	#4-40UNC-3A x .75 LG.	3
AR	B	2158712-1-2-3	SHIM, VENJET	CRES SHIM STOCK	2
16			SOCKET HEAD CAP SCREW	#4-40UNC-3A x .31 LG	1

4			SOCKET HEAD CAP SCREW	#4-40UNC-3A x 1.25 LG.	29
1	D	2158853	MANIFOLD, UPPER	416 CRES	28
2	C	2158272	NOZZLE, FEED-BACK VALVE	416 CRES	27
2	D	2158273	LOWER HOUSING, FEED-BACK VAL.	416 CRES	26
2	D	2158274	UPPER HOUSING, FEED-BACK VAL.	416 CRES	25
8			SOCKET HEAD CAP SCREW	#4-40UNC-3A x .81 LG.	24
2	D	2158787	HOUSING, SUMMING AMPL.	416 CRES	23
2	C	2158786	BUTTON, SUMMING AMPL.	416 CRES	22
1	E	2158270	HOUSING, POWER STAGE	416 CRES	21
1			PLAIN NUT	1/4-28UNF-3A CRES	20
1	B	2158875	VALVE, NEEDLE	416 CRES	19
1			LOCK WASHER	1/4 DIA. CRES	18
2	D	2158266-1	NOZZLE, POWER STAGE	416 CRES	17
AR	B	2158269-1-2-3	SPACER, POWER STAGE	CRES SHIM STOCK	16
2	C	2158267	BUTTON, POWER STAGE	416 CRES	15

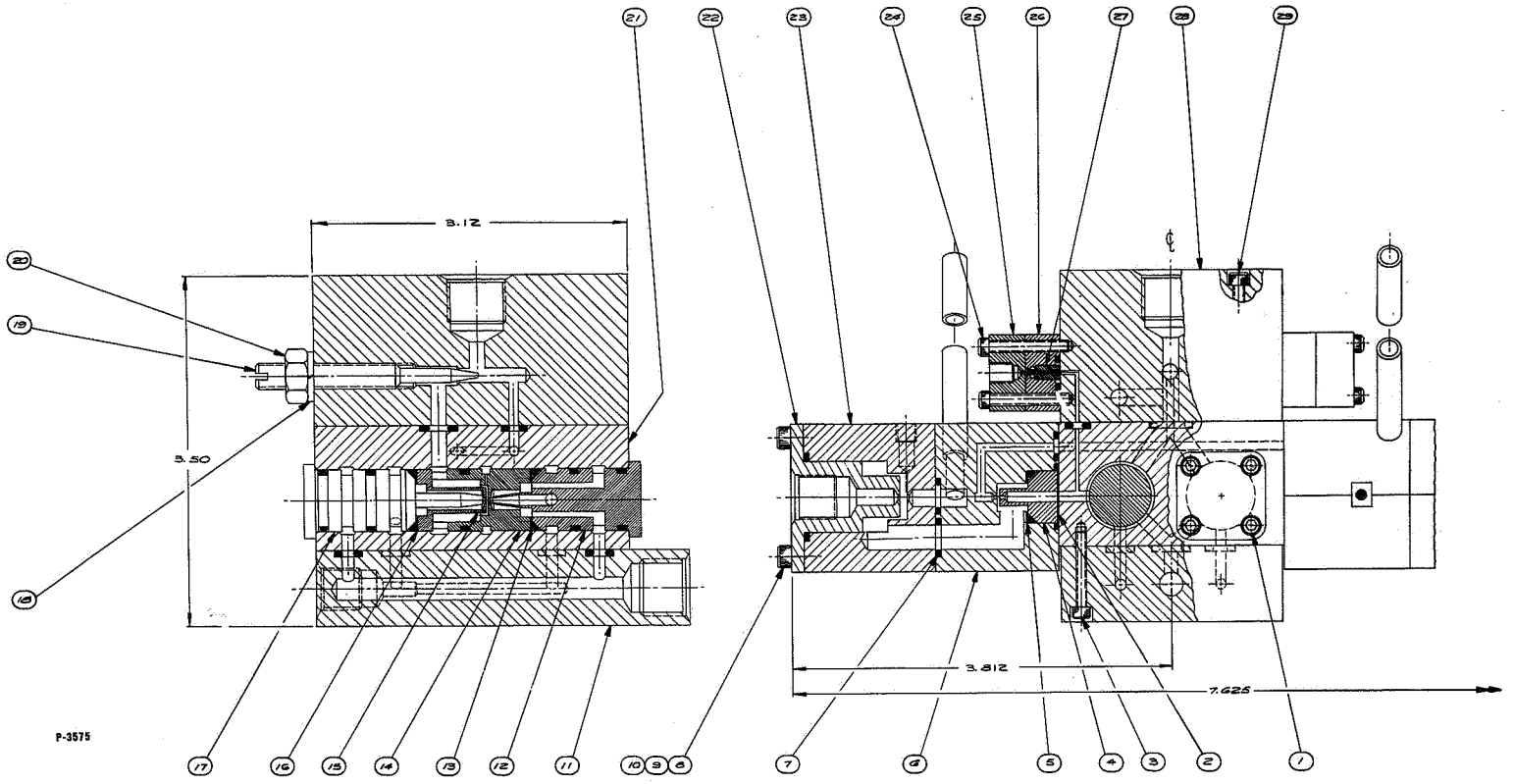

Figure D-1 - Layout Assembly Drawing of Vortex Pressure Amplifier Servovalve

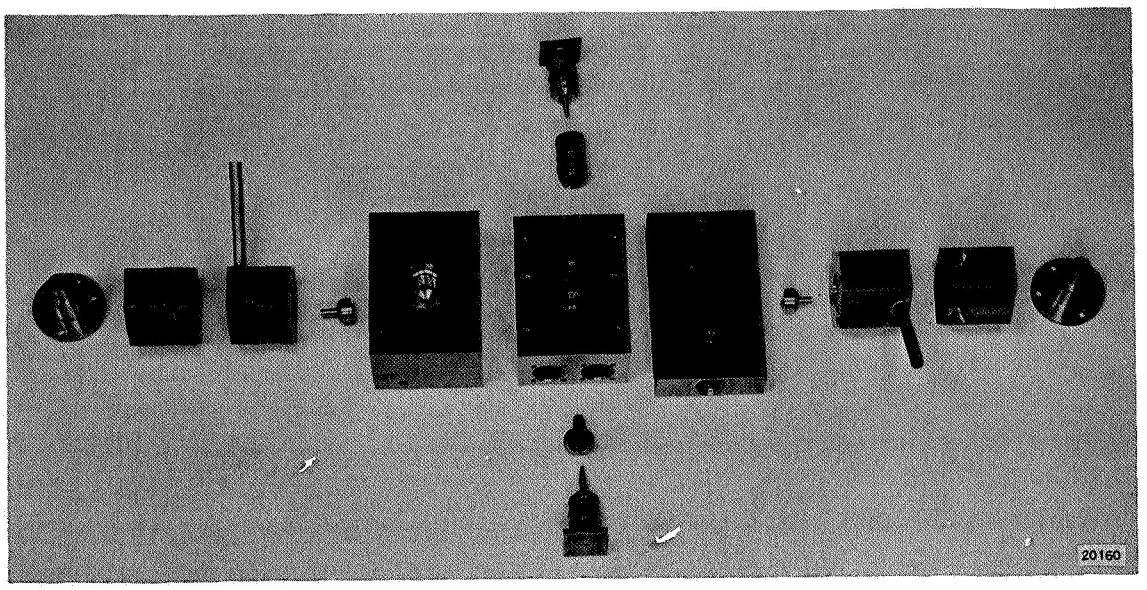

Photograph

Figure D-2 - Vortex Pressure Amplifier Servovalve

The significant dimensions of the regenerative-feedback vortex pressure amplifiers are as follows:

Vortex Chamber Diameter	0.178 cm (0.070 in.)
Vortex Chamber Length	0.020 cm (0.008 in.)
Exit Orifice Diameter	0.020 cm (0.008 in.)
Receiver Diameter	0.020 cm (0.008 in.)
Distance Between Exit Orifice and Receiver	0.010 cm (0.003 in.)

2. VORTEX VALVE BRIDGE SERVOVALVE

The vortex chamber dimensions of both supply and exhaust valve are as follows:

Chamber Diameter	1.11 cm (0.437 in.)
Chamber Length	0.094 cm (0.037 in.)
Button Diameter (Supply Valve)	1.09 cm (0.428 in.)
Button Diameter (Exhaust Valve)	1.06 cm (0.418 in.)
Orifice Diameters	(See Figure 4-9, page 4-8)

APPENDIX E

SERVOVALVE TEST EQUIPMENT AND PROCEDURE

Data in this appendix cover the test equipment and procedure for evaluating both the vortex pressure amplifier and vortex bridge servovalves.

1. TEST EQUIPMENT

Transient response, frequency response, output stability, hysteresis, and symmetry tests were conducted using the test setup shown schematically in Figure E-1. An electropneumatic flapper-nozzle type valve was used to control the input control pressures. The electropneumatic valve was controlled by an amplifier, and the input signal was varied by a function generator. The differential output and input pressures to the servovalve were measured by means of differential pressure transducers. The pressures were recorded on an X-Y plotter or an oscillograph.

Tests of input admittance, control input power, and output flow versus differential output pressure were conducted using the test setup as shown in Figure E-2 for the vortex pressure amplifier servovalve tests, and in Figure E-3 for the vortex bridge servovalve tests. For these tests, mass flow transducers or float-type flowmeters were used to measure input, control, and load flows, and pressure transducers or standard bourdon tube pressure gages were used to measure pressure.

2. TEST PROCEDURE

2.1 Transient Response

The transient response of the servovalve was measured by introducing a step input and by recording both the input and output pressures as a function of time. The load volumes were equal and the load throttle was closed.

2.2 Frequency Response

The frequency response was measured by introducing a constant-amplitude sine-wave input signal. The output and input differential pressures were measured as a function of time at various frequencies. The load volumes were each about 4.9 cm^3 (0.3 in^3), and the load throttle was closed.

2.3 Output Stability

The output stability was measured by recording output differential pressure versus time with a constant input signal. This test

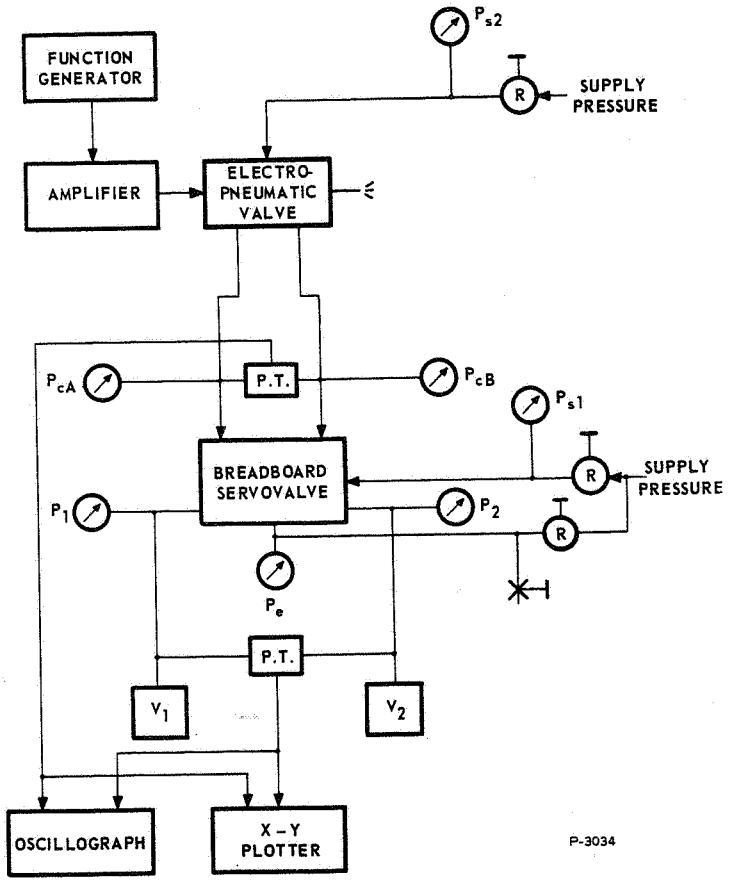

Figure E-1 - Flueric Pressure Amplifier Servovalve Test Setup No. 1

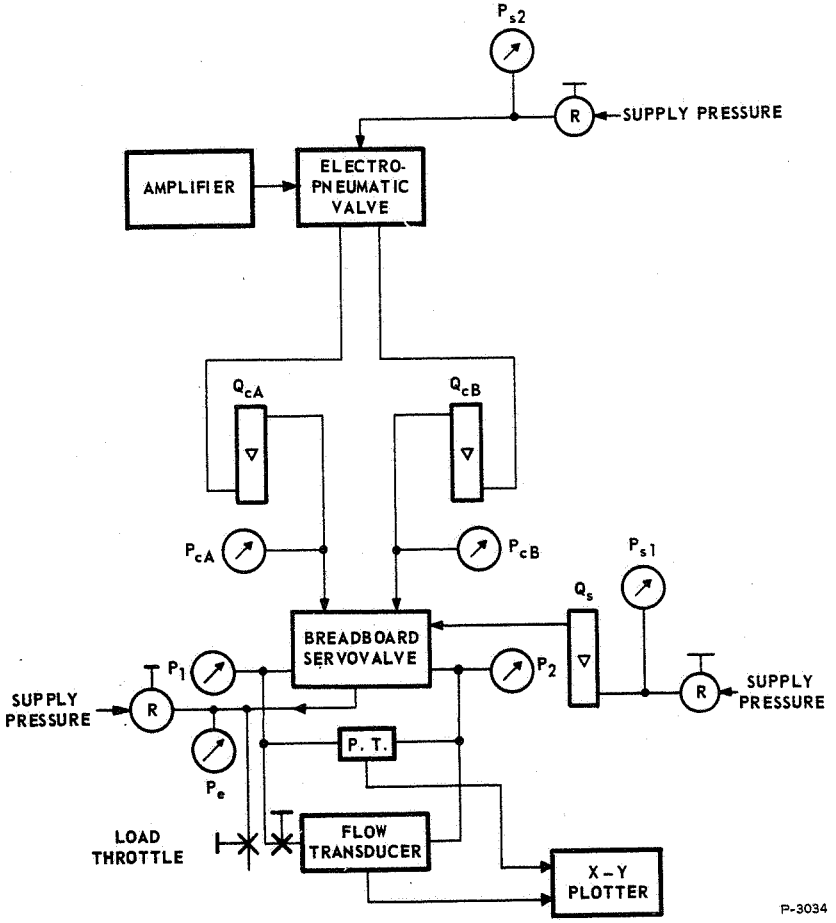

Figure E-2 - Flueric Pressure Amplifier Servovalve Test Setup No. 2

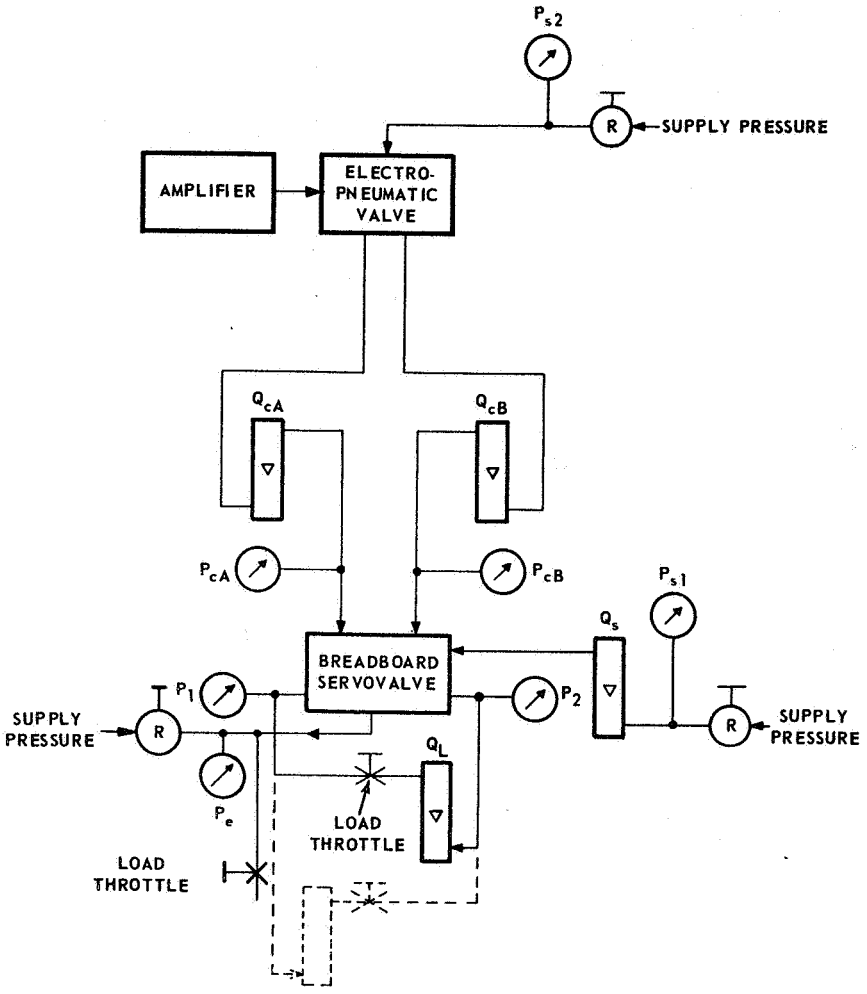

Figure E-3 - Flueric Vortex Valve Bridge Servovalve Test Setup No. 3

was performed with closed load throttle and with various load volume sizes and input-signal levels. The load volumes used were:

(1) $V_1 = 139\ cm^3\ (8.5\ in^3)$; $V_2 = 24.6\ cm^3\ (1.5\ in^3)$

(2) $V_1 = V_2 = 82\ cm^3\ (5\ in^3)$

(3) $V_1 = 24.6\ cm^3\ (1.5\ in^3)$; $V_2 = 139\ cm^3\ (8.5\ in^3)$

2.4 Threshold

The threshold was measured by recording the input and output differential pressures as a function of time with a sine-wave input. The input signal was gradually decreased until the output no longer followed the input.

2.5 Hysteresis and Linearity

The differential output pressure was recorded as a function of the differential input pressure on an X-Y plotter as the input signal varied slowly from plus to minus and back to a plus-rated input signal.

2.6 Input Admittance

The input admittance was established by recording the control unit pressures and flows and the load flow for various throttle openings with a constant input signal.

2.7 Control Input Power

The control input pressures and flows and output pressures were measured at various input-signal levels with closed load throttle.

2.8 Output Flow Versus Differential Output Pressure

The differential output pressure, load flow and supply flow were recorded at various settings of the load throttle with constant input signal.

DISTRIBUTION

NASA-Lewis Research Center (10)
21000 Brookpark Road
Cleveland, Ohio 44135 M.S. 86-6
Attention: Vernon D. Gebben

NASA-Lewis Research Center (2)
21000 Brookpark Road
Cleveland, Ohio 44135
Attention: Lewis Library

NASA-Lewis Research Center (1)
21000 Brookpark Road
Cleveland, Ohio 44135
Attention: James E. Burnett, Technology Utilization Office

NASA-Ames Research Center (1)
Moffett Field, California 94035
Attention: Library

NASA-Goddard Space Flight Center (1)
Greenbelt, Maryland 20771
Attention: Library

NASA-Marshall Space Flight Center (2)
Huntsville, Alabama 35812
Attention: Michael A. Kalange, R-ASTR-NF

NASA-Western Operations (1)
150 Pico Boulevard
Santa Monica, California 90406

NASA Scientific & Technical Information Facility (6 & Reproducible)
Box 5700
Bethesda, Maryland
Attention: NASA Representative

NASA-Lewis Research Center (1)
21000 Brookpark Road
Cleveland, Ohio 44135
Attention: John Danicic

NASA-Lewis Research Center (1)
21000 Brookpark Road
Cleveland, Ohio 44135
Attention: Lewis Technical Information Division

NASA Headquarters (1)
Washington, D.C. 20546
Attention: F. C. Schwenk, NPO

NASA-Flight Research Center (1)
P.O. Box 273
Edwards AFB, California 93523
Attention: Library

NASA-Langley Research Center (1)
Langley Station
Hampton, Virginia 23365
Attention: Library

NASA-Manned Spacecraft Center (1)
Houston, Texas 77001
Attention: Library

Jet Propulsion Laboratory (1)
4800 Oak Grove Drive
Pasadena, California 91103
Attention: Library

NASA-Marshall Space Flight Center (1)
Huntsville, Alabama 35812
Attention: Library

Harry Diamond Laboratories (3)
Washington, D.C. 20438
Attention: Joseph M. Kirshner

Harry Diamond Laboratories (2)
Washington, D. C. 20438
Attention: Library

Wright-Patterson Air Force Base (2)
Ohio 45433
Attention: Library

NASA-Ames Research Center (1)
Moffett Field, California 94035
Attention: E. Perkins

NASA-Manned Spacecraft Center (1)
Houston, Texas 77058
Attention: R. Chilton

NASA-Goddard Space Flight Center (1)
Greenbelt, Maryland 20771
Attention: H. Hoffman

NASA-Langley Research Center (1)
Langley Station
Hampton, Virginia 23365
Attention: Harry V. Fuller

NASA-Lewis Research Center (1)
Plum Brook Station
Sandusky, Ohio 44871
Attention: W. E. Kirchmeier

Jet Propulsion Laboratory (1)
4800 Oak Grove Drive
Pasadena, California 91103
Attention: J. Scull

Aerojet-General Corporation (1)
Liquid Rocket Plant
Sacramento, California
Attention: Earl Sheridan

University of California (1)
Lawrence Radiation Laboratory
P.O. Box 308
Livermore, California
Attention: Jim Day

U. S. ATTAC, AMSTA-Z (1)
Warren, Michigan 48090
Attention: Gregory Arutunian

Aeronautical Engine Dept. (1)
Naval Air Propulsion Test Center
Philadelphia, Pennsylvania 19112
Attention: Joseph A. Avbel

SEG (SEJPF) (1)
Wright-Patterson Air Force Base
Ohio 45433
Attention: Charles Bleidorn

Commanding Officer Wilbert F. Buie (1)
Frankford Arsenal
Philadelphia, Pennsylvania 19137
Attention: SMUFA-J52/00-220-1

U.S. Army Electronic Command (1)
AMSEL-VL-M
Fort Monmouth, New Jersey 07703
Attention: S. Bracy

Naval Air Systems Command (1)
Air 52022A
18th and Constitution Avenue, N.W.
Washington, D. C. 20360
Attention: John Burns

Naval Ship Systems Command (1)
Ships 03414
Washington, D. C. 20360
Attention: Art Chaikin

NASA - ERC (1)
575 Technology Square
Cambridge, Massachusetts 02139
Attention: Dennis F. Collins

D/830
U.S. Naval Avionics Facility (1)
6100 East 21 Street
Indianapolis, Indiana 46218
Attention: Robert K. Davis

Commanding General
Capt. Stephen D. Donahue, Jr. (1)
U.S. Electronics Proving Ground
Ft. Huachuca, Arizona 85613
Attention: STEEP-TD-C (Capt. Donahue)

Harry Diamond Laboratories, Br. 430 (1)
Washington, D. C. 20438
Attention: Evan D. Fisher

Harry Diamond Laboratories, Br. 310 (1)
Washington, D. C. 20438
Attention: Richard N. Gottron

Naval Weapons Center (1)
Weapons Development Dept., Code 4044
China Lake, California 93555
Attention: Rolf O. Gilbertson

AFFDL (FDCL) (1)
Wright-Patterson AFB, Ohio 45433
Attention: James F. Hall

Aeronautical Engine Dept. (1)
Naval Air Propulsion Test Center
Philadelphia, Pennsylvania 19112
Attention: Russell J. Houston

MSFC/NASA R-ASTR-NFM (1)
Huntsville, Alabama 35812
Attention: William L. Howard

Naval Weapons Center (1)
Corona Laboratory, Code 75
Corona, California 91270
Attention: Stanley F. Johnson

Hq. U.S. Army Material Command (1)
Washington, D. C. 20315
Attention: Daniel J. Jones AMCRD-RP

Office of Chief of Research & Development (1)
Department of the Army
Washington, D. C. 20310
Attention: Maj. B. P. Manderville, Jr.
CRDPES

NASA-Ames Research Center (1)
Moffett Field, California 94035
Attention: Curt Muehl

U.S. Naval Ordnance Laboratory (1)
White Oak, Silver Spring, Maryland 20910
Attention: Charles F. Peer

AFAPL (APTC) (1)
Wright-Patterson AFB, Ohio 45433
Attention: Stephen J. Przybylko

Naval Air Systems Command (1)
AIR-52022
18th and Constitution Ave., N.W.
Washington, D. C. 20360
Attention: Richard A. Retta

AFRPL (REA) (1)
Edwards AFB, California 93523
Attention: K. O. Rimer

AFOSR (1)
1400 Wilson Boulevard
Arlington, Virginia 22209
Attention: Milton Rogers

Harry Diamond Laboratories, Br. 310 (1)
Washington, D. C. 20438
Attention: Kenneth R. Scudder

Frankford Arsenal, SMUFA-M-2200 (1)
Philadelphia, Pennsylvania 19137
Attention: Robert A. Shaffer

ONR, Code 461 (1)
Department of the Navy
Washington, D. C. 20360
Attention: David S. Siegel

NAVSEC Philadelphia Div., Code 6772 (1)
Philadelphia, Pennsylvania 19112
Attention: Wilbur L. Smith

AFFDL (FDCL) (1)
Wright-Patterson AFB, Ohio 45433
Attention: Harry Snowball

NED AADL-B65, Picatinny Arsenal (1)
Dover, New Jersey 07801
Attention: George R. Taylor

NASA-Marshall Space Flight Center (1)
Huntsville, Alabama 35812
Attention: Zack Thompson

NASA Headquarters, Code REI (1)
Washington, D. C. 20546
Attention: Stuart H. Vogt

Watervliet Arsenal (1)
Watervliet, New York 12189
Attention: Rolf E. Wagner

Harry Diamond Laboratories, Br. 430 (1)
Washington, D. C. 20438
Attention: Raymond W. Warren

Commanding Officer (1)
Frankford Arsenal
Philadelphia, Pennsylvania 19137
Attention: Manuel Weinstock MUFA-J5400-220-1

Naval Air Development Center (1)
Johnsville, Pennsylvania 18974
Attention: Horace Welk

AFWL (1)
Kirtland AFB, New Mexico 87117
Attention: Lt. John J. Wozniak

NASA-Lewis Research Center (1)
Nuclear Systems Division
21000 Brookpark Road
Cleveland, Ohio 44135
Attention: Lyle O. Wright

AFAL (AVNE) (1)
Wright-Patterson AFB, Ohio 45433
Attention: Seth A. Young